UNIVERSITY OF OKLAHOMA

GRADUATE COLLEGE

FUTURE IMPACT ON THE LOW-LEVEL JET AND ITS EFFECTS ON WIND ENERGY GENERATION IN OKLAHOMA

A THESIS

SUBMITTED TO THE GRADUATE FACULTY

In partial fulfillment of the requirements for the

Degree of

MASTER OF SCIENCE IN ENVIRONMENTAL SUSTAINABILITY

By

JOSHUA JON WIMHURST

Norman, Oklahoma

2019

FUTURE IMPACT ON THE LOW-LEVEL JET AND ITS EFFECTS ON WIND ENERGY GENERATION IN OKLAHOMA

A THESIS APPROVED FOR THE

DEPARTMENT OF GEOGRAPHY AND ENVIRONMENTAL SUSTAINABILITY

BY

Dr. John Scott Greene, Chair

Dr. Stephen Stadler

Dr. Renee McPherson

Acknowledgements

This work represents a culmination of my interests in understanding the mechanisms behind the long-term evolution of wind energy resources, and to be given the opportunity to study this topic for my Master's thesis is something for which I am very grateful. I would like to give thanks to my advisor and committee chair, Dr. Scott Greene, for giving me the academic support that I needed in pursing this work, and still believing in my ideas when the amount of necessary research looked to be difficult to present concisely. Thanks also to Dr. Renee McPherson and Dr. Stephen Stadler, my other committee members, for the advice that they provided in shaping the final document and asking the necessary questions to ensure I executed the work in a way that made sense not only to others but also to myself. I would also like to extend my gratitude to the Oklahoma Mesonet for providing observations that were used in this work, and also to Dr. Elinor Martin at the School of Meteorology for allowing me to have access to climate model data from the National Weather Center's remote access server. Finally, thank you so much to all of my friends and family that have been interested in knowing about this work and also provided the personal support that I needed to produce a successful document, but most of all to my partner, Russell, for always being there whenever I needed to say out loud what I was trying to do or whenever I needed a laugh throughout the process ("Patterns! It's all about the patterns!").

Table of Contents

List of Tables

List of Figures

Abstract

Future increases of wind energy density for the United States' South-Central Plains region have been projected by several previous research examples. These increases oppose the decreases in wind energy density that have been projected for the rest of the country. Simultaneously, the Central Plains' low-level jet has been projected to become faster and more frequent by the end of the century. Given the influence that observed low-level jets have been known to exert on hub-height wind speeds, it is reasonable to suggest that projected changes of wind energy resources over Oklahoma could be a consequence of strengthening of the low-level jet.

This work sought to determine the existence of a significant and explicable climatological relationship between the low-level jet and wind energy resources. The approach of this work was therefore to explore several low-level jet characteristics and wind energy metrics, some of which have seldom been analyzed on climatological timescales, such as low-level jet height, frequency of ramp up/ramp down events, and frequency of cut-in/cut-out events. Another objective of this work was to update projections of low-level jet characteristics and wind energy metrics before exploring their relationships, since many previous studies have based projections of these quantities on older climate model outputs.

Outputs from a collection of recent climate models were enlisted to evaluate projected changes in the low-level jet's speed, height, and frequency. Analysis of these outputs over the 21st Century substantiated the projected low-level jet strengthening concluded in previous work, in particular an increase of low-level jet frequency and a poleward shifting of the most common sites of its formation. This study also indicated statistically significant increases in low-level jet frequency in autumn, a time of year when the low-level jet occurs less frequently. The necessity of enlisting

multiple model outputs in such work was also highlighted, given the tendency of lower-resolution General Circulation Models (GCMs) to project reductions in these low-level jet characteristics, and the known biases that several of these GCMs possess, e.g. underestimation of historical low-level jet frequency, particularly amongst lower-resolution GCMs.

The current study evaluated wind energy metrics by enlisting a climatological delta method to statistically downscale model-projected wind speed changes onto wind measurements from a collection of Oklahoma Mesonet stations, thereby producing high-resolution future pseudo-observations at these locations. The current study showed some disagreement with results from previous work, with reductions in wind speed and wind power density projected by the end of the century, and consistent increases (reductions) in the frequency of cut-out (cut-in) events. There was also evidence for diurnal and seasonal variability in the frequency of ramp up/down events, with both quantities possessing higher frequency in spring and summer and during the day. This finding possessed consistency with observations of ramp events. There were notable differences in projected changes of these metrics between models, with the ACCESS 1.0 GCM in particular more consistently projecting increases in these quantities than the other GCMs used in this work. The known biases of these GCMs in underestimating spring and summer wind speed over the Central Plains was highlighted as reasons for these results.

Simple linear regression showed that increases in low-level jet frequency possess a consistent and statistically significant relationship with the wind energy metrics studied in this work, especially for spring and summer and during the night – times of day at which the low-level jet's occurrence is typically more frequent. The relationship between increased future low-level jet frequency and reductions of ramp event frequency is of interest, given its implications for the grid management of Oklahoma's future wind energy generation. It was noted in this work,

however, that the strong relationships between low-level jet frequency and these wind energy metrics were not always consistent with the sign of projected changes in low-level jet characteristics and wind energy metrics. As such, whilst the low-level jet probably does exert some influence on wind energy metrics and could continue to do so in future decades, the effects of other climatological processes and climate variability cycles could also be important.

Chapter 1: Introduction

1.1. Scope of Thesis

Wind energy generation in the state of Oklahoma has grown considerably in recent years. As of the fourth quarter of 2018, Oklahoma possesses the third highest statewide wind energy capacity in the United States (8,072 Megawatts), which comprises almost one-third (31.9%) of the state's total electrical generation capacity (American Wind Energy Association, 2018). This increase in wind energy has largely been driven by the decreasing cost of its commission and installation. Wind energy now possesses the lowest levelized cost of energy ($37/Megawatt hour) of all means of generating electricity available to the United States (Energy Information Administration, 2018) – an undeniable economic asset to Oklahoma's energy infrastructure.

In the past, the use of wind energy and other renewable energy resources has been encouraged by Oklahoma's state government. Chapter 801.4 of the 2010 Oklahoma Energy Security Act states that "it is in the public interest to promote renewable energy development in order to best utilize the abundant natural resources found in this state" (Oklahoma State Courts Network, 2015), with wind energy being included in its list of promoted forms of energy. There has, however, been legislative pushback in recent years, with the state government ending income tax credits for Oklahoma's zero-emission energy generation in July 2017 (McCall and Schulz, 2017), and the decision to prohibit wind turbine construction within 1.5 miles of the state's airports, hospitals, and schools (Bingman and Sears, 2015). This forms part of a wider national effort to discontinue government-issued incentives for green energy technologies. These legislative motions have, however, had little effect on the growth of Oklahoma's wind energy industry, consequently

assisting in reducing the United States' dependence on fossil fuel imports and strengthening national energy security.

Reliance on wind energy in Oklahoma has produced many economic and environmental benefits, such as supporting up to 9,000 jobs in connection with the wind energy industry, and the avoidance of 10.7 million metric tons of carbon emissions in 2017 alone (American Wind Energy Association, 2018). Benefits of wind energy production are likely to amass and continue in future decades, with the United States' Department of Energy's Wind Vision report projecting a 500-Gigawatt nationwide onshore wind energy capacity by 2050, which would constitute around 35% of the country's electricity supply (Department of Energy, 2018). Oklahoma's wind energy capacity, according to this report, is predicted to have a statewide installed capacity of 15 Gigawatts by 2050. Such growth would represent a doubling of the state's current capacity.

Although Oklahoma's burgeoning wind energy industry affords multiple benefits, whether they be employment, public service funding, or energy independence, it is of interest to research the perpetuity of these benefits. As such, many examples in the research literature have hitherto considered the longevity of wind energy in light of a potential climate change. Spatial and temporal analyses using climate models have generally concluded that climate change could be associated with a negative impact on wind energy in the coming decades. This conclusion has been made by studies of projected wind speed evolution on local scales, such as the Pacific Northwest (Sailor et al., 2008) and the Central Plains (Greene et al., 2012), as well as national scales encompassing the contiguous United States (Breslow and Sailor, 2002; Pryor and Barthelmie, 2011; Johnson and Erhardt, 2016). These results are indicative of a shift of the most optimal locations for wind energy generation to other regions of the United States. Given that many countries are increasingly relying on renewable energy resources as a replacement for

more physically and economically restricted reserves of fossil fuels (Höök and Tang, 2013), the dilemma of maintaining the United States' energy infrastructure using potentially decreasingly available wind energy resources becomes a point of concern.

However, projections of climate change's impacts on wind energy resources possess spatial variability, such that projections for Oklahoma and the wider South-Central Plains region are not consistent with those for the rest of the United States. Analysis of Oklahoma's future wind climate by Stadler et al. (2015) projects springtime wind speed increases of over 7% between 2000 and 2070. Studies focusing on national length-scales corroborate this finding, with work by Segal et al. (2001), Holt and Wung (2012), Kulkarni and Huang (2014), and Johnson and Erhardt (2016) all concluding that the increase in wind speed projected to occur over the South-Central Plains is incongruent with the projected reductions (or lack of change) for the rest of the United States.

Based on the results of these previous studies, it becomes interesting to ask why the use of wind energy resources of states including and around Oklahoma may evolve in a different manner than the rest of the United States. There have been several studies, such as Cook et al. (2008), which have concluded that the springtime low-level jet (powerful nocturnal southerly winds that form frequently over the Central Plains at this time of year – detailed definition of the low-level jet is given in Section 2.2) could be as much as 25% faster by the end of the century, as well as occurring more frequently at times of year when low-level jets are typically less common, such as autumn. More recent work by Tang et al. (2017) found results consistent with Cook et al. (2008), revealing that annual low-level jet frequency could be up to 20% higher by 2070. An enhancement of low-level jet speed and frequency is an important result, since this phenomenon has been documented in various observational studies to have a notable influence on hub-height

level wind speeds, whether for the South-Central Plains or otherwise (Greene et al., 2009; Emeis, 2014b; Lampert et al., 2016). It is therefore reasonable to suggest that an increase in the low-level jet's speed and frequency over the next few decades could be an important contributing factor to the positive wind speed trends over Oklahoma in the aforementioned studies. The low-level jet is of interest to the current study since it is a phenomenon that occurs most frequently over the United States' Central Plains, frequently forming over the state of Oklahoma.

1.2. Justification for this Work

The objective of this thesis is to determine whether model-projected changes in Oklahoma's wind energy resources presented in previous work possess a link with evolution of the Central Plains' low-level jet. Since Oklahoma's dependence on wind energy is growing quickly, it is of interest to the state's government, stakeholders in the wind energy industry, and the scientific community to understand why Oklahoma's wind energy resources may evolve in the manner that has been projected by climate models. This work therefore serves three purposes in particular:

1. *Filling a gap of understanding regarding the vulnerability of the United States' wind energy resources to climate change.* There are several examples of existing research that have explored how the viability of wind energy generation over Oklahoma, and the Central Plains more widely, could change as the 21st Century progresses, typically by quantifying future changes in wind speed and wind power density (Greene et al., 2010; Greene et al., 2012; Stadler et al., 2015). However, there are no United States-focused research examples that consider why these changes in wind climatology might take place. Some studies, such as Holt and Wung (2012), have suggested that the low-level jet's evolution could explain a considerable amount of the trends in wind energy resources over the South-Central Plains region. By combining this proposition with results that

indicate climate change potentially having significant effects on the average state of the low-level jet (Cook et al., 2008; Tang et al., 2017), it is reasonable to specifically assess the low-level jet's role in the changes in extractable wind energy resources that Oklahoma could experience.

2. *Providing insight for long-term energy planning at state and national levels.* Oklahoma is an interesting case study for this work because its wind energy capacity has grown quickly, having had no capacity prior to 2003, and now having the third highest statewide wind energy capacity across the United States (WINDExchange, 2018a). Much of this growth in wind energy development has happened with little to no legislative assistance or formal government policy. Given the focus of the current study, Oklahoma's state government and the private sector may find its results useful for informing energy policy and continued investment into Oklahoma's wind energy industry. Such a finding would hopefully lead to the construction of guided procedures to develop and expand the infrastructure that is already in place. For example, information about future changes in the frequency of cut-in events (shutting down of wind turbines when wind speeds drop below 3 m s^{-1}) could lead to new standards for wind turbine blade construction.
3. *Updating previous work in this field using more contemporary data.* Many previous studies that have considered future changes in the United States' wind energy resources or the low-level jet have been conducted using outputs from similar sets of General Circulation Models (GCMs) from the Third Generation of the Coupled Model Intercomparison Project (CMIP3; Meehl et al., 2007). Whilst these studies have produced many scientifically credible results, the outputs of Fifth Generation (CMIP5) GCMs have been publicly available for several years, having been developed to improve upon CMIP3

in several ways, such as grid resolution, more ensemble members, and improving/increasing the climate system processes that can be simulated (Taylor et al., 2012). Although the newer Sixth Generation (CMIP6) of GCM outputs are gradually being made available to the public, not enough wind speed outputs were available to compare projections from multiple GCMs (WRCP, 2019) at the time of the current study. As such, GCM outputs from the CMIP5 generation are used in the current study, in order to assess linkages between wind energy resources and low-level jet characteristics and therefore update findings from previous work.

It is important to justify why the low-level jet has been selected as an explanation for the evolution of Oklahoma's wind energy resources. The low-level jet has been recognized in previous work to be a significant feature of the United States' wind climatology, particularly during the spring months (Doubler et al., 2015; Yu et al., 2017). This significance is one reason why several studies have evaluated the features of the low-level jet's climatology and its relationship to other climatological features (Song et al., 2005; Harding et al., 2013; Danco and Martin, 2017). Secondly, observational studies that link low-level jets to near-surface winds (Emeis, 2014b; Lampert et al., 2016) all give credence to the low-level jet's influence on wind energy generation. Finally, non-extreme extratropical cyclones over North America are expected to shift poleward and also reduce in strength and frequency (Yin, 2005; Bengtsson et al., 2006; Zappa et al., 2013). This contribution to reduced wind speed over the South-Central Plains would suggest that large synoptic scale processes have less importance in explaining the wind speed increases that have been found to occur in this region. Overall, the low-level jet's pertinence and strong influence on Oklahoma's wind climatology means that it makes sense to study the low-level jet specifically in explaining the effects on the state's future wind energy resources.

As mentioned above, the results of this study could have relevance to stakeholders in the wind energy industry. A core component of this study is therefore to relate the evolution of the low-level jet to various metrics for measuring wind energy generation, therefore producing results that are more tangible when informing long-term investment and policy decisions. The selected metrics are all relevant to the productivity of wind turbines, consisting of wind speed, wind power density, frequency of winds below cut-in/above cut-out speed, and frequency of ramp up/down events (see Section 3.2 for definitions and significance of these indicators).

Bearing all of this in mind, the following three research questions are asked by the current study, which shall be answered based on the obtained results and comparisons with previous literature:

1. A United States-based multi-GCM analysis of historical versus future low-level jet climatology using model outputs from the CMIP5 generation is yet to be done. Previous studies either used outputs from the CMIP3 generation (Tang et al., 2017) or only one or two CMIP5 climate model outputs (Harding and Snyder, 2014). Studies that enlisted a contemporary multi-model ensemble only considered the jet's historical state, such as Harding et al. (2013) and Danco and Martin (2017). Also, none of these studies have considered projected changes in low-level jet height. As such, how does using more recent climate model outputs of wind speed and consideration of a wider range of low-level jet characteristics change the current understanding of projected low-level jet climatology over the South-Central Plains region?

2. Previous examples of research concerning United States-focused climatological projections of wind energy resources have not enlisted as holistic a range of wind energy metrics as the current study. Most of these studies have only considered wind speed (Pryor and Barthelmie, 2011) or wind power density (Stadler et al., 2015; Johnson and Erhardt, 2016), many of which again enlisted model outputs from the CMIP3 generation to project these quantities. Kulkarni and

Huang (2014) is one of the only examples in the literature of CMIP5-based projections of the United States' wind energy resources, but this study used a different combination of GCMs than that of the current study (see Section 3.1 for details of GCMs enlisted). In what way does using more recent climate model projections to calculate changes in a range of wind energy metrics yield notable results concerning Oklahoma's future wind energy resources?

3. The linkage between the low-level jet and near-surface winds in its vicinity has been suggested by studies such as Holt and Wung (2012) and Johnson and Erhardt (2016), but is still yet to be assessed explicitly. How can changes in the low-level jet climatology projected in the current study be linked to changes in Oklahoma's wind energy resources in ways that are conceptually sound, owing to suggested influences of the low-level jet on near-surface winds? For example, it is reasonable that increases in wind power density could occur alongside a simultaneous increase in low-level jet frequency. The range of quantities analyzed in the current study allows for assessment of this link across a range of different low-level jet characteristics and wind energy metrics, as opposed to simply linking near-surface and upper-level wind speeds.

This thesis is broken down into the following chapters. Chapter 2 consists of a literature overview of previous work that underpins the current study. Chapter 3 details and justifies the methods used to obtain this work's findings. Chapters 4 contains results that answer the first research question, concerning projected changes in low-level jet characteristics. Chapter 5 contains results that answer the second and third research questions, concerning changes in wind energy metrics and their linkages to the low-level jet characteristics. Chapter 6 summarizes the results and limitations of the study, and also suggests avenues for future work on this subject.

Chapter 2: Literature Overview

2.1. Influences of Climate Change on Wind Power Production

Climate change has been considered a relevant factor in influencing wind energy resources due to its effects on geographical distribution and variability of wind speed and direction (Sailor et al., 2008; Pryor and Barthelmie, 2010; Johnson and Erhardt, 2016). Outside of the tropics, mountainous terrain, and coastal boundaries, the prevailing winds that provide most of a region's wind energy resource are largely derived from synoptic-scale weather patterns, such as those associated with the Northern Hemisphere jet stream. Several studies of jet stream climatology (Bengtsson et al., 2006; Woollings and Blackburn, 2012) have concluded that future decades could play host to a poleward shift of these storm tracks, perhaps resulting from weakened meridional (equator-to-pole) temperature gradients. This shift could consequently relocate the most profitable and sustainable locations for wind energy production, as evidenced by the potential link between surface and jet stream-level wind speeds (Wimhurst et al., 2017).

The resulting decrease of wind power density (the amount of energy present in the wind that can hypothetically be extracted by wind turbines) over North America has been presented in several studies. Regional examples include Greene et al. (2012) and their study of wind power density changes over the Central Plains region. Their use of aggregated model outputs from the North American Regional Climate Change Assessment Program (NARCCAP) archive found that spring and summer median wind speeds over this region (between 2000 and 2070) are expected to increase, but also decrease by as much as 6% in the winter months (Figure 1). This study also concluded that a poleward shift of storm tracks over North America could explain some of these results, based on the overall reduction in extractable wind energy over the Central Plains that is

projected. Consistent results were found in another regional study by Sailor et al. (2008), who enlisted outputs from four statistically downscaled GCMs to verify the role of climate change in projections of wind power density for the Pacific-Northwest. Their results demonstrated reductions of summertime wind power density between 2000 and 2050 of as much as 40%, with much smaller to negligible decreases in other seasons.

This link between climate change and reductions of wind power density has also been explored in studies that considered greater spatial scales, such as the contiguous United States. Research by Pryor and Barthelmie (2011) used outputs from three GCMs that had been dynamically downscaled by a selection of Regional Climate Models (RCMs) to diagnose statistically significant changes ($p < 0.05$) of 50-meter wind power density between 2000 and 2062. Figure 2

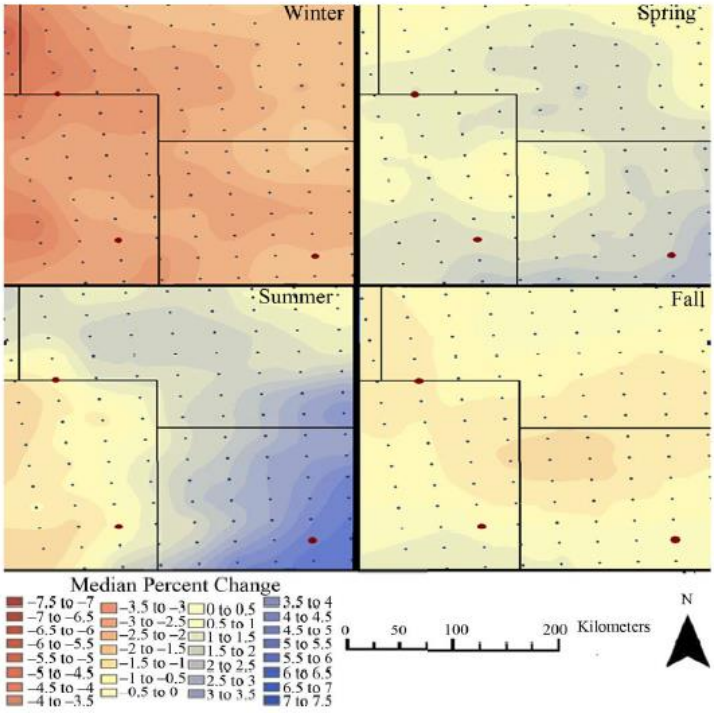

Figure 1: Spatial analysis of median wind speed changes over the Central Plains region (in %) between 1970-2000 and 2040-2070 using NARCCAP model outputs.
- Outputs are seasonally averaged for winter (top-left), spring (top-right), summer (bottom-left), and autumn (bottom-right) (Greene et al., 2012).

presents one of the study's results, which shows that the majority of statistically significant changes of wind power density over the model run period are decreases. Many other studies of nationwide wind energy resources have arrived at the same general conclusion, whether based on projections using climate models (Segal et al., 2001; Breslow and Sailor, 2002; Kulkarni and Huang, 2014), or observations and reanalysis of previous wind climatology (Pryor et al., 2009; Greene et al., 2010). As such, the broad synoptic estimation for the United States is a reduction of wind energy availability in the coming decades, potentially resulting from a multi-decadal poleward shift in storm tracks displacing optimal sites for wind energy generation.

However, the South-Central Plains region consistently has not adhered to the same projected changes in available wind energy resources for rest of the United States. This discrepancy can be

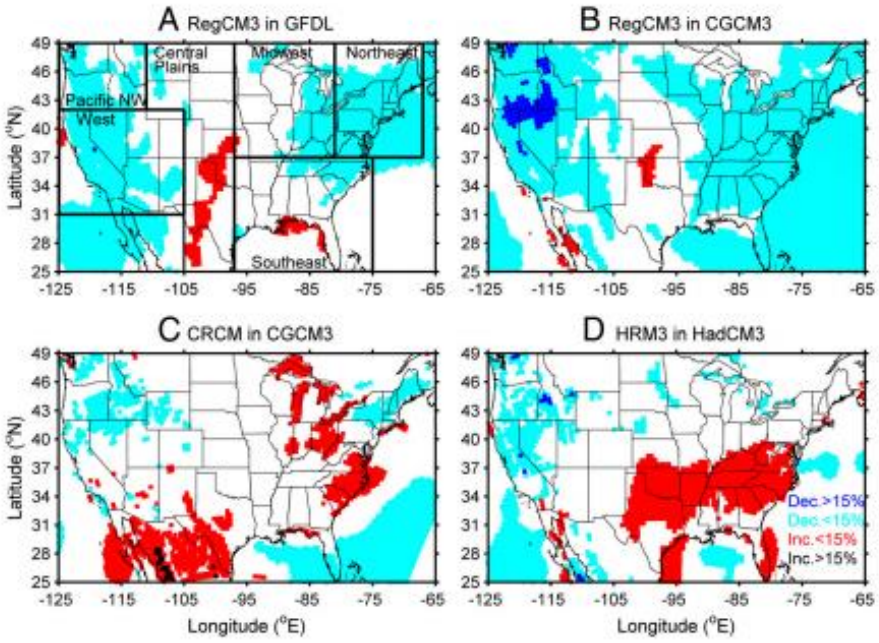

Figure 2: Changes of mean wind power density (in %) between 1979-2000 and 2041-2062 with different GCM-RCM combinations.
- Colors are attributed to changes of mean wind power density that are statistically significant at the 95% confidence level, i.e. at least 2 standard deviations greater than 1979-2000 mean wind power density in that location (Pryor and Barthelmie, 2011).

seen in Figure 2, which shows that the only region of the United States that might experience a statistically significant increase of mean wind power density in all GCM-RCM combinations is the South-Central Plains region of Kansas, Texas, and Oklahoma. As mentioned above, Greene et al. (2012) also projected increases of wind energy resources in spring and summer over Colorado and Kansas, which helps to corroborate the existence of this inconsistency. The same result was found by Johnson and Erhardt (2016) in their study of changes in 50-meter wind speeds over the contiguous United States. Their analysis of dynamically downscaled model outputs from NARCCAP found that the South-Central Plains region was, across all outputs, the only region of the United States that could experience a >2% mean wind power density increase between 2000 and 2070, particularly over the Oklahoma Panhandle. This increase of wind speed across the South-Central Plains region can in fact already be seen in data derived from observations. Holt and Wung (2012) concluded that the most significant increases of 80-meter wind speed across the United States from 1979 to 2009 have happened across the region of Texas, Louisiana, and Oklahoma. Their use of North American Regional Reanalysis (NARR) output data found an approximate wind speed increase of 0.12 m s^{-1} $decade^{-1}$ for this region.

When looking at smaller spatial scales, such as Oklahoma alone, this same result holds. Spatial analysis of NARR data by Greene et al. (2010) exemplifies the increase of 80-meter wind power density in Oklahoma that happened between 1979 and 2008. As well as changes in observational wind speed across Oklahoma, projected changes have also been studied, such as in research by Stadler et al. (2015) that analyzed outputs from two GCM-RCMs of 10-meter wind speed across Oklahoma. Under a "business as usual" emissions scenario (Scenario A2 from the Special Report on Emission Scenarios (SRES, Nakićenović et al. (2000))), they found that median spring and

summer wind speeds could be 6-8% higher by the 2060's versus the 1990's (Figure 3), with negligible changes in autumn and winter.

These literature examples collectively indicate that the projected wind climatology of the South-Central Plains is influenced by more than just synoptic-scale processes that affect the Contiguous

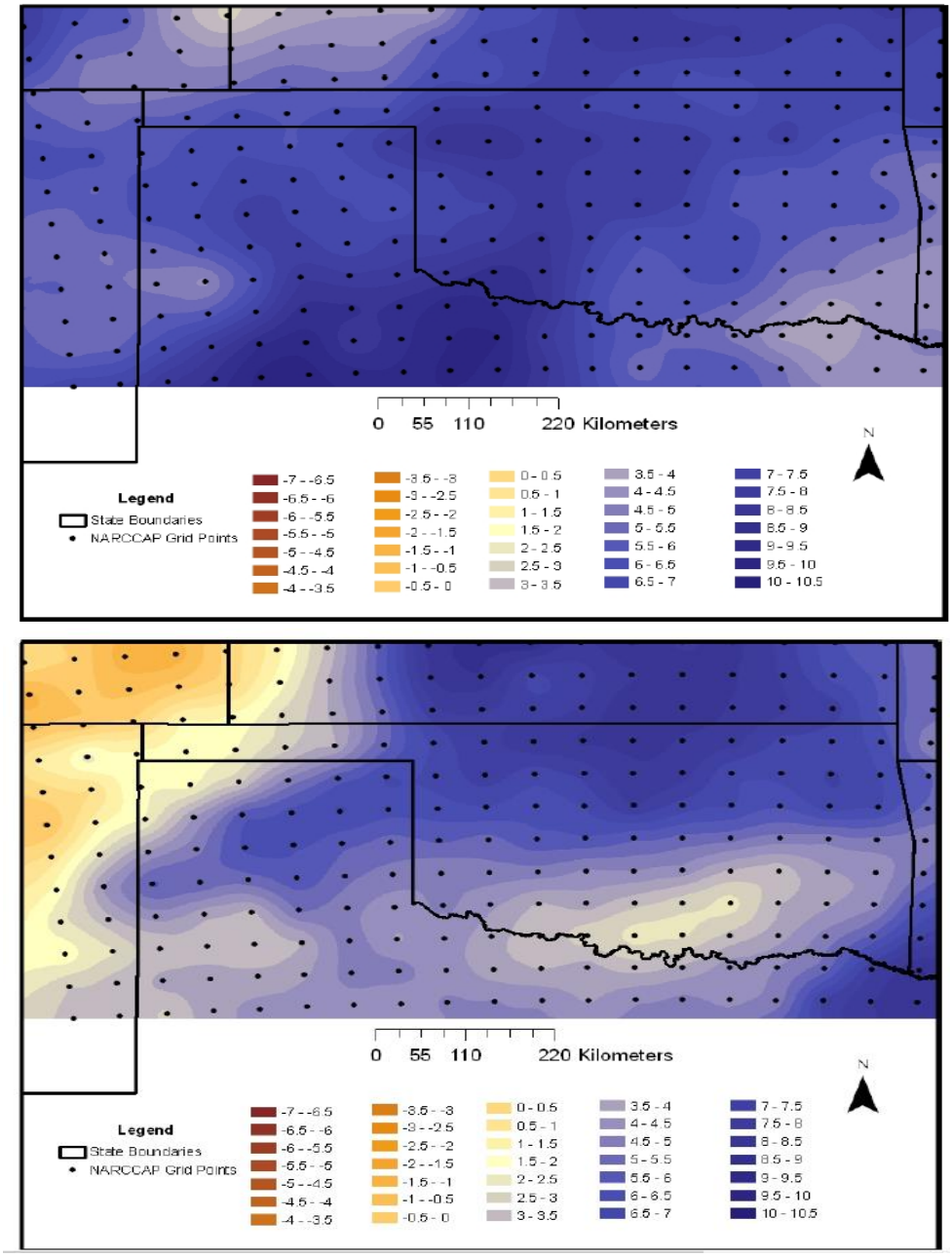

Figure 3: Changes of median 10-meter wind speed (in %) for spring (top) and summer (bottom) between 2060-2069 and 1990-1999 using NARCCAP model outputs (Stadler et al., 2015).

United States, particularly over the state of Oklahoma. It is therefore of interest to investigate a potential reason for this discrepancy in projected wind climatology changes.

2.2. The Central Plains' Low-Level Jet

2.2.1. Climatology of the Low-Level Jet

The low-level jet, henceforth referred to as the LLJ, is a mostly nocturnal meteorological phenomenon that occurs over the United States' Central Plains. It is comprised of powerful, supergeostrophic winds that are much stronger than the calmer winds of the surface layer (the lowest region of a nocturnal atmospheric boundary layer) below (Stull, 1988). The LLJ's features and formation process have been described in various studies, such as Blackadar (1957), Wexler (1961), and more recently by Shapiro and Fedorovich (2010). These studies stipulate that the LLJ's formation occurs due to strong radiational cooling that decouples the surface layer from the Ekman layer above, occurring most easily under cloud-free conditions. The consequent cutting off of turbulent mixing that was formerly associated with the daytime convective boundary layer significantly reduces atmospheric friction, therefore resulting in northward acceleration in the Ekman layer. This mechanism is what produces the LLJ's southerly winds across the Central Plains. LLJs that form are generally faster and closer to the ground the greater the reduction in turbulent mixing.

LLJs can also be produced by extratropical cyclones travelling across the Central Plains, such that the isobars within a cyclone's warm sector are oriented in a north-south direction (Djurić and Ladwig, 1983). However, this process of LLJ formation typically produces less frequent and slower jets in the absence of the radiational cooling effect (Uccellini, 1980). Most previous studies of LLJ climatology (Doubler et al., 2015; Tang et al., 2017; Yu et al., 2017) acknowledge

that extratropical cyclones do have an influence on detected patterns in LLJ characteristics, but these influences are small compared to the boundary layer formation mechanism described by Shapiro and Fedorovich (2010). Furthermore, these studies (and the current study) have been more concerned over the LLJs themselves when evaluating this climatology, less so the mechanisms that produce them.

Generally, the height of the LLJ's core (level of maximum wind speed) forms between 150 to 500 meters above the ground (Emeis, 2014a), with the wind itself being as much as 70% stronger than daytime winds over the Central Plains (Shapiro and Fedorovich, 2010). The formation of such high-magnitude supergeostrophic winds is assisted by the differential radiational cooling between the Rocky Mountains (faster cooling) and the Central Plains themselves (slower cooling). The altitude difference is what enhances radiative forcing, establishing an east-west pressure gradient and southerly winds even more powerful and frequent than otherwise (Emeis, 2014a).

Climatologically, the LLJ has been observed to occur most frequently during spring and summer, since the conditions necessary to form the LLJ are more often satisfied at these times of year (radiational cooling, decoupling of surface layer from air above, altitude differences resulting in differential cooling). A study by Doubler et al. (2015) that used NARR data from 1979 to 2009 came to this conclusion, with the LLJ being observed to occur on 25-30% of nights in these spring and summer over the South-Central Plains. The frequency of LLJ formation in April over from this study is shown in Figure 4, which demonstrates the climatological significance of this phenomenon. However, the study does concede that an LLJ that forms outside of spring and summer (whether formed by boundary layer dynamics and/or extratropical cyclones) tends to be somewhat stronger, averaging 18-22 m s^{-1} at around 2000 meters above sea level. Song et al.

(2005) also came to this realization in their analysis of observed wind profiles at the Atmospheric Boundary Layer Experiments (ABLE) site in South-Central Kansas. Their study reasoned that the east-west misalignment of air density and pressure gradients (baroclinicity) that characterizes LLJ formation is typically stronger in colder seasons, hence the higher LLJ speed at this time of year.

Other papers that have used NARR as a data source to diagnose the LLJ's climatology (Weaver and Nigam, 2008; Yu et al., 2017) have made similar conclusions about its frequency of occurrence. Both of these studies also made interesting deductions about some of the LLJ's recurring features and the climate variability cycles that may influence them:

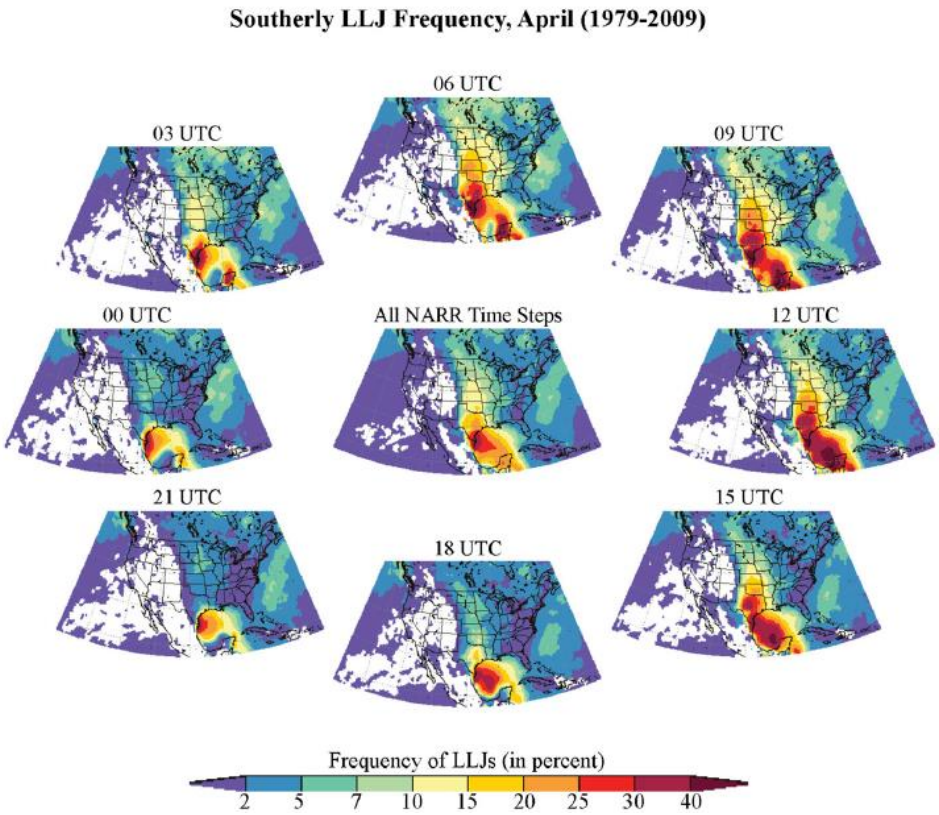

Figure 4: Frequency of Southerly LLJ formation (in %) during all months of April from 1979-2009, averaged over 3-hourly time steps using NARR output data.
- White indicates no LLJ formation or locations that are more than 2000 meters above sea level (Doubler et al., 2015).

1. Empirical Orthogonal Analysis (EOF) of the LLJ's climatological features reveals that it possesses specific spatial patterns. Weaver and Nigam (2008) assessed characteristics of the LLJ over a jet core region of 25°–35°N and 102°–97°W, and found that almost 75% of the LLJ's variance derived from monthly-averaged wind fields over this region (based on NARR outputs) can be explained by three distinct modes – a latitudinal expansion of the jet core (38% of variability), a south-west shift in rainfall associated with the LLJ (23% of the variability), and an in-place strengthening (12% of the variability). Similarly, Yu et al. (2017) used an EOF approach and identified two modal features in the LLJ's spatial patterns. In 30% (20%) of LLJ occurrences in the warm (cool) season, the LLJ frequency is relatively high and the jet core over the South-Central Plains becomes stronger. By contrast, in 20% (15%) of LLJ occurrences in the warm (cool) season, the jet core undergoes a sub-seasonal latitudinal shift, such that its frequency of formation drops over the Gulf of Mexico and increases over the Central Plains.
2. In both of these studies, the aforementioned EOFs can be partially attributed to climate variability cycles. For example, Weaver and Nigam (2008) found that stronger meridional winds over the Central Plains at the 900 hectopascal (hPa) level are somewhat negatively correlated with a negative phase of the North Atlantic Oscillation (NAO) ($r = -0.46$ in the correlation of the NAO index and the study's enlisted LLJ index). Moreover, Yu et al. (2017) made conclusions that faster and stronger LLJs are positively correlated with the summertime Atlantic Multidecadal Oscillation (AMO) and negatively correlated with the Pacific Decadal Oscillation (PDO) in spring and summer. Danco and Martin (2017) concluded that the LLJ is also influenced by changes in the El Niño-Southern Oscillation's (ENSO) phase. Using several reanalysis datasets and historical

model outputs from 42 different CMIP5 ensemble members, they found that an El Niño event that occurs during winter is statistically significantly linked ($p < 0.05$) to weaker LLJs in the following spring ($r \approx -0.4$) and stronger LLJs in summer ($r \approx 0.3$), based on correlation between ENSO and LLJ indices. Observational studies have found similar links, such as Song et al. (2005). Over their study's six-year observational period, they discovered that LLJs occurred more often during a colder PDO phase and during La Niña events.

A feature of climatological studies of the LLJ that is of importance to this study's motivation is the LLJ's most frequent site of formation. In a study of LLJ climatology by Tang et al. (2016), dynamically downscaled model outputs from four NARCCAP datasets were compared to observational soundings of wind profiles, with all data sources encompassing the period of 1979 to 2000. The downscaled models were able to identify the three locations where LLJ formation most frequently occurred according to the observational soundings – South Texas, Central Texas, and the Kansas/Oklahoma border. The frequency of warm season LLJ formation over the South-Central Plains and the agreement between observations and model outputs is shown in Figure 5. Yu et al. (2017), made the same deduction based on their analysis of NARR outputs, observing that annually averaged LLJ frequency is at its greatest over South Texas and the Gulf of Mexico, with high frequencies also occurring over Oklahoma and Kansas during the warm season. As discussed earlier in this section, LLJ formation is common over the Central Plains due to ideal conditions being present, hence high LLJ frequency in this region is expected.

Although it is encouraging when results from observations, reanalysis data, and model outputs are consistent when comparing studies, such consistency does not often occur. For example, Danco and Martin (2017) found that despite different GCMs being consistent with each other in

recreating features of ENSO, many of them are negatively biased in their simulation of the LLJ strength and frequency seen in reanalysis outputs. Further compounding this issue, Doubler et al. (2015) concede in their work that reanalysis datasets, such as NARR, tend to underestimate the frequency of LLJ formation, but nevertheless are preferable to observations due to issues with the latter's coverage and temporal availability. With this consistent underestimation of true LLJ speed and frequency, it is possible that data received from model outputs used in the current study would therefore be biased in its characterization of future changes in Oklahoma's wind climatology. A lack of consistency from different data sources due to model biases and/or differences in spatial and temporal coverage means that care must be

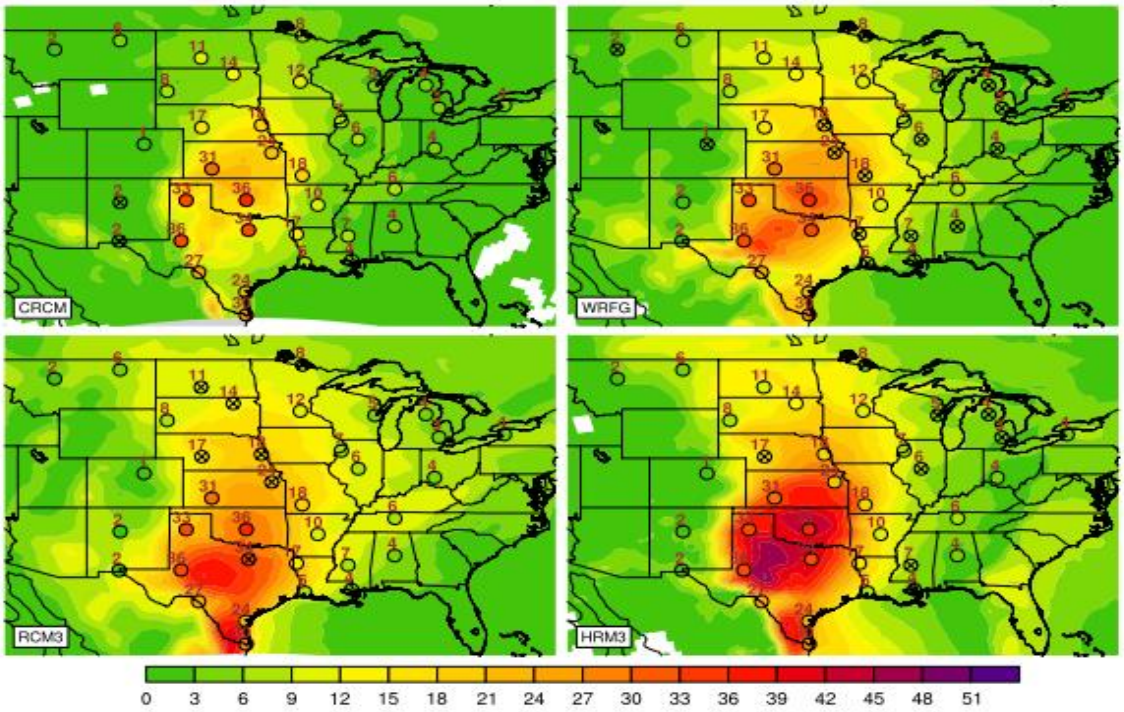

Figure 5: Comparison of observational soundings (circles) and 4 different NARCCAP model outputs in terms of warm season 1200 UTC average LLJ frequency of occurrence (in %) from 1979-2000.
- Percentages for the observations are indicated next to each sounding location. A circle not containing a cross means indicates that the observations and model outputs produced statistically significantly different results (Tang et al., 2016).

taken when deriving conclusions from projections for LLJ climatology and wind energy resources.

The results from the summarized literature in this section provide important insight into the LLJ's various climatological features, such as its speed, height of formation, and common geographical location. This last feature is especially important, given the result from Pryor and Barthelmie (2011) that projected increases of wind power density are located in the same region of the United States as in the LLJ's greatest frequency – the South-Central Plains. Such consistency in location positions the LLJ as a viable candidate to explain, at least partially, why the projected changes of Oklahoma's wind energy resources are not consistent with the rest of the United States in climate model projections.

2.2.2. Response of the Low-Level Jet to Climate Change

There have been few studies that have specifically considered how the LLJ itself responds to climate change, with most studies focusing instead on changes in its associated features. Furthermore, as discussed in Section 1.2, most studies that have considered LLJ climatology have based their projections on the outputs of climate models from CMIP3, with these outputs having been available since the mid-2000s (Meehl et al., 2007). For instance, Cook et al. (2008) analyzed projected intensification of the LLJ and its association with climate change, using the outputs of 18 CMIP3 GCMs. These models were used to simulate recorded states of the LLJ seen in NARR and NCEP (National Centers for Environmental Prediction) reanalysis data from 1979 to 1999, as well as to project 2079 to 2099 meridionally-averaged 850 hPa winds over the Central Plains region to quantify sensitivity to climate change. The models consistently projected that the LLJ could become approximately 25% stronger in the months of April, May, and June from the historical period to the future period, with smaller increases for the autumn months. It

was suggested by this study that an LLJ strengthening could occur due to the westward extension of the subtropical Bermuda High, owing to an increase in oceanic temperatures. The influence of the Bermuda High on the LLJ is also acknowledged by Holt and Wung (2012) and Zhu and Liang (2013).

A more recent study by Tang et al. (2017) considered the same topic, but was specifically motivated by the decision made in Cook et al. (2008) to use model runs to derive the state of the LLJ using meridionally-averaged winds over a constant pressure level (850 hPa), rather than wind shear across multiple pressure levels, as also used in other recent literature examples (Doubler et al., 2015; Yu et al., 2017). Tang et al. (2017) also used dynamically downscaled climate model outputs from a selection of CMIP3 GCMs from the NARCCAP archive, as opposed to the coarser, non-downscaled outputs used in Cook et al. (2008). Using wind speed projections over a historical (1970 to 2000) and future (2040 to 2070) model run period, forced by the SRES A2 emissions scenario, they found an average increase of 20% in nighttime LLJ frequency ($p < 0.1$) over Texas and Oklahoma. An LLJ speed increase of 0.5 to 1 m s^{-1} was also projected, though it lacked statistical significance. This study also linked changes of the LLJ's speed and frequency to the westward expansion and strengthening of the Bermuda High.

As mentioned earlier in this section, some studies have used climate models and reanalysis data to infer changes in the state of the LLJ based on its relationship with associated meteorological features. Barandiran et al. (2013) is a good example of such work, having used outputs from the NARR dataset from 1979 to 2012 to analyze precipitation patterns that have occurred over the Central Plains, subsequently relating them to changes in the LLJ's strength and position. Their results showed that the northward edge of the LLJ has gradually moved poleward, with these jets also becoming stronger over this period. This poleward shift has led to the South-Central Plains

experiencing up to 50% reductions in annual precipitation amounts during April, May, and June. The greatest monthly rainfall amounts also moved poleward with this shifting of the LLJ.

Work by Harding and Snyder (2014) conducted the same analysis using the outputs of two CMIP5 climate models (CMCC-CM and CNRM-CM5, dynamically downscaled by the Weather Research and Forecasting (WRF) model) out to the year 2100. This study is one of few about LLJ climatology that used climate model outputs more recent than those from the CMIP3 generation, with future runs forced by the Representative Concentration Pathway (RCP) 4.5 and 8.5 emissions scenarios (Riahi et al., 2011). Their results show the same trend of northward displacement and greater rainfall during spring months as in Barandiran et al. (2013), which were attributed in part to the expected strengthening of the LLJ.

The studies reviewed in this section suggest a strong consensus that the LLJ has become faster and more frequent in the last few decades, and that these trends are expected to continue. Changes in the methods used to evaluate and project LLJ climatology are also apparent, with a transition to using outputs from newer climate models (Harding and Snyder, 2014) as well as more specific criteria for determining an LLJ's presence at a certain point in time (Tang et al., 2017). Most importantly, given these LLJ projections, and the factors that are altering wind climatology over the South-Central Plains (see Section 2.1 and Section 2.2.1), these findings give credence to the changing state of the LLJ being a viable explanation for evolution of Oklahoma's wind energy resources.

2.3. Linking the Low-Level Jet to Oklahoma's Wind Energy Generation

This chapter has up to now considered projections of wind energy production in Oklahoma and state of the LLJ separately. Based on published literature, there does appear to be a precedent for

studying a physical connection between the two. For example, it has been seen that the LLJ is expected to experience an increase in speed and frequency in the coming decades, particularly during spring months (Cook et al., 2008; Barandiran et al., 2013; Tang et al., 2017). This finding is consistent with model-projected increases of wind speed/power density over Oklahoma in spring and summer (Stadler et al., 2015). However, proposing a climatological link between the LLJ and near-surface winds based on separate studies is not sufficient, especially when the studies in question used different methods.

Fortunately, there have been several studies that have specifically analyzed the link between the presence and features of LLJs and the capturing of energy using wind turbines. An observational study by Cosack et al. (2007) based in Northern Germany considered the validity of scaling near-surface wind speeds up to given turbine hub-heights, ranging from 85 to 130 meters, in the presence of an LLJ. Their results found that LLJs were associated with in an increase of wind turbine energy generation, as well as an increase in the generation's standard deviation. It was, however, conceded that basing hub-height wind speeds on upscaled near-surface winds is associated with errors in calculated energy generation of as much as 30%. This error is likely due to the questionable validity in using a logarithmic power law to upscale near-surface winds when an LLJ is present. Emeis (2014b) came to the same conclusion that the presence of the LLJ is able to influence wind energy generation, based on their analysis of two years of SODAR (SOund Detection And Ranging) observations of vertical wind profiles, also in Northern Germany. Both this study and Cosack et al. (2007) state that LLJs are favorable for wind energy generation because the decoupling of the atmosphere that occurs at night due to the removal of convection produces a surface layer that is on the order of 100 meters deep. The decoupling process is a consequence of the inversion layer that forms due to radiative cooling that permeates

the surface layer from the ground, thus separating this lowest layer from the Ekman layer above (Lampert et al., 2016). With the surface layer being around 100 meters deep, the blades of typical utility-scale wind turbines are frequently within the Ekman layer, thus exposing them to the LLJ's enhanced winds. This result is consistent with the basic LLJ theory discussed in Section 2.2.1 (Blackadar, 1957; Wexler, 1961; Shapiro and Fedorovich, 2010). Emeis (2014b) also states that there is an apparent limit to the extent of an LLJ's effects on wind shear, which can be seen in Figure 6. This result indicates that the wind shear below an LLJ cannot physically exceed approximately 0.08 s^{-1}, which means that there exists a critical limit to how much an increase in LLJ speed or frequency could influence the magnitude of wind energy generation.

As well as distinguishing the existence of a relationship between the LLJ and wind energy generation in observations, it is also of interest to characterize its nature. An important aspect of this relationship is the vertical wind profile below the LLJ core, since such profiles are commonly used to scale near-surface wind speed data to a given turbine hub-height in wind

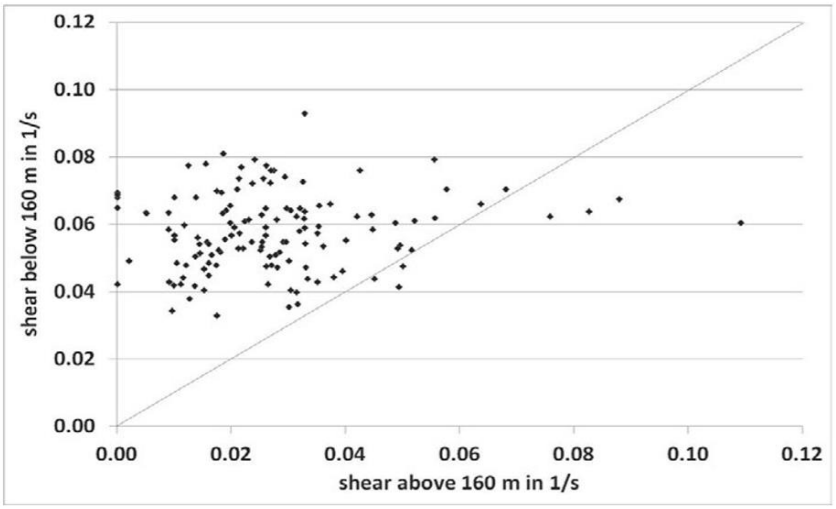

Figure 6: Comparison of mean vertical wind shear between 160 meters and the ground versus 160 meters and the jet core height (in s^{-1}) (Emeis, 2014b).

power density calculations. In many examples of research concerning wind energy, this scaling is achieved using the power law equation (Equation 1):

$$V(z_H) = V_r \left(\frac{z_H}{z_r}\right)^{\alpha} \quad \textbf{(1)}$$

Where $V(z_H)$ is the wind speed at hub-height, z_H, V_r is the wind speed at the reference height (z_r) at which data are obtained (typically 10 meters), and α is the exponent for the wind shear, which is typically given the value of 1/7 as an average for all atmospheric stability modes (Storm et al., 2009).

The power law has been observed to be invalid in observational studies of vertical wind profiles in the presence of an LLJ. Storm et al. (2009) came to this conclusion in their reanalysis of notable LLJ occurrences in the Central Plains. Their study attempted to recreate vertical wind profiles on two particular nights (that each featured an LLJ) using the WRF model, with 24-hour forecast runs conducted using different boundary layer and radiative transfer schemes. They came to the conclusion that WRF was much more capable at matching observations of wind speeds from the two occasions than extrapolations of near-surface wind speeds using the power law, with the latter significantly underestimating wind speed magnitudes. The value of α was also observed to be highly inconsistent, ranging in value from 0.2 to 0.45 in the course of one night. The consequent implication is that the power law is not able to accurately extrapolate wind speeds from a given measurement height in the presence of an LLJ, thus attesting to the LLJ's importance in influencing wind energy generation.

It follows that the lack of consistency in the value of α in an LLJ's presence results in vertical wind profiles that are not logarithmic at all. This conclusion is made from studies of wind speed measured by observational towers in Oklahoma by Greene et al. (2009), and also from studies of

lidar observations in Northern Germany by Lampert et al. (2016). Figure 7 gives an example of a typical wind profile when an LLJ presides over a given area. The profile itself is near-logarithmic closer to the surface, but is perfectly linear up the LLJ's wind speed maximum. As such, it can be argued that upscaling of near-surface winds to turbine hub-height is more accurately approximated by a linear relationship than the power law when considering wind speeds in the presence of an LLJ. An important caveat to the effect of LLJs on wind energy generation, however, is that non-logarithmic wind profiles can also be a consequence of synoptic scale weather systems in the vicinity (Emeis, 2014b; Lampert et al., 2016), since extratropical cyclones are also capable of generating LLJs (Djurić and Ladwig, 1983).

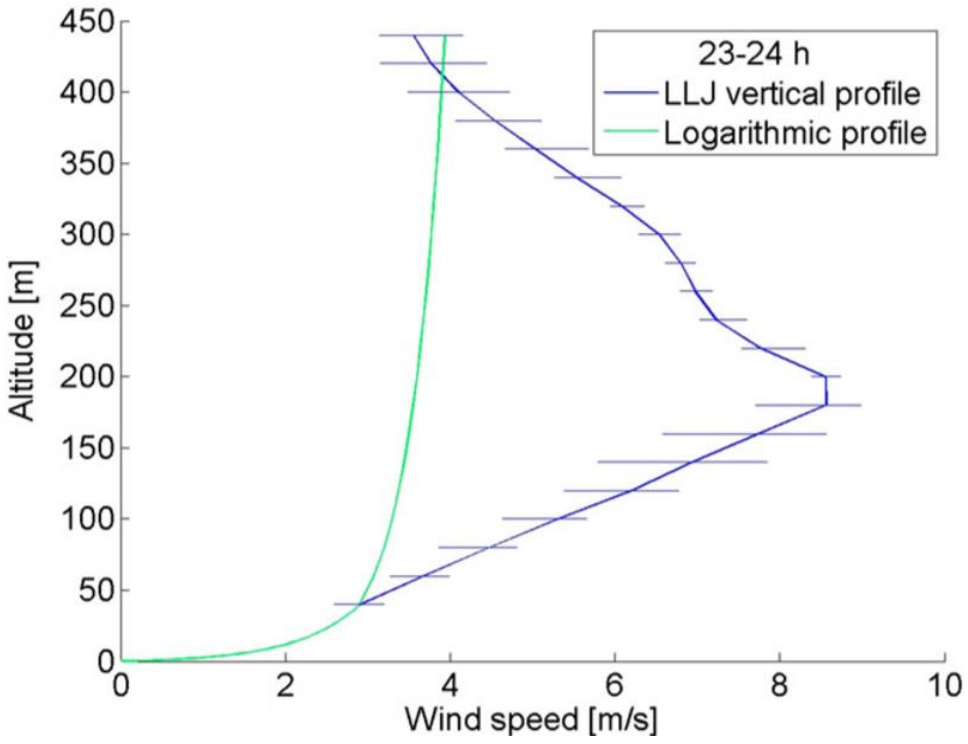

Figure 7: An example of a standard logarithmic wind profile and the wind profile associated with the presence of an LLJ, derived from one hour of lidar observations from December 13th 2013 (Lampert et al., 2016).

Overall, it is clear that the LLJ has notable effects on wind speeds between the jet-core height and the surface, such as by increasing wind speeds and also by modifying the vertical distribution of these winds, such that they cease to be logarithmic. Given the apparent strength of the link between the state of the LLJ and wind energy generation, as well as the projections of LLJ changes in the coming decades (see Section 2.2.2), it can be hypothesized that changes in the LLJ's speed, height, and frequency could feasibly explain projected changes in Oklahoma's wind energy resources.

Chapter 3: Data and Methods

3.1. Data Sources

Much of the research that has been conducted in this field of study, especially that into projected changes of wind energy resources across the United States, has been conducted using outputs from Third Generation climate models, i.e. CMIP3 models (Meehl et al., 2007). Several recently conducted studies, such as Stadler et al. (2015), Johnson and Erhardt (2016), and Tang et al. (2017) used dynamically downscaled outputs from them, which were accessed through NARCCAP (NARCCAP, 2012). The current study, however, is interested in using the more recently available climate models and climate change emissions scenarios under CMIP5 (Taylor et al., 2012), and the more recent Sixth Generation of climate model outputs, CMIP6 (Eyring et al., 2016). Since many climate research institutes contributing to CMIP6 had not made outputs of wind speed available at the time of the current study, outputs from a collection of CMIP5 GCMs have been enlisted instead.

Table 1 lists the names and grid resolutions (in decimal degrees) of the six CMIP5 GCMs from which wind speed outputs were used. The outputs from these GCMs were sourced from the National Weather Center's open access server, therefore limiting the current study to using outputs with a complete and robust data record. It is also important to consider that all of these GCMs have been shown to possess documented biases in relation to the LLJ. Harding et al. (2013) considered the ability of an ensemble of CMIP5 GCMs to resolve the historical mean and standard deviation of the jet's summertime speed and location when compared to NARR reanalysis outputs. Their use of z-scores to assess the difference between the GCMs and NARR data indicated that their multi-model ensemble was effective in simulating the mean and standard

deviation of these LLJ features. They also found that GFDL-ESM2M simulated the LLJ's summertime historical speed and location the most accurately of the six GCMs enlisted in the current study, with the other five GCMs exhibiting larger amounts of bias.

Danco and Martin (2017) also found that these GCMs possess notable amounts of bias in simulating the LLJ when comparing their outputs to reanalysis datasets compiled by the European Centre for Medium-Range Weather Forecasting (ECMWF) and the Twentieth Century Reanalysis (20CR) dataset. They found that all of these GCMs (except for ACCESS 1.0, which was not included in this work), underestimate the LLJ's springtime speed to varying degrees, with only HadGEM2-ES overestimating its historical summertime speed. Nevertheless, their results showed that whilst these GCMs do slightly underestimate the speed of LLJs, they quite successfully simulate their annual frequency and daily time of occurrence.

Kulkarni and Huang (2014) also noted in their study of projected changes of wind speed across the United States that IPSL GCMs from the CMIP5 generation (such as the one used in the

Model Name	Latitudinal Resolution	Longitudinal Resolution	Reference
ACCESS 1.0	1.25	1.875	Collier and Uhe (2012)
GFDL-CM3	2	2.5	Donner et al. (2011)
GFDL-ESM2G	2.0225	2.5	Donner et al. (2011)
GFDL-ESM2M	2.0225	2.5	Donner et al. (2011)
HadGEM2-ES	1.25	1.875	Jones et al. (2011)
IPSL-CM5A-MR	1.2676	2.5	Dufresne et al. (2013)

Table 1: Names, grid resolutions (in decimal degrees), and references for the climate models enlisted in the current study.

current study) have a tendency to underestimate the LLJ's general occurrences. Since the GCM outputs enlisted in the current study have not been bias-corrected for over/underestimation of wind speeds on different timescales, it is important to be mindful of these known biases moving forward, since they can affect the interpretation of this study's results. It should also be clarified that the current study has not enlisted reanalysis data to examine the biases of these GCMs in simulations historical LLJ characteristics or near-surface wind energy metrics, since these aforementioned studies have already identified them.

The data from each model's output consist of six-hourly wind speeds across each model's atmospheric height levels. These outputs are given in Coordinated Universal Time (UTC - 00Z, 06Z, 12Z, and 18Z), placing them six hours ahead of Central Standard Time (CST) over the South-Central Plains region (e.g. outputs at 12Z are those for 6am CST). The future runs of these climate models were forced by the RCP 8.5 emissions scenario – a high-emissions "business as usual" scenario for projections of climate change (Riahi et al., 2011). Other RCP scenarios have not been enlisted in the current study due to data limitations, the implications of which are discussed in Section 6.2.

Studies that enlist climate model outputs typically consider a data period of 30 years, in order to account for the periodicity of Earth's longest natural climate variability cycles, as defined by the World Meteorological Organization (World Meteorological Organization, 2011) and used in much of the literature (Greene et al., 2012; Holt and Wung, 2012; Doubler et al., 2015). Wind speed data were instead extracted from historical (1981 to 2005), and future (two periods of extraction are used – near future (2035 to 2059) and far future (2075 to 2099) – in order to assess mid-Century and end-of-Century projections) runs of each of the six models over a data period of 25 years per time frame, rather than 30 years. This model run period was used to match the

number of years of available Oklahoma Mesonet data – the source of observations used in the current study. The use of 25 years of Mesonet data to conduct analysis in this study has the caveat of being short of the recommended 30-year climatological period (World Meteorological Organization, 2011) by five years. However, similar studies of future changes of wind energy resources have also not used 30 years of data as their climatological period, such as Pryor and Barthelmie (2011).

The Oklahoma Panhandle and segments of the states surrounding it have been selected as the spatial domain for the current study, as illustrated in Figure 8. This location has been selected for two reasons:

1. As discussed in Section 2.2.1, the South-Central Plains region experiences the greatest southerly LLJ frequency of any location in the contiguous United States, especially over the state

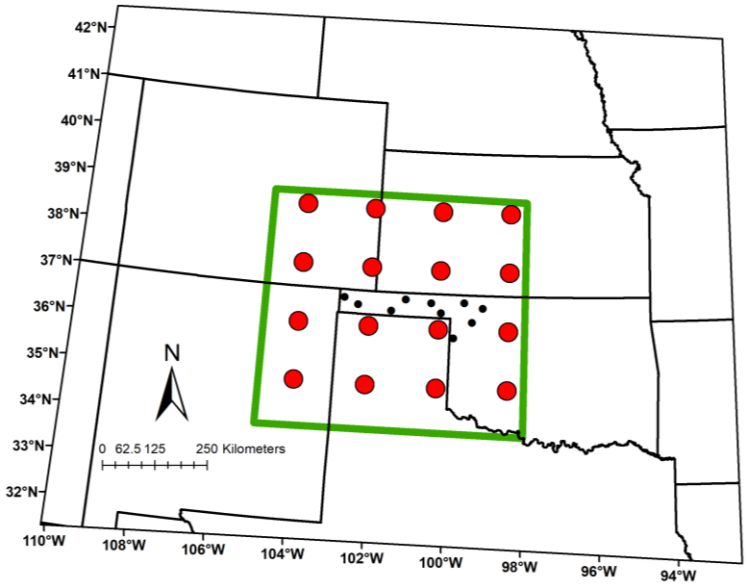

Figure 8: The spatial domain of the current study.
- The green box indicates the bounds of the South-Central Plains region, within which grid points (red dots, the example being the grid resolution of ACCESS 1.0) of the selected climate models are studied for LLJ occurrences. The black dots show the locations of the 10 Oklahoma Mesonet stations used in the current study, many of which fall within the Oklahoma Panhandle.

of Oklahoma (Doubler et al., 2015). Furthermore, the Oklahoma Panhandle was identified by Johnson and Erhardt (2016) as a specific location where increases of near-surface wind speeds are expected to take place.

2. As discussed in Section 1.1, Oklahoma's wind energy industry has grown quickly in the last 15 years, and much of its greatest wind energy resources exist within the Oklahoma Panhandle (WINDExchange, 2018b). There has also been previous interest in developing wind energy capacity in this area, such as the Wind Catcher Energy Connection Project, which was expected to have produced the largest (by capacity) wind farm in the United States (American Electric Power, 2018). Despite the project being cancelled for political reasons in July 2018, it still attests to the interest in developing wind energy capacity in the Oklahoma Panhandle.

Figure 8 illustrates that the Oklahoma Panhandle (black dotted box) is a relatively fine-scale geographical location, when considering that its approximate size is 3° longitude x 0.5° latitude – a resolution that is too fine for some of GCMs used in the current study to capture. Since the provided climate model outputs have been neither statistically nor dynamically downscaled, observational outputs from the Oklahoma Mesonet were enlisted in order to capture the high-resolution wind energy resource climatology necessary for this domain of study.

The Oklahoma Mesonet network is a collection of more than 110 weather observation sites across the state of Oklahoma, with the objectives of creating a quality-assured database that is as representative of Oklahoma weather and climate as possible, and by extension affording the creation of products and information dissemination for customers (Brock et al., 1995; McPherson et al., 2007). Ten of these Mesonet sites (excluding Eva, a new station with an observation record that is too short for use in the current study) are contained within the black dotted box shown in Figure 8, from which 10-meter average wind speed data were extracted for the purpose of this

study (Mesonet, 2018). Table 2 details the names and locations of the 10 Oklahoma Mesonet stations enlisted in the current study. Stations in other nearby states, such as Texas, have not been included because their observational records are too short.

The Mesonet's wind speed data possess a temporal resolution of five minutes, with data records taken from January 1st 1994 (when the Mesonet began regular weather observations) to December 31st 2018 – a 25-year time period (as mentioned previously when discussing the years of climate model outputs enlisted). With such a high temporal and spatial resolution, these observations are able to successfully simulate the climatology of wind energy resources in the Oklahoma Panhandle. However, obtaining an accurate representation of this climatology

Name (Mesonet Abbreviation)	Location (degrees N, degrees W)
Arnett (ARNE)	36.07N, -99.90W
Beaver (BEAV)	36.80N, -100.53W
Boise City (BOIS)	36.70N, -102.50W
Buffalo (BUFF)	36.83N, -99.64W
Freedom (FREE)	36.72N, -99.14W
Goodwell (GOOD)	36.60N, -101.60W
Hooker (HOOK)	36.86N, -101.23W
Kenton (KENT)	36.82N, -102.88W
Slapout (SLAP)	36.60N, -100.26W
Woodward (WOOD)	36.42N, -99.41W

Table 2: Names and locations of the 10 Oklahoma Mesonet stations that are enlisted in the current study.
- Latitudes and longitudes are given to 2 decimal places, with information being sourced from Mesonet (2018).

depends on adequate quality assurance in collecting and preparing the Mesonet observations. Fiebrich et al. (2010) provides details of recommended quality assurance procedures for preparation of mesoscale meteorological datasets, many of which are utilized by the Oklahoma Mesonet. These procedures include adequate station siting, archiving and flagging of collected observations when needed, and wind speed-specific procedures such as testing observations at different heights to better identify incorrect wind speed measurements.

Data from the Oklahoma Mesonet were enlisted in the current study to statistically downscale the outputs of the six GCMs listed in Table 1 to a finer resolution, so that a set of future "pseudo-observations" could be created using the Mesonet data and the projections of these GCMs. The resulting high-resolution values afforded assessment of wind energy metrics over the Oklahoma Panhandle – a region too small for most of the GCMs enlisted in the current study to resolve without prior downscaling.

A climatological delta method (henceforth referred to as the "delta method") was selected as the method for downscaling the outputs of these GCMs onto the Oklahoma Mesonet data. The delta method is the practice of downscaling climate model outputs to produce projections of a higher-resolution set of values by adding/multiplying the projected change from a GCM to the historical observations of the same set of data (Walsh et al., 2018). In the case of the current study, the factor changes (or "delta") in annual median near-surface wind speed projected by each GCM (averaged across all grid points in the South-Central Plains region defined in Figure 8) were applied to the observations at each Mesonet location in the Oklahoma Panhandle. The delta method has been used to statistically downscale climate model outputs in several literature examples, hence its use in the current study, most frequently for outputs of temperature and precipitation (Déqué, 2007; Maraun et al., 2010; Pourmokhtarian et al., 2016). Wind speed,

however, has not been statistically downscaled frequently using the delta method. Cox et al. (2015) decided in their examination of climatological heating and cooling demands for buildings that statistically downscaled wind speeds were not important enough to consider, and although Eames et al. (2012) did consider such wind speeds, they were not generated using the delta method. Nevertheless, the pseudo-observations of future wind speed produced in the current study have the same temporal and spatial coverage as the historical (1994 to 2018) Mesonet data, and thus constitute high-resolution values for comparison against historical observations.

Different sets of pseudo-observations resulted from different combinations of GCM used and future time frame (near future versus far future) considered in calculating factor changes (multiplicative differences of wind speed between time frames) using the delta method. Furthermore, these factor changes were broken down seasonally and diurnally, since the LLJ is known to have well-defined seasonal and diurnal cycles (Doubler et al., 2015), and an interest of this study is evaluating the relationship between LLJ characteristics and wind energy metrics. Discussion of assumptions when calculating these factor changes, and the validity of these pseudo-observations is discussed in Section 3.3.2.

3.2.Defining Wind Energy Metrics

As mentioned in Section 1.2, the current study uses multiple metrics for the projection of changes in Oklahoma's wind energy resources. Six such metrics, all commonly used by the wind industry, have been selected based on their ability to quantify features of a wind turbine's productivity, as well as their relevance in long-term planning for future wind farm installations.

3.2.1. Wind Power Density

Wind power density (henceforth referred to as WPD) describes the potential for capturing energy for electricity production. WPD's usefulness is its ability to approximate the potential available resource for transforming kinetic energy in the wind into electrical energy using wind turbines. A projected increase of wind speed (and by extension WPD) based on climate model outputs means greater potential wind energy capture, therefore enhancing prospects for wind energy's ability to meet the demands of future generations. Multiple research examples (Pryor and Barthelmie, 2011; Greene et al., 2012; Stadler et al., 2015) have used WPD calculations to transform climate model outputs of wind speed over a given area and time into a quantity that has more significance for wind energy generation. This is achieved using Equation 2:

$$WPD = \frac{1}{2}\rho(z_H)V(z_H)^3 \quad \textbf{(2)}$$

Where *WPD* has units of W m^{-2}, $\rho(z_H)$ is the air density at wind turbine hub-height, z_H, in kg m^{-3}, and $V(z_H)$ is the wind speed at hub-height in m s^{-1}. Conducting this calculation thus requires selecting a hub height at which to determine wind speed and air density. For example, prior to the Wind Catcher Energy Connection Project's cancellation in July 2018 (American Electric Power, 2018), the project's intention was to enlist 800 2.5 Megawatt General Electric (GE) wind turbines, each with a hub-height of 110 meters. Thus, z_H is equal to 110 m in the current study. As for air density, given that the average height above sea level of the Oklahoma Panhandle ranges from approximately 500 meters to the east and 1300 meters to the west, the value of $\rho(z_H)$ ranges from 1.03 to 1.13 kg m^{-3} (Engineering Toolbox, 2003) which has been averaged to 1.08 kg m^{-3} for simplicity. Since Equation 2 states that WPD is proportional to the cube of the wind speed and to half of the air density, inaccuracy in the value of air density for

each of the 10 Mesonet locations in the study region should not notably affect the calculated values of WPD, relative to an inaccurate value of wind speed.

Calculations of $V(z_H)$ are typically conducted by extrapolating near-surface wind speeds from observations (Emeis, 2014b; Lampert et al., 2016) or model outputs (Storm et al., 2009; Johnson and Erhardt, 2016) to a given wind turbine hub-height, traditionally done so using the power law (Equation 1). However, as discussed in Section 2.3, Equation 1 is invalid when the LLJ is present, because of its existence being associated with surface to jet-core wind profiles that are near-linear rather than logarithmic (Lampert et al., 2016). Multiple studies have also either directly (Pichugina et al., 2016) or indirectly (Baas et al., 2009; Kallistratova et al., 2013; Guiterrez et al., 2017) provided confirmation that the vertical wind profile below a low-level jet has a linear shape. There is currently no established formula for extrapolating near-surface wind speeds to a given hub-height in this circumstance. Such a formula's derivation would require an in-depth analysis of empirical wind profile formulations in the LLJ's presence, which goes beyond the scope of this study. As such, results from the cited literature have been used to approximate a linear equation that can used to obtain more accurate hub-height wind speeds when the LLJ is present. The proposed equation is shown below as Equation 3:

$$V(z_H) = V(z_r) + 0.05z_H \quad \textbf{(3)}$$

Where $V(z_H)$ is the wind speed at hub-height, z_H, $V(z_r)$ is the wind speed at the height of the model output, z_r (equal to 10 meters, the height at which the Oklahoma Mesonet records wind speeds), and 0.05 (in s^{-1}) is the coefficient that represents the linear increase of wind speed with height from the surface to the LLJ's core. It must be stressed that this equation does not hold when the LLJ is absent, or when considering heights above the LLJ's core. The value of 0.05 s^{-1} has been obtained by approximating the surface to jet-core gradient presented in results such as

from Lampert et al. (2016) (see Figure 7 of the current study), as well as results from Baas et al. (2009), Kallistratova et al. (2013), Pichugina et al. (2016), and Guiterrez et al. (2017). In circumstances where the LLJ is indeed absent, Equation 1 is used instead.

The changes of annual median wind speed and WPD (broken down diurnally, seasonally, and by time frame – as discussed in Section 3.1) between the historical and future Mesonet values are used as two of the wind energy metrics in this study.

3.2.2. Wind Speeds Below Cut-In and Above Cut-Out Thresholds

Cut-in and cut-out wind speed (henceforth referred to as V_{in} and V_{out} respectively) are the two wind speeds that signify the range within which the blades of wind turbines are permitted to rotate. Their respective purposes are to prevent turbine blades from being rotated only by a wind turbine's generator, and to prevent turbine damage in high winds (Abdullah et al., 2012). V_{in} and V_{out} are consequently important for protecting wind turbine investments and reducing the need for maintenance. Most importantly, these two thresholds place upper and lower bounds on the amount of electricity that wind turbines can generate in a given time. These thresholds allow for assessment of climatological significance because if model-projected wind speed changes are overall reductions, increases in frequency of winds below V_{in} could occur, therefore decreasing the amount of extractable wind energy.

Manufacturers of wind turbines assign V_{in} and V_{out} to their products based on the minimum wind speed required to rotate their turbines' blades (V_{in}) and the maximum wind speed at which their blades can rotate without resulting in mechanical damage (V_{out}), such as damage to the gearbox or the blades themselves. These values are typically within the range of 2.5-3.5 m s^{-1} for V_{in}, and 20-25 m s^{-1} for V_{out} (Mabel and Fernandez, 2007). Indeed, the 2.5 Megawatt GE wind turbine

model enlisted for this study possesses manufacturing specifications with V_{in} and V_{out} values in these ranges, being 3 m s^{-1} and 25 m s^{-1} respectively (Wind Turbine Models, 2014). By using the power curve characteristics of a specific wind turbine model in this way, it becomes possible to evaluate how much of an available wind energy resource can feasibly be transformed into electrical energy. As such, determination of wind speeds being between V_{in} and V_{out} provides essential context to the WPD values calculated from Equations 2 and 3, since the mechanical limitations of wind turbines permit energy to be generated between specific values of $V(z_H)$. This method is consistent with approaches in studies of wind energy resource projections based on a specific wind turbine model, such as Greene et al. (2012) and Stadler et al. (2015).

In projecting changes of Oklahoma's wind energy resources, the interest is in the changing frequency of wind speeds being below V_{in} and above V_{out} between a historical and future model run, based on five-minute observations from data at each Mesonet location. The observation of hub-height wind speed being below 3 m s^{-1} at a particular Mesonet location is counted as a "below cut-in" event, with an "above cut-out" event being counted if the wind speed is above 25 m s^{-1}. The annual V_{in} and V_{out} frequencies (again broken down diurnally, seasonally, and by time frame) obtained from the historical and future Mesonet data are another two metrics used in the current study to evaluate significant changes in their occurrence in relation to the changing state of the LLJ.

3.2.3. Ramp Up and Ramp Down Events

Ramp events are defined as "a large variation in wind power output that is observed on a wind farm (or in a portfolio) within a short period of time (up to a few hours)" (Gallego et al., 2014). Prediction of ramp events is a challenge for the wind energy industry, because their erratic nature can result in intermittent electricity supply, thus making the distribution of electricity to meet

demand difficult for grid managers (Zhang et al., 2017). Consequently, if Oklahoma's future wind speeds were to become more variable resulting from potential influences such as faster and/or more frequent LLJs, the consequence could be more ramp events and greater difficulties for grid managers controlling electricity supply.

A ramp event can be described in terms of a change in capacity factor – a percentage quantification of a wind turbine's power output (Boccard, 2009). For example, a GE 2.5 Megawatt (MW) wind turbine (Wind Turbine Models, 2014) operating at a capacity factor of 50% produces 1.25 MW of power, i.e. half of its maximum output. Figure 9 is a graphical example of how ramp up and ramp down events look when plotting a wind turbine's capacity factor against time – rapid changes in capacity factor within the maximum allotted time constitute a ramp event.

However, one of the common disagreements with analyzing ramp event occurrences is the change in capacity factor that must occur in a given amount of time in order to declare that a ramp event has occurred. Whereas Bradford et al. (2010) and Kamath (2011) examined ramp

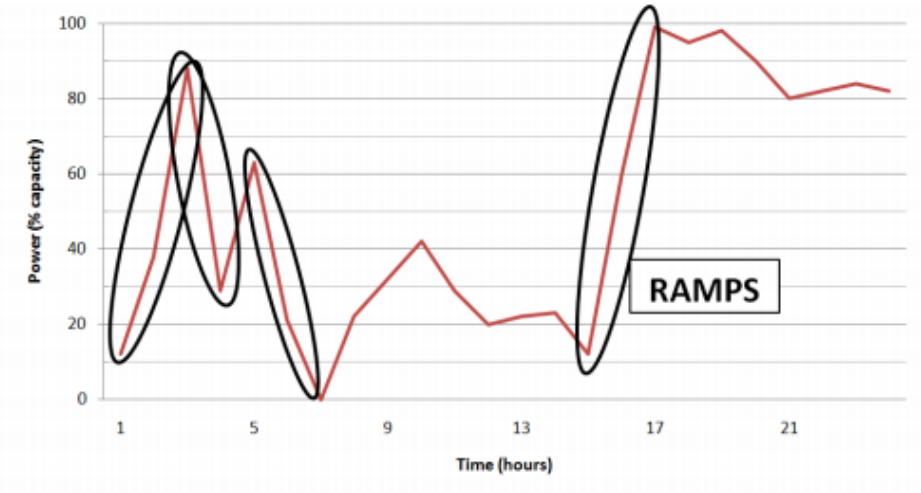

Figure 9: Example of what ramp events look like (black circles) on a plot of wind turbine capacity factor (%) against time (hours) (Ferreria et al., 2010).

events by considering turbine capacity factor increases or decreases of at least 20% in one hour, work by Greaves et al. (2009) and Ferreira et al. (2010) both use the definition of at least 50% in four hours or less. Since ramp events are able to take place over a matter of minutes, and high-resolution information is typically more useful to grid managers (Ela and Kemper 2009), the ramp event criteria used in Bradford et al. (2010) and Kamath (2011) is used in the current study.

Obtaining capacity factors from wind speed outputs depends on having knowledge of how much power the GE 2.5 MW wind turbine produces at different wind speeds. Ramp event occurrences can thus be determined by creating a polynomial expression for this wind turbine's power curve (Figure 10), which relates $V(z_H)$ to the turbine's power output in Watts. Since power output is proportional to the cube of the wind speed, the plot in Figure 10 can be expressed as a cubic polynomial. The approximate polynomial equation derived from this plot is shown below as Equation 4, using the same formulaic construction as in Stadler et al. (2015):

$$P = -9.3549\,V(z_H)^3 + 201.83\,V(z_H)^2 - 984.02\,V(z_H) + 1412.5 \quad \textbf{(4)}$$

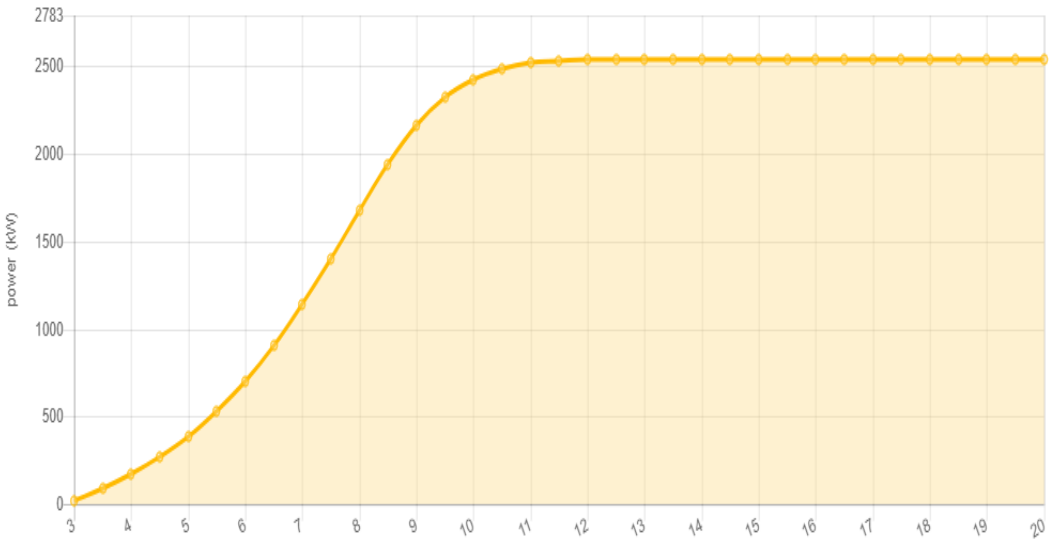

Figure 10: Power curve for a GE 2.5 – 120 wind turbine (Wind Turbine Models, 2014).

Where P is power output in W, and the numbers in front of each $V(z_H)$ term are coefficients of the polynomial equation. It is important to remember that a wind turbine does not produce power at wind speeds below V_{in} or above V_{out} (see Section 3.3.2), meaning that P is taken to equal 0 when the hub-height level winds at a location and point in time are below cut-in or above cut-out speed.

Having calculated the power output associated with a particular value of $V(z_H)$, the capacity factor can then be calculated by expressing P as a fraction of the maximum power output, P_{max} (2.5 MW for this particular wind turbine model), as shown in Equation 5 below:

$$Capacity\ Factor(\%) = \frac{P}{P_{max}} * 100 \quad \textbf{(5)}$$

The existence of a ramp up (down) event is then determined based on whether a capacity factor change of at least 20% occurs in an hour or less of wind speed observations at a Mesonet location. By contrasting the change in annual frequency (again broken down diurnally, seasonally, and by time frame) of ramp events between the historical and future time frame at all Mesonet stations, deductions can be made about projected changes in the consistency of extractable wind energy. Ramp up and ramp down frequency thus serve as the final two wind energy metrics in the current study. These metrics supplement the changes in magnitude provided by WPD/wind speed, and enhance the consistency of the wind energy resource detailed by cut-in/cut-out frequency calculations.

3.3. Methods Used

This section describes the theories and statistical approaches that shall be used in order to analyze the data discussed in Section 3.1, and to consequently evaluate these data using the wind energy metrics discussed in Section 3.2.

3.3.1. Updating LLJ Projections

It was highlighted in Section 3.1 that many of the previous studies into projected changes of the LLJ's state and wind energy resources over the South-Central Plains have been conducted using climate model outputs from the CMIP3 generation (Stadler et al., 2015; Johnson and Erhardt, 2016; Tang et al., 2017). Whilst there have been some studies that have used CMIP5 climate model outputs to analyze wind climatology, these studies did not encompass the objectives of the current study, whether due to enlisting GCMs not used by the current study or too small a number of them (Harding and Snyder, 2014; Kulkarni and Huang, 2014), focusing only on the LLJ's historical state (Harding et al., 2013; Danco and Martin, 2017), or examining wind climatology without a specific focus on the United States (Karnauskas et al., 2018). Much projected wind climatology research that enlisted outputs of CMIP5 climate models has been focused on Europe, such as Zappa et al. (2013), Tobin et al. (2016), and Carvalho et al. (2017). Finally, there is a significant lack of studies that have considered climatological changes of LLJ height, or wind energy resource evolution in terms of metrics besides wind speed or wind power density. As such, the lack of studies applying more recent generations of GCMs to the United States along with this combination of LLJ characteristics and wind energy metrics makes updates to their projections in the current study's context essential before assessing any linkage between them.

The first task was to use the wind speed outputs from each of the six GCMs (see Table 1) to create vertical wind profiles in the historical, near future, and far future time frames (time frame lengths are specified in Section 3.1) for each model's grid points encased within the South-Central Plains region (the green box of Figure 8). Within the three time frames, the existence of an LLJ at each grid point was determined in the six-hourly time step of each model. The LLJ

definition used was the same as that by Doubler et al. (2015) and Yu et al. (2017) in their studies of LLJ climatology, which reads as follows: “wind direction from 113° to 247° (southerly winds throughout the profile), a wind speed maximum ≥ 12 m s^{-1} at or below 3000 m above ground level (AGL), a decreasing wind speed by ≥ 6 m s^{-1} above the maximum wind level to the minimum or to 5000 m AGL (whichever is lower), and a decreasing wind speed by ≥ 6 m s^{-1} below the maximum wind level” (Yu et al., 2017, page III). This definition therefore requires knowledge of wind speeds at multiple height levels. Different models tend to have different numbers of atmospheric layers between two given heights of the atmosphere, which can result in some models more effectively resolving the existence of LLJs than others.

From applying this definition and determining LLJ occurrences, LLJ annual frequency and annual median speed and height within each time frame were calculated. The median was used as the measure of central tendency in all time frames of the current study, due to probability density functions (PDFs) of wind speed tending to be right skewed, thus making other central tendency metrics, such as the mean, inappropriate (Greene et al., 2012).

The calculations and projections of the three LLJ characteristics were broken down by time of day (00Z, 06Z, 12Z, 18Z), season, and the model used in order to identify output differences and diurnal and seasonal trends in LLJ projections, much like the approach taken by Doubler et al. (2015) and Tang et al. (2017). LLJ height was determined from vertical profiles constructed from each GCM’s discrete height levels (which ranged in number from 12 to 16 between the surface and 3000 m AGL). Due to differences in vertical model resolution and the fact that some of the models, such as the GFDL models, enlisted hybrid sigma-pressure (a definition of height levels based on proximity to the ground, which transitions to an isobaric definition further away from

the surface) to define each vertical level, changes in annual median height were instead expressed as a change in height level, rather than height in meters.

The results from the LLJ projections were presented spatially for individual grid points, using the spatial convention presented in Figure 8, where each grid point's size and color corresponds to the sign and magnitude of the change in LLJ frequency, speed, or height. In order to gauge changes in central tendency and variability of these LLJ characteristics, tables showing percentage changes and boxplots that illustrate the spread of the annual values of these characteristics were also created. Each boxplot and each line of the tables combined the projected changes in LLJ characteristics across all grid points, which is consistent with the methods of work such as Doubler et al. (2015).

Given the spatial nature of these projections of LLJ characteristics and the non-parametric nature of wind speed data, statistically significant changes ($p < 0.05$) for the maps, percentage tables, and boxplots were assessed by conducting Mann-Whitney U-tests. These tests were conducted by using rankings of annual historical LLJ characteristics versus their respective annual near future/far future characteristics, with each pair of ranks existing for a particular season, time of day, and model time frame (e.g., historical annual LLJ frequency for Spring 00Z versus far future annual LLJ frequency for Spring 00Z, both of which calculated from the HadGEM2-ES model). Each ranked group consisted of the LLJ characteristic in question grouped across all grid points that a given model possessed within the South-Central Plains region. Mann-Whitney U-tests have been applied to spatial data in this manner in previous studies, such as in work by Baidya Roy and Traiteur (2010) in their analysis of wind turbines' effects on local temperature climatology. The overall intention of this data presentation and analysis of statistical significance is to determine whether climate model projections of LLJ features found in previous studies with

older generations of climate models, such as Cook et al. (2008) and Tang et al. (2017), are still valid or have perhaps changed.

3.3.2. Updating Projections of Oklahoma's Wind Energy Resources

Section 3.1 described the application of the delta method (Déqué, 2007) to statistically downscale the GCMs' annual median near-surface wind speed projections onto the higher-resolution Oklahoma Mesonet locations (Mesonet, 2018) over the Oklahoma Panhandle. In this case, "near-surface" wind speed refer to that at the lowest height level of each model. These factor changes obtained from using the delta method were averaged across each GCM's grid points that fell within the South-Central Plains region (Figure 8), with factor change calculations broken down by future time frame being considered, by season, and by time of day (as in Section 3.3.1). Applying the factor changes projected by these six GCMs to all 10 Mesonet locations (see Table 2) results in multiple sets of future pseudo-observations, the calculation for which is shown below as Equation 6:

$$V_{future} = F * V_{historical} \quad \textbf{(6)}$$

Where $V_{historical}$ is a historical Mesonet of wind speed for a given 5-minute time period and Mesonet location, F is the multiplicative factor change of near-surface annual median wind speed between time frames of a GCM's output (with this factor change being for a particular combination of time frames (i.e. historical and near future/far future), season, and time of day), and V_{future} is the pseudo-observation that is produced from applying the factor change to the historical wind speed observation. These future and historical values were then used to compute projected changes in the wind energy metrics discussed in Section 3.2, therefore producing the

projections in Oklahoma's wind energy resources that were sought at the beginning of the current study.

The delta method's advantage when statistically downscaling climate model outputs onto observations (such as those of the Oklahoma Mesonet) is its ability to implicitly bias-correct climate model projections (Walsh et al., 2018). However, the delta method is not able to correct the bias in climate model outputs within separate time frames. Such bias correction is sometimes done by quantile-mapping an observed variable (in this case near-surface wind speed from the Oklahoma Mesonet) against the model outputs of the same variable. This mapping is subsequently used to adjust the model outputs for biases that are identified (Maraun et al., 2010). Although such mapping was not performed here, the biases that these six GCMs possess have been examined in previous work (see Section 3.1), meaning that the results of the current study can still be evaluated against knowledge of these biases.

Another assumption of this approach is that the variability of the near-surface wind speeds in the historical and future time frames are similar (if not the same) (Déqué, 2007). An additive/multiplicative factor change only accounts for changes in the position of PDFs of measured wind speeds, not their shape (Pourmokhtarian et al., 2016). Multiple studies have argued for the PDF of measured wind speeds possessing a right-skewed Weibull distribution, which also persists in future time frames of climate model outputs (Pryor et al., 2005; Altunkaynak et al., 2012). Furthermore, studies of projected changes in wind speed variability across the United States, such as Goddard et al. (2015), have found that the variability of near-surface winds across the United States (especially diurnal variability) might not change as much in future decades as their magnitude.

It is, however, necessary to construct PDFs of each GCM's near-surface wind speed outputs over the historical, near future, and far future time frames in order to validate this assumption of no change in wind speed variability. Figure 11 presents the PDFs constructed from these data, such that each PDF consists of 25 years of six-hourly wind speed outputs from all grid points that each GCM possesses within the South-Central Plains region (Figure 8). Two descriptive statistics have been included for each PDF. The first of these is the interquartile range, the difference between the 75th and 25th percentile of a distribution of data (Yuan 1999; Riaz, 2013). The interquartile range is a more appropriate measure of variability than standard deviation given

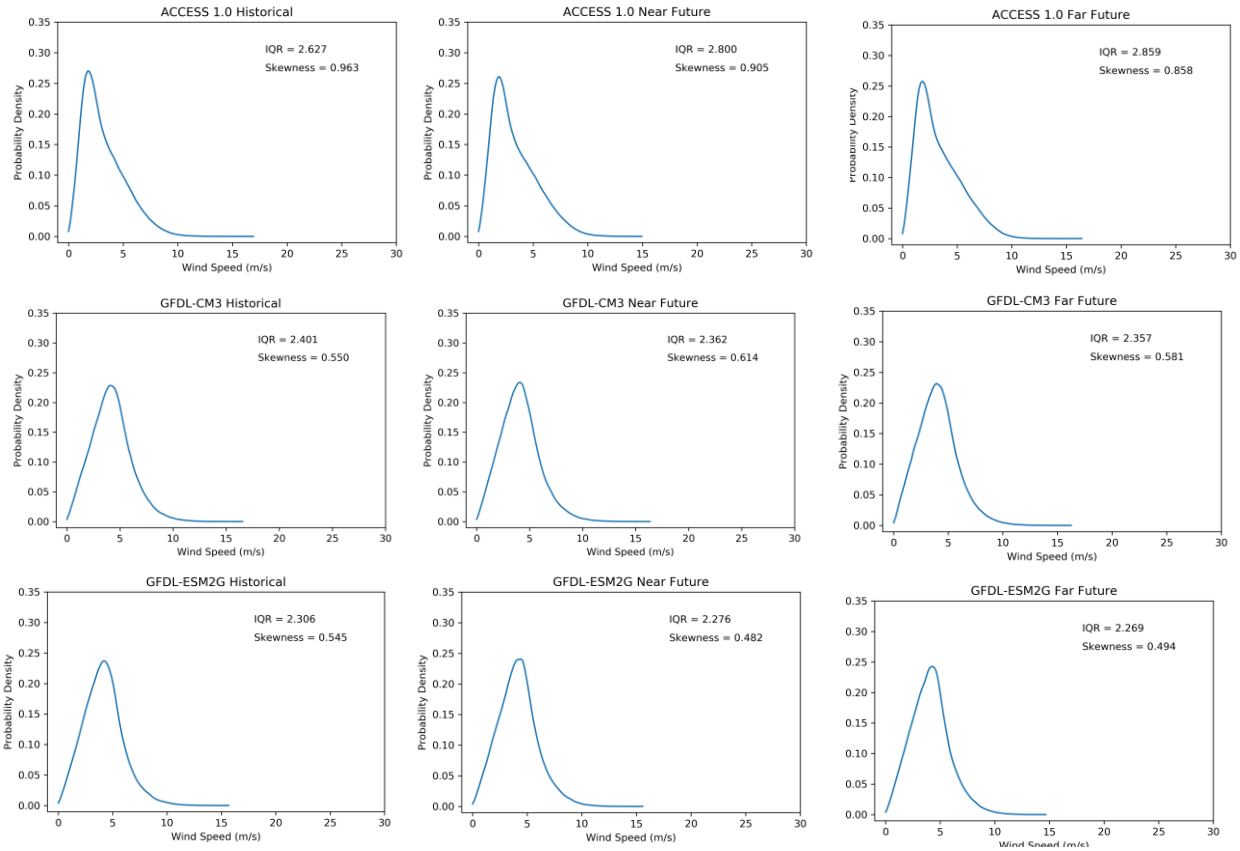

Figure 11: Probability density functions of six-hourly near-surface wind speed from all enlisted GCMs.
- Each function consists of all wind speed outputs from a given time frame (historical, near future, or far future) for each GCM. Values of interquartile range (IQR) and skewness are given for each function. This first half of the figure contains the functions of the following GCMs: ACCESS 1.0 (top row), GFDL-CM3 (middle row), and GFDL-ESM2G (bottom row).

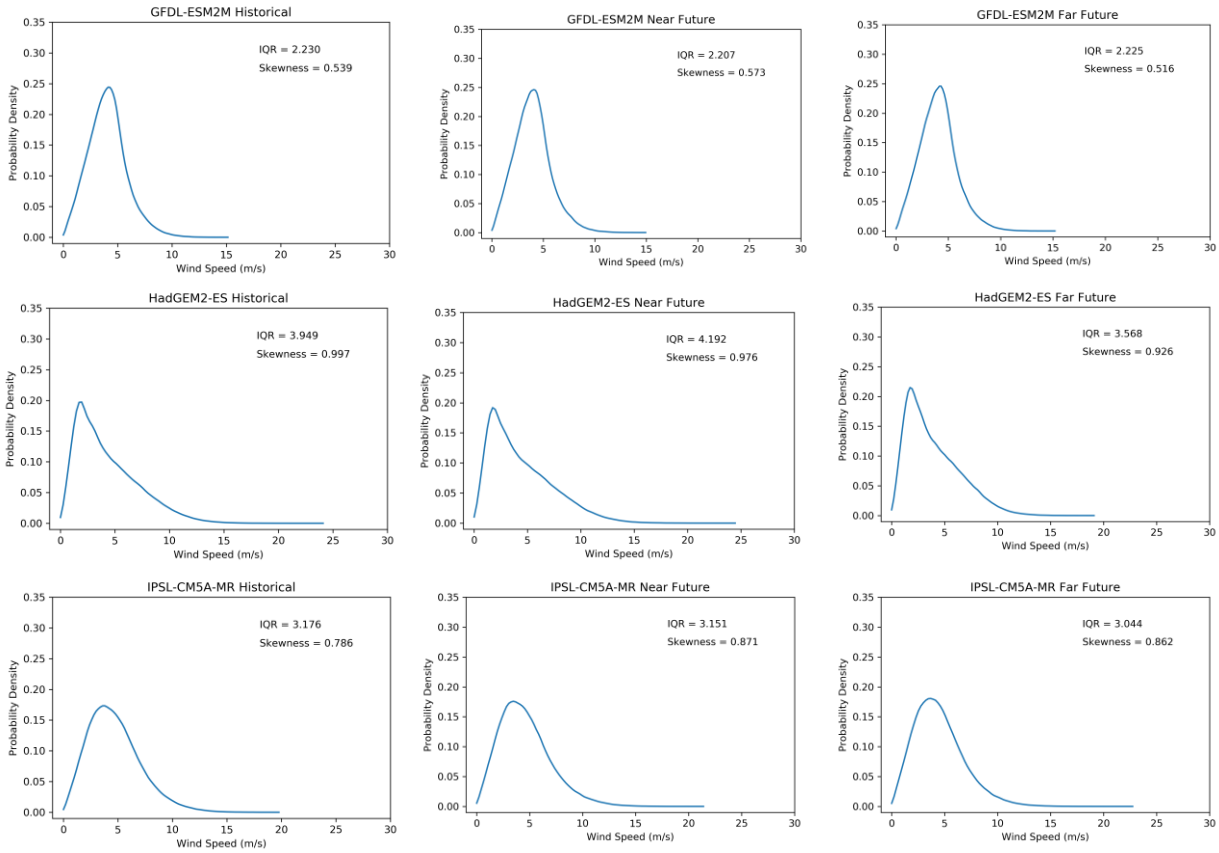

Continuation of Figure 11, containing the probability density functions of the following GCMs: GFDL-ESM2M (top row), HadGEM2-ES (middle row), and IPSL-CM5A-MR (bottom row).

the positive skewness that wind speed data often possess (Greene et al., 2012). The second statistic is skewness, a measure of a PDFs difference from a parametric distribution (Doane and Seward, 2017), such that a skewness value greater than 1 represents an extreme amount of positive (right) skewness (Groeneveld and Meeden, 1984).

Although comparisons of PDFs produced from each GCM's timeframes show slight differences, e.g. ACCESS 1.0's mode is more peaked in the historical than in the future time frames, the distributions' shapes across timeframes are broadly similar. All of these distributions of near-surface wind speed retain the expected right-skewed shape seen in previous literature (Pryor et al., 2005; Altunkaynak et al., 2012). Moreover, almost all of the differences of interquartile range

and skewness between the historical and future time frames are within ±10%. The GFDL models in particular express limited differences of interquartile range, all existing within the range of 0 to -2%, which indicates that these models adhere to the assumption (Déqué, 2007) used here.

There are other caveats associated with the approach used in the current study. Firstly, the projected changes in near-surface wind speed were averaged from grid points across the South-Central Plains region (Figure 8) in the same way that they were when projecting changes in LLJ characteristics (see Section 3.3.1). There is consequently a concern of applying projected wind speed changes from a larger area (grid points over the South-Central Plains region) onto wind speed observations over a much smaller region within it (the Oklahoma Panhandle's Mesonet stations). This difference in spatial domains could be seen as a limitation of this study's approach, since the factor changes of median near-surface wind speed from all model grid points are collectively being applied to a smaller area in order to create high-resolution values.

Another potential concern is that the six GCMs used to create these pseudo-observations have a temporal resolution of six hours – much longer than the Oklahoma Mesonet's five-minute resolution. To address this issue, each point of time in a given day (00Z, 06Z, 12Z, and 18Z) was treated as a mid-point, such that each GCM's six-hourly factor changes were applied and time-centered to the five-minute Mesonet observations. For example, the factor changes of spring 12Z (6am CST) near-surface winds by a given GCM were applied to all spring Mesonet observations recorded between 3am and 9am. The selection of the mid-point of each GCM's diurnal time step was used to minimize potential errors associated with the GCM outputs and Oklahoma Mesonet data having different temporal resolutions.

An important final caveat is that the historical runs of the GCMs (1981 to 2005) and the Mesonet data (1994 to 2018) are offset by 13 years, due to the non-existence of Mesonet observations

prior to 1994. Studies using reanalysis datasets by Pryor et al. (2009) and Torralba et al. (2017) both indicate that the trends in wind speed over the Central United States in recent decades have not been consistent between models, as well as not being statistically significant at the 95% confidence level. The consequent stationarity of wind speeds over the United States in recent decades means that the 13-year offset in these different historical datasets should not significantly affect the results of this study. However, since these previous studies considered spatial and temporal scales larger than that of the current study, there is a need to verify that this stationarity assumption holds.

Figures 12 and 13 show time series plots of annual median near-surface wind speed against time calculated from the Oklahoma Mesonet observations and the GCM outputs respectively, with each plot representing the wind speed trends obtained at each station/from each model. The purpose of these time series plots is to determine whether there indeed was not a notable trend in historical wind speed over the South-Central Plains region from 1981 to 2018. In order to satisfy this assumption, a lack of meaningful trend must exist on multiple temporal scales in both the Oklahoma Mesonet observations and the GCM outputs.

Figure 12 shows that the observed changes in wind speed have been small to non-existent over the 25-year period from 1994 to 2018. Six of the Mesonet stations have observed slight increases in wind speed, with the greatest rate of increase occurring at Boise City, at +0.013 m s^{-1} $year^{-1}$. These wind speed trends over a 25-year period range from +0.325 m s^{-1} at Boise City, to -0.280 m s^{-1} at Arnett. This range of trends is comparable to that found by Torralba et al. (2017) in their global-scale reanalysis of wind speed. Diurnal and seasonal trends in these historical wind speeds were also examined. Almost none of these other trends possessed statistically significant changes ($p < 0.05$, according to Spearman's Rho regression analysis (Yue et al., 2002)), and the largest

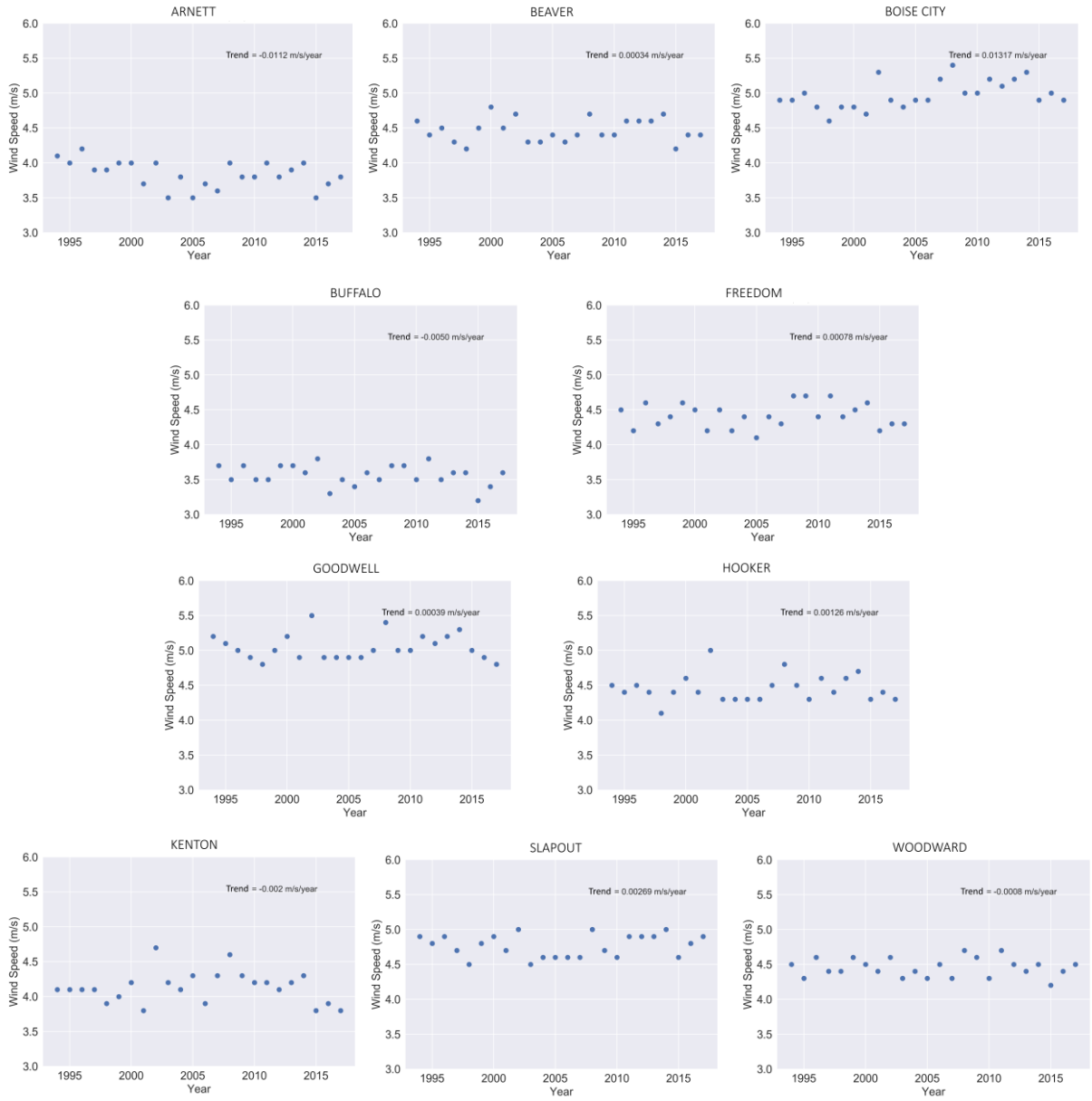

Figure 12: Time series plots from 1994 to 2018 for each individual Oklahoma Mesonet station showing the change of annual median wind speed with time.
- Each plot contains the value of the wind speed/time gradient in m s^{-1} $year^{-1}$.

changes in wind speed were again found at Arnett and Boise City, regardless of season or time of day considered.

Figure 13 shows the same analysis as Figure 12, but instead based on outputs of the six GCMs. Each annual median value was calculated using the values from each model's grid points that fell within the South-Central Plains region, and much like Figure 12, there exists a general absence of strong wind speed trends. The annual trends shown in the figure indicate an overall tendency for increases in historical wind speed, with the strongest trend indicated by HadGEM2-ES at $+0.014$ m s^{-1} $year^{-1}$. Although these trends are more consistent in their sign than those found at the Oklahoma Mesonet locations, they still have notable range and are similarly weak, with the 25-year wind speed trend ranging from $+0.350$ m s^{-1}indicated by HadGEM2-ES, and ± 0 m s^{-1} by IPSL-CM5A-MR. The favoring of positive trends in wind speed continues when examining seasonal and diurnal trends in these historical wind speeds. More statistically significant changes occurred than amongst the Oklahoma Mesonet data on these temporal scales, but the majority of trends were once again weak. These results would suggest that the GCM outputs also abide by the lack of expected wind speed trend seen in previous work that encompassed this region (Pryor et al., 2009; Torralba et al., 2017). As such, the GCM outputs along with observations from the 10 Mesonet locations uphold the stationarity assumption made by the current study.

Despite the apparent validity of this assumption for the South-Central Plains region, Greene et al. (2010) found from their use of NARR data that wind power densities across the Oklahoma Panhandle increased by around 250 Megawatt hours per decade from 1979 to 2008. Such a result would attest to an increase in local wind speeds over the historical time frame. However, Pryor et al. (2009) stated that there can be significant discrepancies in the wind climatology proposed by

observations and reanalysis datasets such as NARR, which means that the inconsistent wind speed trends presented in Figures 12 and 13 are perhaps to be expected.

The presentation of changes in wind energy metrics using these downscaled data was similar to that for the projection of LLJ characteristics detailed in Section 3.3.1 – central tendency and

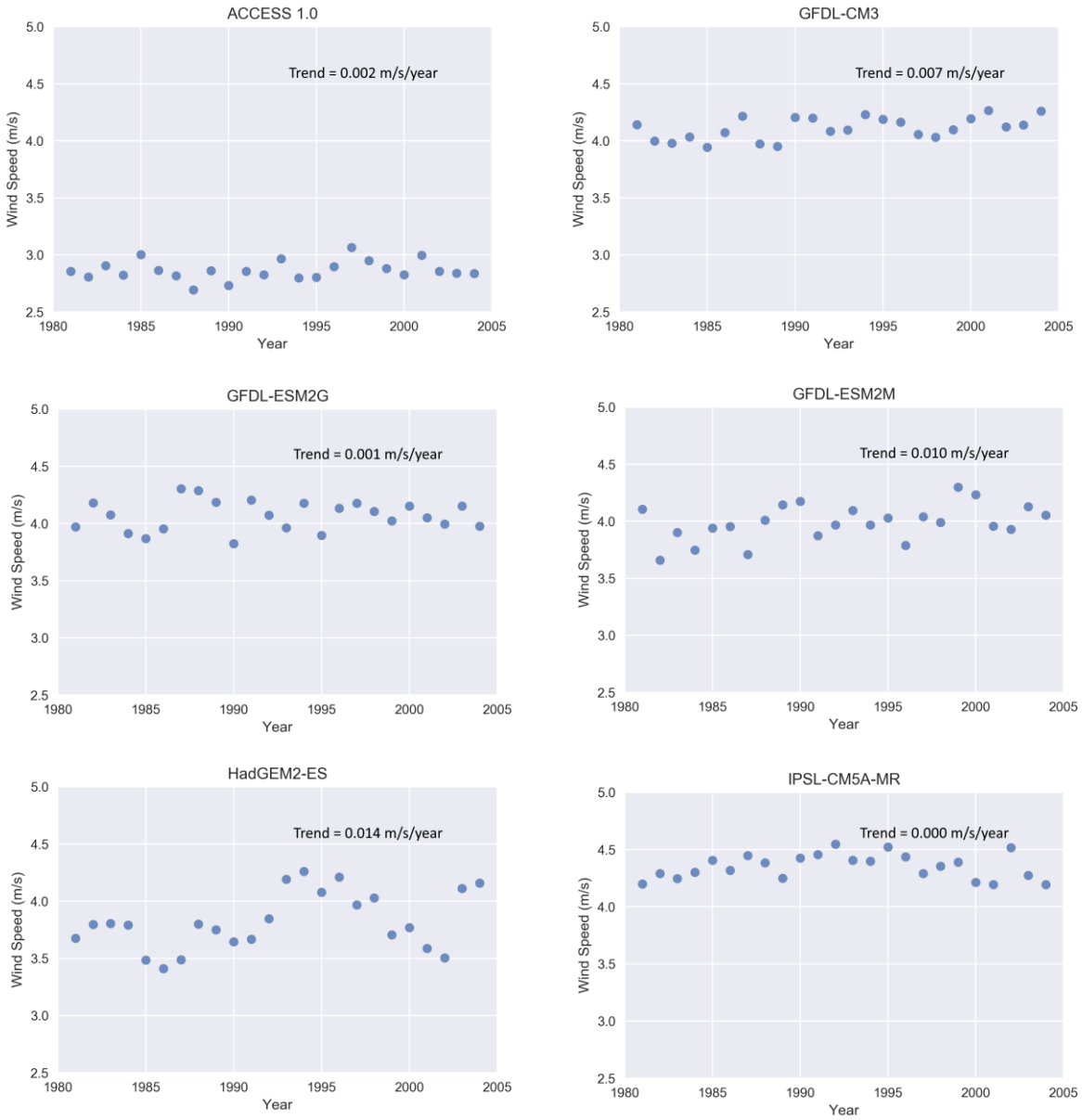

Figure 13: Same as Figure 12 but with annual median near-surface wind speeds obtained from the GCM outputs from 1981 to 2005.

variability in wind energy metrics were presented as percentage change tables and boxplots respectively. In addition, maps of the Oklahoma Panhandle area illustrated spatial variability of trends in these metrics. Since the Oklahoma Mesonet stations have a spatial distribution that is analogous to a GCM's grid points, statistically significant ($p < 0.05$) changes were analyzed in same manner as described in Section 3.3.1. Therefore, Mann-Whitney U-tests of two ranked groups consisting of annual values of a given wind energy metric were computed at all stations for the historical and a future (near future or far future) time frame, broken down further by season and by time of day. The culmination of this analysis is the use of contemporary climate model outputs to deepen and update wind energy resource projections for Oklahoma.

3.3.3. Linking LLJ Characteristics to Wind Energy Metrics

Although it is somewhat unique to projecting changes in three different LLJ characteristics and examining climatological changes in various wind energy metrics, the most novel aspect of the current study is assessing the link between these two features of wind climatology. The decision to examine this link was inspired by Wimhurst et al. (2017) and their analysis of changes in the United Kingdom's wind climatology in connection with the influences of climate change on the North Atlantic Jet's speed and latitude. The linkage between LLJ characteristics and wind energy metrics in the current study was also assessed by linear least-squares regression (Clarke and Cooke, 1998), since the scatterplots produced by this analysis possessed a linear relationship.

Statistical significance ($p < 0.05$) of these regressions of LLJ characteristics against wind energy metrics were assessed using Spearman's Rho analysis (Yue et al., 2002), given the non-parametric distribution of wind speed data (Greene et al., 2012). The independent data were broken down by GCM, seasonally, diurnally, Mesonet station, and most importantly by wind energy metric. The dependent data for these regression analyses came from the LLJ

characteristics, broken down by GCM, seasonally, diurnally, and by characteristic. Such in-depth decomposition of data was done with the interest of identifying any possible relationships between LLJ characteristics and wind energy metrics. If statistically significant relationships were found from this analysis, there would be evidence to suggest that the influence of climate change on the LLJ could be a contributing factor to projected evolutions of Oklahoma's wind energy resources.

Chapter 4: Results – LLJ Characteristics

4.1. Changes in Central Tendency of LLJ Characteristics

Perhaps the most fundamental results from the current study are the changes in central tendency of LLJ speed, height, and frequency over time. In this case, central tendency refers to the changes in median speed and height level of the LLJ, as well changes in its frequency, between the historical and the near/far future time frame. As discussed in Section 3.3.1, projections for these three LLJ characteristics were broken down by model, season, time of day, GCM, and the future time frame considered. Tables 3 and 4 present the outcomes of these projected changes for the near future minus historical, and far future minus historical, model runs of the six GCMs respectively. These projections were calculated as percentage changes, as was also done by Tang et al. (2017), since percentage changes are arguably easier to conceive and possess more meaning than the absolute change in LLJ frequency. It should be pointed out that, in both tables, many of the projected changes in LLJ height are zero percent, which is a consequence of the discrete nature of the height levels that these GCMs possess, as mentioned in Section 3.3.1. If the median height level between two time frames did not change, a projected change of zero percent was produced.

What transpires from comparing these two tables is a much greater number of statistically significant changes ($p < 0.05$, indicated by the red cells) in Table 4, which implies that changes in these LLJ characteristics are greater between the historical and far future model runs than the historical and near future runs. This increase in the number of statistically significant changes when comparing these tables argues for a systematic increase in their occurrence with time. Table 4 also shows that the majority of these statistically significant changes are those of LLJ

	ACCESS 1.0				GFDL-CM3			
	Winter	Spring	Summer	Autumn	Winter	Spring	Summer	Autumn
Speed 00Z	-5.6	-1.2	1.3	-3.6	0.2	-4.2	1.1	-7
Speed 06Z	-0.5	-0.2	2.6	3.6	5.4	-4	-1.9	1.2
Speed 12Z	-0.9	0.2	6.3	0.9	17	0.9	0.2	-0.5
Speed 18Z	2.2	-1.3	3	-0.6	15.6	5.9	0.2	5
Height 00Z	0	0	0	-14.3	0	-7.7	0	-17.2
Height 06Z	0	0	0	0	0	0	-20	-10
Height 12Z	0	0	0	0	0	0	-20	0
Height 18Z	0	0	0	0	9.1	4.5	0	10
Frequency 00Z	-21.4	14.3	56.5	42.9	-33.3	50	100	0
Frequency 06Z	31.8	-9.2	31	7.5	-14.3	5	-34.5	-7.4
Frequency 12Z	20	11.3	36.1	1.3	66.7	23.1	-3.8	34.6
Frequency 18Z	18.2	29.6	88.2	26.1	-16.7	16.7	-40	-25
	GFDL-ESM2G				GFDL-ESM2M			
	Winter	Spring	Summer	Autumn	Winter	Spring	Summer	Autumn
Speed 00Z	11.1	6.5	7	2.5	-15.6	0.8	20.3	6.6
Speed 06Z	6.8	14.8	-0.4	-1	-9.8	4.4	2.5	2.5
Speed 12Z	-4	8.5	-0.6	5.7	-14.5	-2.6	-4.5	-2.4
Speed 18Z	0.6	0.7	-2.7	-4.9	-13.8	-9.9	-1.1	10.7
Height 00Z	20	20	-7.7	-14.3	-16.7	-8.3	25	0
Height 06Z	-4	0	-9.1	0	0	0	0	20
Height 12Z	0	0	-16.7	0	-14.3	0	0	20
Height 18Z	-7.7	0	0	0	-14.3	0	0	4.3
Frequency 00Z	-66.7	0	0	-50	100	0	-50	0
Frequency 06Z	100	0	9.1	-20	0	-12.5	-8.3	-33.3
Frequency 12Z	100	-9.1	17.4	12.5	100	-30	0	-7.7
Frequency 18Z	-50	20	-16.7	0	0	0	-18.2	-11.1
	HadGEM2-ES				IPSL-CM5A-MR			
	Winter	Spring	Summer	Autumn	Winter	Spring	Summer	Autumn
Speed 00Z	-0.6	-0.8	1.8	3.7	15.3	-1.3	0.8	0.2
Speed 06Z	0.1	-0.2	1.4	2.6	-12.8	2.4	1.3	-0.1
Speed 12Z	-1.8	2.8	0	-0.2	6.2	1.7	-1.1	-5.4
Speed 18Z	3.7	2.9	-1.3	-1.5	-1.5	-2.8	2.4	-16.1
Height 00Z	0	0	0	0	-11.1	0	-16.7	-9.1
Height 06Z	25	0	0	0	-28.6	20	0	0
Height 12Z	-11.1	0	0	-10	7.7	-8.3	0	0
Height 18Z	9.1	0	12.5	16.7	-20	-14.3	0	0
Frequency 00Z	0	-16.7	130.8	38.5	0	-5.9	21.4	100
Frequency 06Z	16	2.4	30.2	10.1	33.3	41.7	46.7	58.3
Frequency 12Z	11.1	15.5	31	21.8	20	25	14.3	-33.3
Frequency 18Z	-6.2	-4.3	30.8	9.5	0	0	0	-16.7

Table 3: Percentage changes of median LLJ speed and height level, and LLJ frequency, between the historical and near future time frames.
- Changes in the LLJ characteristics projected by the six GCMs are separated by season and time of day. Red cells indicate changes in annual rank of a given characteristic that were statistically significant according to a Mann-Whitney U-test ($p < 0.05$).

frequency, rather than speed or height. This result is consistent with that of Tang et al. (2017), who found that statistically significant changes ($p < 0.1$, using a student's t-test) of LLJ frequency were projected by their enlisted GCM-RCM combinations quite consistently, with projected changes of LLJ speed being, by contrast, much smaller and lacking statistical significance.

When considering Tables 3 and 4, it can also be seen that the majority of statistically significant changes occur in summer and autumn, with winter being the least frequent season for such changes. This result is perhaps surprising upon a first inspection, considering that the spring season typically experiences the greatest number of LLJs, as found in analysis of historical LLJ climatology by Doubler et al. (2015). It might therefore be expected that spring would experience a larger number of statistically significant projections in these characteristics. However, research by Cook et al. (2008) into springtime LLJ intensification also projected a strengthening of LLJs that occur in autumn over the Central Plains, which they postulated as being a result of the conditions that allow for LLJ formation persisting longer into autumn by the end of the 21st Century. The results from the current study could support this idea, given that many of the statistically significant changes in summer and autumn LLJ frequency are increases, especially in Table 4.

An examination of the diurnal trends identified in these tables reveals that statistically significant changes of jet height and frequency are more common near sunset (00Z) and during the night (06Z). On the other hand, projected changes in jet speed do not seem to possess this diurnal variability, which again is consistent with the idea that projected changes of LLJ speed are expected to be insignificant (Tang et al., 2017). Nevertheless, the idea that LLJ height and

	ACCESS 1.0				GFDL-CM3			
	Winter	Spring	Summer	Autumn	Winter	Spring	Summer	Autumn
Speed 00Z	4.8	1.6	0.5	-4.5	12.4	-5.5	-4.1	4.5
Speed 06Z	1.6	0.7	-1.5	6.6	3.4	-6.1	-2.7	2.2
Speed 12Z	-1.6	0.9	-0.7	2	9	1.9	2.2	-7.4
Speed 18Z	0.2	-0.4	-0.9	0.5	8.6	8.5	-1.3	-13.5
Height 00Z	16.7	0	0	-14.3	16.7	-7.7	7.7	-13.8
Height 06Z	0	20	0	0	-8.3	0	-20	-20
Height 12Z	0	0	0	0	0	-8.3	0	-20
Height 18Z	0	0	12.5	0	9.1	0	15	0
Frequency 00Z	-7.1	-3.6	56.5	92.9	-33.3	25	0	-33.3
Frequency 06Z	0	-1.5	35.2	32.5	-28.6	15	-31	-37
Frequency 12Z	-6.7	28.9	31.5	25.3	0	38.5	-7.7	-15.4
Frequency 18Z	18.2	37	105.9	39.1	0	0	-30	-50
	GFDL-ESM2G				GFDL-ESM2M			
	Winter	Spring	Summer	Autumn	Winter	Spring	Summer	Autumn
Speed 00Z	23.2	-9.5	3.5	-15	0.3	-16	-1.1	5.6
Speed 06Z	-0.9	4.9	-3.9	1	0	2.3	3.4	-4.5
Speed 12Z	7.7	6.1	-0.2	-1.3	-11.3	7	0.5	0.8
Speed 18Z	8.1	3.1	-1.1	-4	2.5	-9.2	2.2	-1.2
Height 00Z	40	30	23.1	0	4.2	0	0	0
Height 06Z	-4	0	-9.1	0	8.3	0	0	0
Height 12Z	0	0	-16.7	0	0	0	0	20
Height 18Z	-7.7	0	0	0	-14.3	0	0	4.3
Frequency 00Z	-66.7	-25	0	0	50	0	-50	50
Frequency 06Z	100	-10	-13.6	25	50	-12.5	-37.5	0
Frequency 12Z	33.3	-18.2	-13	0	200	10	-18.2	76.9
Frequency 18Z	0	-40	-50	0	0	-20	-45.5	-44.4
	HadGEM2-ES				IPSL-CM5A-MR			
	Winter	Spring	Summer	Autumn	Winter	Spring	Summer	Autumn
Speed 00Z	-4.5	-11.8	-9.7	-4.8	6.5	4.6	-1.8	-4
Speed 06Z	-2.2	3.8	-2.9	-1.2	-5.5	2.3	1	0.7
Speed 12Z	-0.2	1.4	-2.4	-6.4	-8	6.7	1.4	-3.3
Speed 18Z	-6	-6.9	-7.3	-4.8	9.5	2.1	5.3	-14.9
Height 00Z	8.3	0	-8.3	0	-11.1	0	-16.7	-9.1
Height 06Z	0	0	0	0	-25	10	0	0
Height 12Z	11.1	0	0	0	-7.7	0	0	-16.7
Height 18Z	9.1	0	12.5	16.7	-20	0	0	-14.3
Frequency 00Z	-10	0	284.6	69.2	0	-17.6	71.4	150
Frequency 06Z	24	-1.6	30.9	30.3	-33.3	50	110	141.7
Frequency 12Z	50	9.7	23.5	31	-60	12.5	100	100
Frequency 18Z	6.2	13	176.9	52.4	0	33.3	0	-33.3

Table 4: Same as Table 3, but instead for changes in LLJ characteristics between the historical and far future time frame.

frequency would change by larger amounts during nocturnal periods is a theoretically sound result, since its formation is much more frequent in the stable atmospheric boundary layers that often form at night (Shapiro and Fedorovich, 2010).

The statistically significant changes that are presented in Tables 3 and 4 are predominantly increases, especially in LLJ frequency, regardless of season, time of day, or the enlisted GCM. Changes in LLJ speed and height are less consistent in their sign than frequency, due to small changes in their projections (Tang et al., 2017) and detectable changes being by coarse vertical GCM resolution respectively. This study thus indicates a future strengthening of the LLJ, based on its projected frequency increase over the South-Central Plains region. Many studies that conducted similar analyses of LLJ frequency came to the same conclusion, regardless of the climate model outputs and methods used (Barandiran et al., 2013; Harding and Snyder, 2014; Tang et al., 2017).

There are also noticeable differences in the number of statistically significant changes projected by each GCM. In both Tables 3 and 4, the GCMs that possess higher (vertical and horizontal) grid resolutions, such as ACCESS 1.0 and HadGEM2-ES (see Table 1 for horizontal resolutions) project a much greater number of such changes, with HadGEM2-ES and GFDL-CM3 projecting by far the largest number of statistically significant changes in LLJ speed. This inconsistency may be a consequence of model resolution differences and the known biases that these GCMs possess, as mentioned previously in Section 3.1.

Besides the statistically significant changes, it is also important to consider the overall pattern in all projections of the three LLJ characteristics. Identifying these patterns in Tables 3 and 4 is quite difficult, however, owing to the large number of rows and columns that they each possess.

Table 5 is a condensed form of Tables 3 and 4, which shows the number of increases and decreases in each LLJ characteristic broken down by time. Not only are the two tables therefore simplified, but their positive and negative trends are summarized more succinctly. There is not a great deal of difference in the most frequent sign for the near future minus historical time frames when compared to the far future minus historical trends, which implies a consistent relationship between these LLJ characteristics and a change in LLJ climatology. The broad patterns shown in Table 5 are as follows: tendency towards increases in LLJ speed, particularly at night (06Z); a lack of change in LLJ height; and consistent increases in LLJ frequency, especially at night and near sunrise (12Z). Although changes in LLJ characteristics that are not statistically significant are arguably of lesser importance, and are therefore less meaningful, Table 5 shows that the sign

	Near Future Positives vs Negatives			Far Future Positives vs Negatives		
Variable Name + Time	**Positive**	**Negative**	**No Change**	**Positive**	**Negative**	**No Change**
Speed 00Z	**15**	**9**	**0**	**11**	**13**	**0**
Speed 06Z	**14**	**10**	**0**	**13**	**10**	**1**
Speed 12Z	**12**	**12**	**0**	**13**	**11**	**0**
Speed 18Z	**12**	**12**	**0**	**11**	**13**	**0**
Height 00Z	**3**	**10**	**11**	**8**	**7**	**9**
Height 06Z	**3**	**5**	**16**	**2**	**6**	**16**
Height 12Z	**2**	**6**	**16**	**2**	**5**	**17**
Height 18Z	**7**	**13**	**4**	**7**	**4**	**13**
Frequency 00Z	**10**	**7**	**7**	**9**	**9**	**5**
Frequency 06Z	**14**	**8**	**2**	**12**	**10**	**2**
Frequency 12Z	**18**	**5**	**1**	**15**	**7**	**2**
Frequency 18Z	**8**	**10**	**6**	**9**	**8**	**7**

Table 5: A condensed form of Tables 3 and 4 that presents the number of cells in each row of these two tables that possess increases, decreases, or no change for a given LLJ characteristic and time.
- The results from the near future minus historical time frames (Table 3) are shown in the three left columns, and far future minus historical (Table 4) in the three right columns. The blue cells indicate the most common sign of the changes in each row of Tables 3 and 4, with the darker blue cells indicating signs that are deemed especially frequent in their occurrence (greater than 16 cells per row).

of all projected changes (significant or otherwise) has some consistency with the expectations of previous literature – increases in LLJ speed and frequency at times when its formation is known to be more frequent (Cook et al., 2008; Barandiran et al., 2013; Tang et al., 2017). However, it should be clarified three of the six models used in the current study are variants on the GFDL GCM (Donner et al., 2011). As such, the results of Table 5 could be somewhat skewed by these three GCMs resolving and projecting the LLJ in a similar manner.

Some of the individual values presented in some of the cells of Tables 3 and 4 should also be discussed, since explanations for their occurrence can be suggested. The first notable values to consider are the large increases in LLJ frequency that many models have projected to take place, especially in Table 4. There are several projections of frequency in this table that are greater than 100%, almost all made by the higher-resolution GCMs (ACCESS 1.0, HadGEM2-ES, IPSL-CM5A-MR), with many of these larger increases of frequency being projected for summer and autumn. HadGEM2-ES in particular projects large increases in LLJ frequency, with summertime frequency near sunset (00Z) and during the day (18Z) in Table 4 being 284.6% and 176.9% respectively. This particular GCM projected its largest physical number of LLJs across all seasons for 06Z and 12Z, making it understandable that a large percentage increase in LLJ occurrence at times of day that are typically less common (i.e., 00Z and 18Z) would occur. By contrast, the projections of LLJ frequency by the lower-resolution GCMs possess a greater tendency for decreases. Though they are typically smaller than the increases projected by the higher-resolution GCMs, they also remain interspersed with increases in some seasons and time frames. For example, in Table 4, GFDL-ESM2M projects changes in spring LLJ frequency ranging from 10% at 12Z to -20% at 18Z. The multi-model pattern therefore remains one of increases in LLJ frequency between the historical time frame and the end of the century. As

stated previously when referencing Cook et al. (2008), these greater LLJ frequencies could be a consequence of stable boundary layer formation over the South-Central Plains in seasons other than spring (such as summer and autumn) perhaps occurring more frequently in the decades to come. The characteristic southerly winds of the LLJ (Shapiro and Fedorovich, 2010) would become a more common occurrence, therefore producing a noticeable change in the region's wind climatology. There also exists somewhat of an argument for higher resolution GCMs projecting greater increases in LLJ frequency, with these larger increases consistently being statistically significant.

Some of the individual projections of LLJ speed are also of interest. As stated in the analysis of Table 5, the overall pattern for LLJ speed is one of slight increases over the next several decades, with the largest of these increases occurring consistently in winter, regardless of the GCM enlisted or time of day. For instance, Table 4 shows GFDL-CM3 projecting increases of speed for winter 00Z LLJs of 12.4%, with GFDL-ESM2G projecting a 23.2% increase. Even some of the higher-resolution GCMs, such as ACCESS 1.0, project larger increases in LLJ speed than seen in the majority of cells, with this GCM projecting a mid-century (Table 3) LLJ speed increase of 6.3% for summer 12Z LLJs. It has been pointed out in multiple studies, such as Holt and Wung (2012) and Zhu and Liang (2013) that a faster LLJ is commonly associated with a westward expansion of the Bermuda High. An enhanced future expansion could form part of the reason why the slight increase in LLJ speed that has been presented in the current study might take place. As such, not only could the South-Central Plains experience southerly winds more frequently, but they could also be slightly faster when they occur.

4.2. Changes in Variability of LLJ Characteristics.

The percentage change tables in Section 4.1 present projections of central tendency of the three LLJ characteristics examined in the current study. Given the LLJ's susceptibility and influence that it experiences from climate variability cycles, such as ENSO (Danco and Martin, 2017) and the NAO and PDO (Weaver and Nigam, 2008), examination of projected changes in the LLJ's variability is also of worth. As discussed in Section 3.3, variability of LLJ speed, height, and frequency was considered in the current study by constructing boxplots of annual median speed/height level, and annual frequency count, constructed from each GCM's grid points across the South-Central Plains region. As such, each boxplot is comprised of 25 plot points, one for each annual value of speed/height/frequency. In maintaining consistency with Tables 3 and 4, boxplot construction is separated by LLJ characteristic, enlisted GCM, season, and time of day, thus maintaining this study's holistic analysis of the LLJ. Boxplot construction was also separated by time frame (historical, near future, and far future), rather than calculating projected changes as done for Tables 3 and 4, since the interest of constructing boxplots is in determining the change of the LLJ's variability with time.

4.2.1. Variability of LLJ Speed

Boxplots presenting results from median LLJ speed are shown in Figure 14. Since these boxplots were grouped by season and enlisted GCM, 24 sets of boxplots for each LLJ characteristic were produced. Boxplots that best summarize the results of the current study are shown here. Figure 14 (see Appendix A1 for the rest of the boxplots) presents the findings from 10 of the 24 sets of boxplots, with each set of three boxplots on a given set of axes representing the spread of annual median LLJ speed for a given time of day. Although Doubler et al. (2015) tells us that LLJs are not a frequent occurrence in winter (top row of Figure 14), those that do occur could experience

a greater variability in speed by the end of the 21st Century. This result was especially true of LLJs that form at night (06Z) and near sunrise (12Z), based on the spread of the boxplot data. LLJs that occur outside of spring and summer tend to be faster, as mentioned in Section 4.1, thus offering an explanation for greater variability in jet speed in these seasons.

A common result conveyed by these boxplots is changes of median LLJ speed that are quite small, regardless of the time of day, season, or GCM considered. Most of these changes are on the order of ± 1 m s^{-1} – a projected change that is consistent with results from Tang et al. (2017). Some of the largest changes of LLJ speed are projected for spring and summer by the higher resolution models (second and third rows of Figure 14), with several of these changes in LLJ speed being statistically significant ($p < 0.05$, lighter-colored boxplots), based on the results of the Mann-Whitney U-tests. Despite these somewhat larger changes in LLJ speed, spring and summer speed variability are small compared to that of autumn and winter, and are also small when comparing the boxplots of the historical and future time frames.

In terms of the projected changes of LLJ speed between time frames, there are some notable results. Slight increases of nighttime spring jet speed (06Z and 12Z) of approximately +1 m s^{-1} are suggested by some of the higher resolution GCMs, particularly ACCESS 1.0 and HadGEM2-ES (second row of Figure 14). Also, all of the GCMs agree on projected reductions of autumn jet speed at all times of day, with the reductions reaching slightly over -2 m s^{-1} for daytime (18Z) LLJs. These changes of median value between time frames are somewhat notable, based on the lower diurnal variability of wind speed that spring and summer possess (second and third row).

However, the seasonal variability of LLJ speed and its differences within time frames can be much larger than across them. The LLJ's speed appears to be approximately 3-5 m s^{-1} higher in

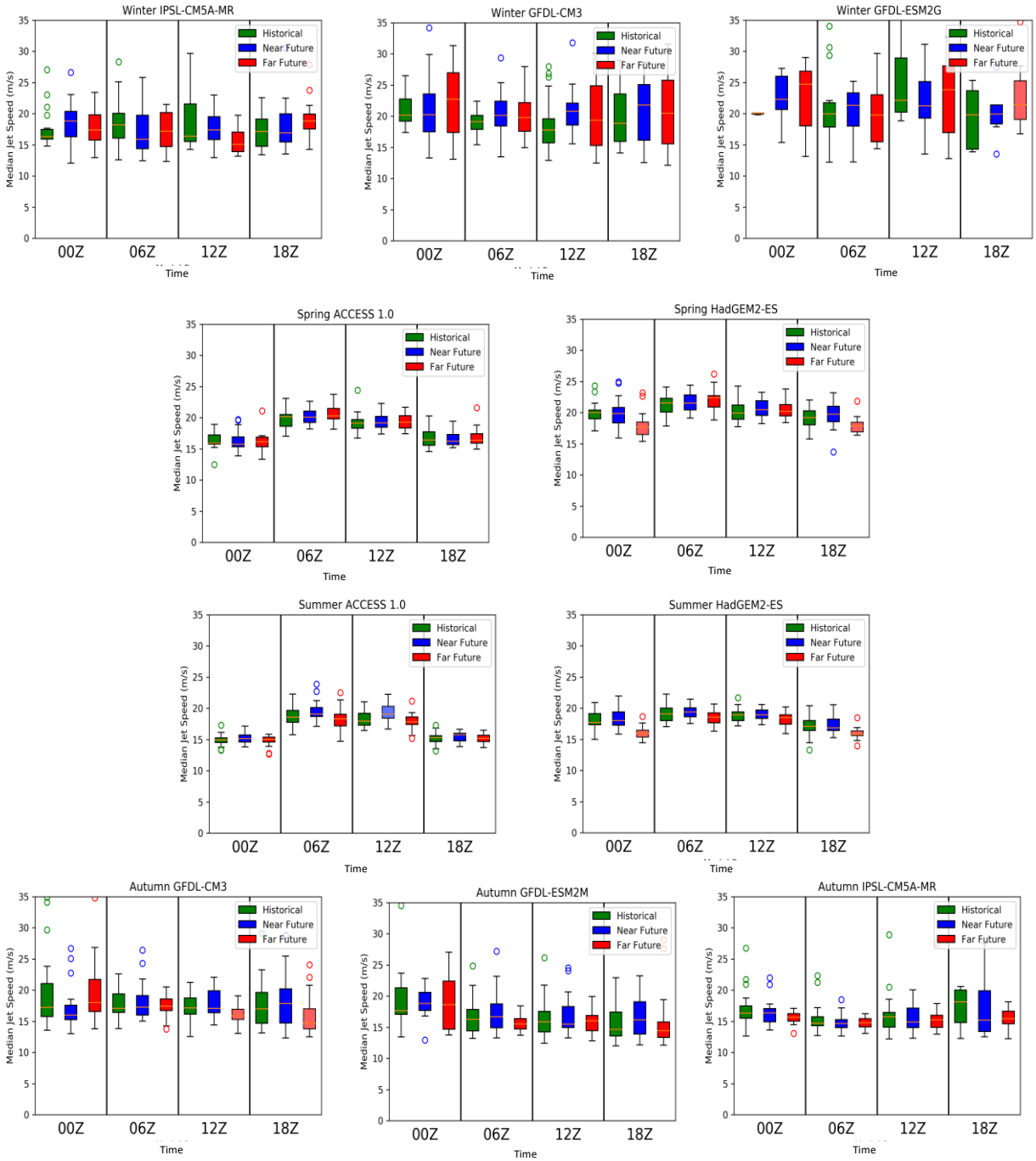

Figure 14: Boxplots showing annual median LLJ speed in (m s^{-1}) for each individual time frame across each GCM's grid points within the South-Central Plains region.
- The boxplots are grouped by season and the GCM that was used to produce them, with each set of three boxplots on a given pair of axes representing the historical (green), near future (blue), and far future (red) spread of annual median LLJ speeds for a given time of day (00Z, 06Z, 12Z, 18Z). Lighter-colored boxplots indicate future time frames (compared to the historical time frame of a given season, model, and time of day) that possess a statistically significant change ($p < 0.05$) in median LLJ speed when enlisting a Mann-Whitney U-test.

autumn and winter than spring and summer, which agrees with expectations from Doubler et al. (2015) that LLJs that form outside of spring and summer are typically faster. The greatest variability and changes in median LLJ speed for autumn and winter seem to be projected by the GFDL GCMs (top and bottom row), with the variability in the remaining GCMs for these seasons being slightly smaller. The heightened LLJ variability in autumn and winter and its greater change into the future perhaps is related to lower frequency of formation at these points in the year. It may also be linked to the climate variability cycles that can influence the LLJ's formation; both of these possibilities shall be discussed in Chapter 6.

Regardless, the projected changes of LLJ speed between time frames are quite small, both in terms of change and spread of the median values of these boxplots, meaning that any change in wind energy resources linked to a change in LLJ speed could be somewhat limited. Recall from Danco and Martin (2017) that several of these GCMs (except for HadGEM2-ES) have a tendency to underestimate the LLJ's historical speed. This bias could have an impact on these models' ability to project changes in LLJ speed, beyond the physical changes simply being small.

4.2.2. Variability of LLJ Height

As described in the methods of this work, median LLJ height and its projections were inferred from changes in the height level of the LLJ's maximum winds for a given GCM and point in time (see Section 3.3.1). As such, the boxplots shown in Figure 15 (and Appendix A2) present the variability of the LLJ's height level rather than its physical height in meters, with the most noteworthy results presented in the same manner as in Figure 14. It is important to clarify, however, that because these boxplots of LLJ height have been constructed based on the relatively low-resolution height levels of these six GCMs, care must be taken to not overstate what they are

conveying. The number of height levels that these GCMs possess up to 3000 meters AGL, as per the definition of LLJ occurrence used by Doubler et al. (2015) and Yu et al. (2017), ranges from 12 to 16 levels. The distance in meters between subsequent lower height levels can be as much as 50 meters. With such large differences in height between levels and a consequently discrete and categorical nature of these height measurements, it was more appropriate to display the y-axis of Figure 15 as the median height level presented by each GCM's output, as opposed to physical height in meters. It is important to mention, however, that two (or more) GCMs that indicate the same height level often do not indicate the same height, due to vertical resolution differences.

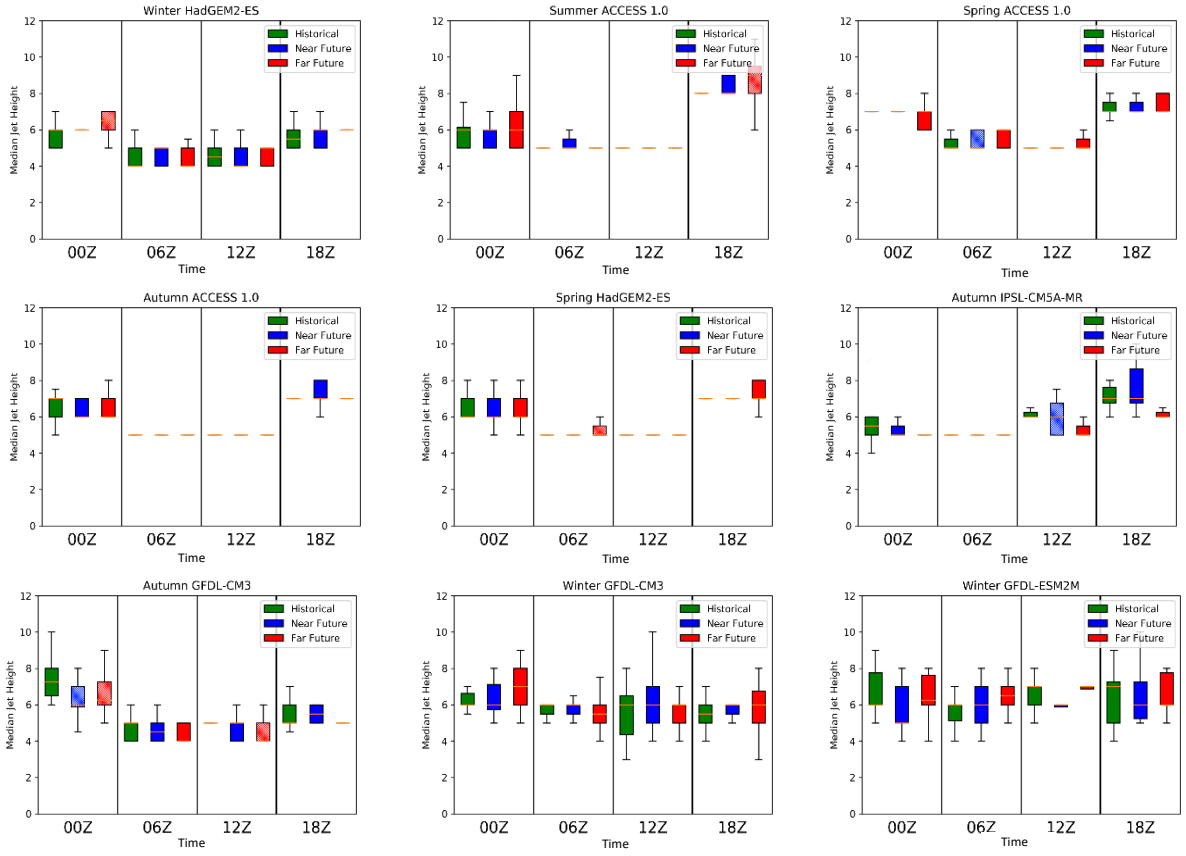

Figure 15: Same as Figure 14 but for annual median LLJ height (expressed as height levels) rather than speed.

Finally, since LLJ height is presented on discrete height levels and therefore is a categorical variable, it is inappropriate to determine the existence of outliers in the construction of these boxplots, hence their absence in Figure 15.

One common result from these boxplots was height of LLJs that formed during the night being less than those that formed during the day (00Z and 18Z). The majority of GCMs, but particularly those with a higher resolution such as ACCESS 1.0, indicated a daytime (06Z and 12Z) height level of approximately level 7, with the most common median height level of LLJ formation at night across GCMs being level 5 (top row of Figure 15). This lower nighttime LLJ was a consistent feature across all three time frames, perhaps owing to the low vertical resolution of the GCMs' height levels preventing notable differences from being projected. However, upon converting the height levels of these six GCMs into meters, height level 5 corresponds to a height over the South-Central Plains region of 200-400 m AGL, depending on the GCM in question. This range of LLJ height is comparable to heights obtained from several studies of LLJ features using SODAR (Emeis, 2014a; Lampert et al., 2016). As such, despite issues regarding GCMs having relatively low vertical height resolution when compared to the vertical wind profile detail afforded by SODAR, they are still able to simulate and project LLJ heights that are realistic.

Not only is LLJ height typically lower at night than that of LLJs that form during the day, but the variability of those that form during the night is also smaller. The second row of Figure 15 suggests such a result, illustrating the median height level of the LLJ not deviating from level 5 at 06Z and 12Z across all time frames. The consequent implication is formation and structure of the LLJ being more consistent at night, which is probably true since stable boundary layers that produce LLJs are typically a nocturnal feature (Stull, 1988).

It can also be argued that projected changes in LLJ height and changes in its variability are larger in autumn and winter (bottom row of Figure 15) than spring and summer, according to the spread of annual median LLJ heights in the former two seasons. These autumn and winter spreads were particularly large when looking at the results of some of the lower-resolution GCMs, with GFDL-CM3 indicating winter LLJs (bottom row, center) ranging in height from as low as level 3 and up to level 10 at 12Z. By contrast, the spread of heights indicated by HadGEM2-ES in winter (top row, left) is much smaller, ranging from level 4 at night to level 7 during the day. This seasonal variability could be related to the greater consistency of LLJ formation at night and during spring and summer (Shapiro and Fedorovich, 2010), with differences in GCM outputs perhaps resulting from biases when characterizing LLJ formation (Harding et al., 2013; Danco and Martin, 2017), thus complicating the overall result.

4.2.3. Variability of LLJ Frequency

Of the three LLJ characteristics examined in the current study, the diurnal, seasonal, and inter-model variability of LLJ frequency is perhaps of greatest interest. The creation of boxplots revealed stark differences between LLJs that form during the day versus at night, as well as those which form in spring and summer versus autumn and winter. Figure 16 (and Appendix A3) presents a collection of boxplots of annual LLJ frequency, again in the same vein as Figures 14 and 15. What should be made clear about Figure 16, however, is that the differences in LLJ frequency when comparing different seasons and GCM outputs can be large, with the higher-resolution GCMs, such as HadGEM2-ES, indicating frequency changes into the hundreds for a given year of data. These differences in frequency can largely be attributed to the higher-resolution GCMs possessing a greater number of grid points over the South-Central Plains region (Figure 8), therefore increasing the number of LLJs that can be detected. As such, the boxplots

presented in Figure 16 do not all have the same y-axis scale, so care should be taken when comparing them.

Perhaps the most notable result from these boxplots was the large difference in LLJ frequency when comparing those that formed during the day against those at night. As evidenced by the first two rows of Figure 16, annual LLJ frequency can be as much as 2-4 times greater at night than during the day (regardless of time frame considered). The first row of Figure 16 shows two good examples of this result, with the daytime frequency indicated by GFDL-ESM2G for spring LLJs being between two and 15 in a given year, with the frequency of nighttime LLJ formation ranging from two to almost 35. Such a greater LLJ frequency should be expected, since the conditions that favor LLJ formation over the South-Central Plains region are more common at night (Stull, 1988). However, this disparity in frequency seems not to occur in winter as significantly as it does in autumn, spring, or summer. When comparing the LLJ frequencies for GFDL-ESM2M in winter (second row, right) to the other boxplots, the median annual frequency indicated by this boxplot is typically around one to two LLJ occurrences higher in 06Z and 12Z than during the day – a much smaller difference than that indicated by other seasons. Previous work has also provided evidence for a low historical climatological LLJ frequency in winter months (Doubler et al., 2015).

The consistency of diurnal and seasonal trends in established LLJ frequency between the current study and previous literature continues when examining variability across time frames. Several of the enlisted GCMs projected particularly large increases in LLJ frequency across all time frames, with ACCESS 1.0 and HadGEM2-ES, with IPSL-CM5A-MR also projecting substantial changes in the variability of this annual frequency, particularly at night (third row of Figure 16). For example, projections for IPSL-CM5A-MR in summer and autumn (third row,

center and right) indicate increases in median 06Z frequency of 20 and 30 more LLJs in a given year respectively by the end of the century. Many of these large increases in LLJ frequency between historical and future time frames were statistically significant ($p < 0.05$), as was also seen in Tables 3 and 4, but what Figure 16 shows is that this significance could be a consequence of these large changes in the variability of LLJ frequency. It is also possible that the variability of

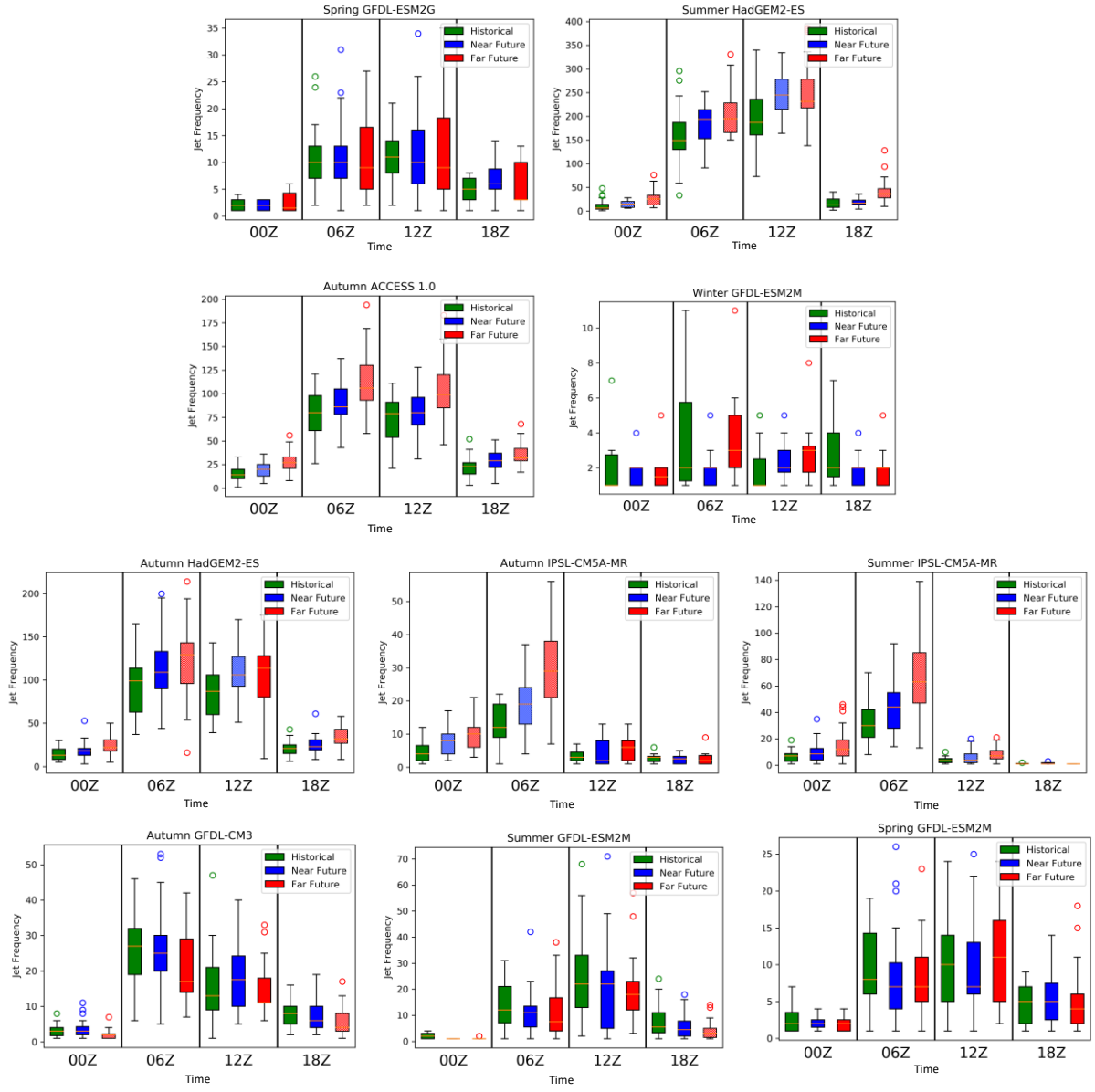

Figure 16: Same as Figure 14 but for annual LLJ frequency rather than speed.

LLJ frequency could be scaling with its central tendency, given the multitude of significant LLJ frequency increases noted in Section 4.1. Indeed, Cosack et al. (2007) found that occurrence of LLJs was associated with an increase in the magnitude and spread of observed winds, so a positive relationship between the magnitude and spread of LLJ frequency on climatological scales has some credence. Increases in LLJ frequency by the end of this century are consistent with multiple studies that have examined projected changes of LLJ characteristics (Cook et al., 2008; Barandiran et al., 2013; Tang et al., 2017).

A final result to mention is the sometimes large differences in projections of LLJ frequency made by different GCMs. Despite the general agreement of increasing LLJ frequency between historical and future time frames, the GFDL models do not always agree with this pattern for certain seasons and times of day. The bottom row of Figure 16 shows several outputs from the GFDL models in which the change in frequency ranges from no notable change to even slight decreases in annual LLJ frequency of approximately 5 to 10 fewer LLJs in a given year, regardless of the season or time of day being considered. The GFDL models may possess resolutions and parameterizations that result in these projections not matching the overall pattern presented in Section 4.1.

More importantly, as mentioned at the beginning of this discussion of LLJ frequency, the higher-resolution GCMs consistently indicate much greater LLJ frequencies in a given time frame than those with a lower resolution. The effects of higher resolution are evident when comparing the boxplots produced for summer by HadGEM2-ES (top row, right), and autumn by ACCESS 1.0 (second row, left) and HadGEM2-ES (third row, left), to the other boxplots in Figure 16. The LLJ frequencies of nighttime LLJs indicated by these boxplots can be upwards of 200 LLJ occurrences for a single year of data. These higher resolution models indicate frequencies that

are several factors higher in some seasons and times of day than those of the lower-resolution GCMs. Having a greater horizontal resolution over the South-Central Plains region should increase the probability of detecting an LLJ's occurrence, which seems to have been the case when comparing GCM outputs.

These differences in projected LLJ frequency and frequency within single time frames are indicative of the biases that these GCMs possess. In their study of historical LLJ climatology from 1979-2009, Doubler et al. (2015) found that the diurnally-averaged annual southerly LLJ frequency over the South-Central Plains had the following approximate values: 5-7% in January, 10-15% in April and October, and 20-25% in July (peaking at 40% from 06Z to 12Z). Given the result from Figure 16 that HadGEM2-ES indicates a historical frequency of approximately 150 LLJs occurring in a single summer at 06Z (top row, right), this represents an LLJ frequency of 40.8% (considering that these boxplots were comprised of six-hourly wind speed data, and there are 368 six-hourly time periods in a single summer). Given the results from Doubler et al. (2015) stated above, this would indicate that HadGEM2-ES simulates historical LLJ frequency with little bias. Extending this same analysis to other GCMs, seasons, and times of day would indicate that the higher-resolution GCMs, especially HadGEM2-ES and ACCESS 1.0, possess much lower bias in their simulations of historical LLJ frequency. This would also indicate that the lower-resolution GCMs considerably underestimate the occurrence of LLJs.

Recall as well from Section 3.1 that these six GCMs have been shown to possess biases in their simulation of historical LLJ features in previous work (Harding et al., 2013; Danco and Martin, 2017), such that they tend to underestimate simulated speed and mischaracterize the location of typical LLJ formation. Discrepancies with observations of LLJ frequency and known biases of these GCMs therefore provide explanations for the multi-model differences that Figure 13

possesses. Discussion of the impacts and solutions for bias mitigation for the current study shall be discussed further in Chapter 6.

4.3. Spatial Patterns of LLJ Characteristics

The third examined quality regarding these three LLJ characteristics is the spatial distribution of projections across the South-Central Plains region. Multiple studies have found that there exist notable spatial differences in wind climatology away from the surface across the United States. Holt and Wung (2012) and Johnson and Erhardt (2016) presented increases of wind speed in previous and future decades respectively over the Central Plains, and Harding and Snyder (2014) found that a stronger and poleward-shifted LLJ could become a more common occurrence in future decades. The results from this section serve to supplement these previous studies by considering projected changes in the three selected LLJ characteristics using multiple GCM outputs, whilst also considering projections for individual seasons and times of day.

4.3.1. Spatial Pattern of LLJ Speed Projections

Much like Section 4.2, the results from the analysis of each LLJ characteristic are presented separately, starting with LLJ speed. In all presented maps, the color and size of the circles corresponds to the sign and magnitude of the projected change of the given LLJ characteristic at each GCM's grid points over the South-Central Plains region. Due to the large number of maps than could potentially be created, owing to the number of combinations of time of day, season, time frame, and GCM, the maps shown here are representative of the current study's results. Furthermore, all of the presented maps possess statistical significance ($p < 0.05$) based on the Mann Whitney U-test of rank changes of each LLJ characteristic between time frames (see Section 3.3).

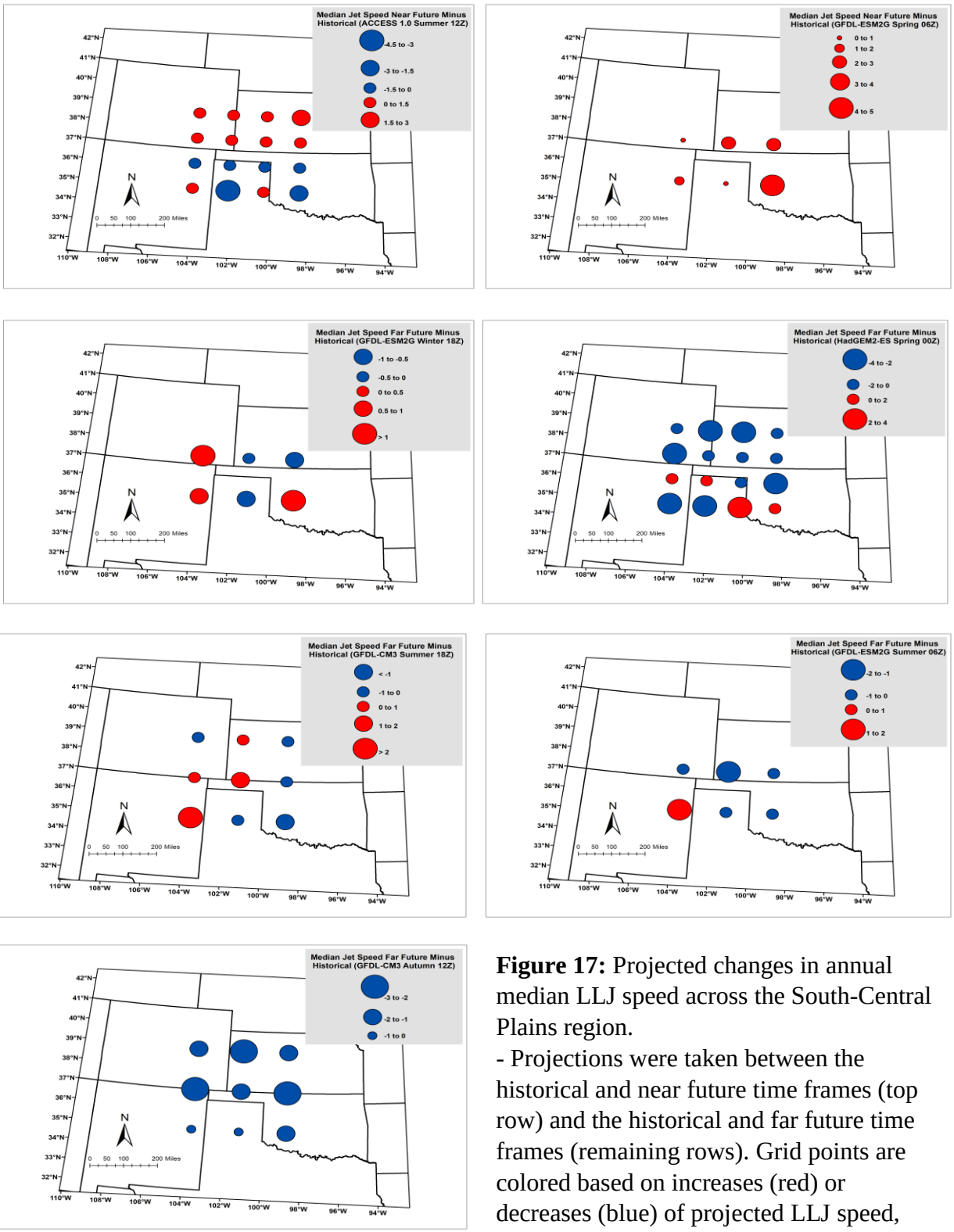

Figure 17: Projected changes in annual median LLJ speed across the South-Central Plains region.
- Projections were taken between the historical and near future time frames (top row) and the historical and far future time frames (remaining rows). Grid points are colored based on increases (red) or decreases (blue) of projected LLJ speed, with their size proportional to the projection's magnitude.

Figure 17 shows seven projections of median LLJ speed across the South-Central Plains region, with maps created for the difference between the historical and near future (top row), as well as historical and far future (remaining rows) time frames. As in the analysis of central tendency and variability, there is a lack of overall discernible pattern in projected LLJ speed in these maps. The projected changes from one grid point to the next are inconsistent, except for the overall increases projected by GFDL-ESM2G for springtime LLJs that form at night, and the decreases of autumn LLJ speed near sunrise that GFDL-CM3 projects. Given the lack of sign consistency in most of these wind speed projections, the common LLJ speed projection range of ± 3 m s^{-1} presented in these maps averages out to little change overall. An argument can be made that increases in LLJ speed occur more to the south and west of the South-Central Plains region, but the consistency of this trend is weak.

Though some studies have concluded from climate model projections that the LLJ may experience a strengthening in the coming decades, especially in April, May, and June (Cook et al., 2008), more recent studies such as Harding and Snyder (2014) and Tang et al. (2017) found that the LLJ could experience greater changes in its frequency than speed. The latter study found a multi-model LLJ speed change across the Central Plains that does not exceed ± 1 m s^{-1}. Such an inconclusive projection in LLJ speed is consistent with the results presented in Figure 17.

4.3.2. Spatial Pattern of LLJ Height Projections

Maps of projections in median LLJ height show a similar lack of overall spatial pattern or meaningful diurnal and seasonal differences as seen in Figure 17 for LLJ speed. Projecting changes in LLJ height, like the other characteristics considered in this work, depends on the GCMs being able to simulate the historical state of LLJ height effectively. Previous work such as Doubler et al. (2015) and Lampert et al. (2016) found that the LLJ's typical height ranges from

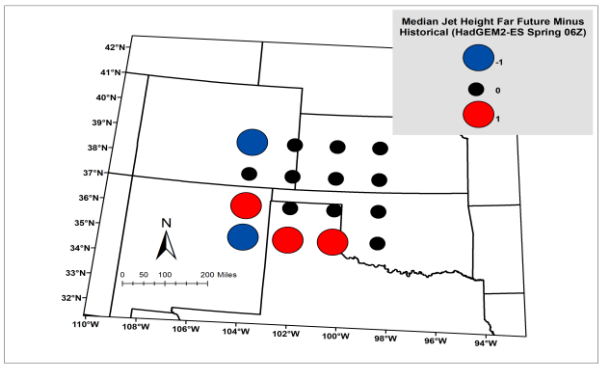

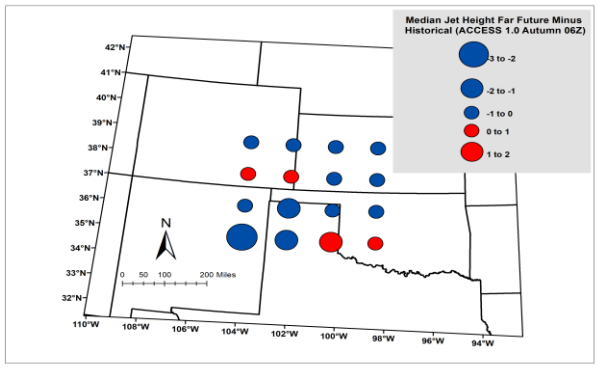

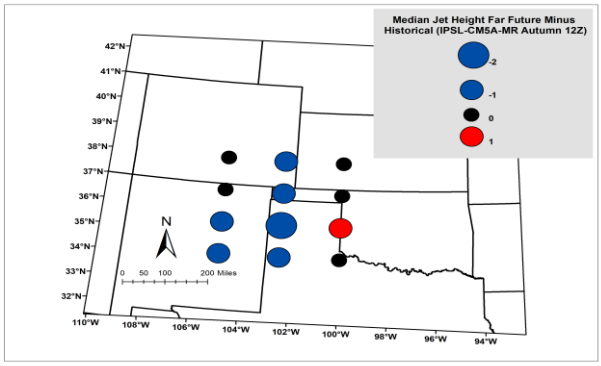

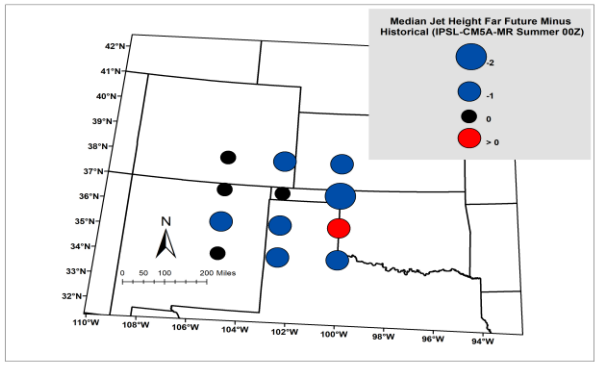

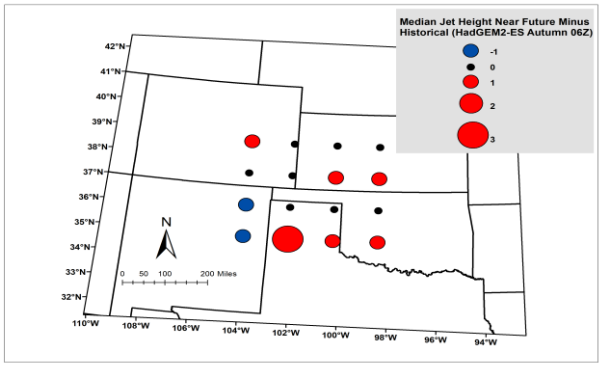

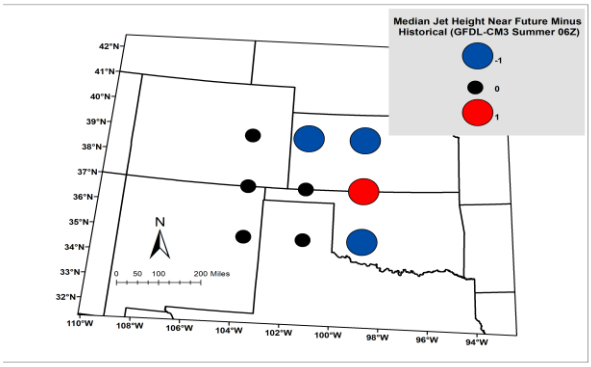

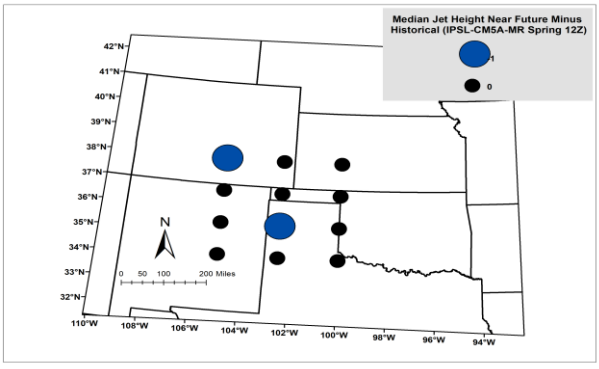

Figure 18: Same as Figure 17 but for annual median projections of LLJ height.
- Black circles indicate grid points that experience no change in height level.

200 to 600 meters above ground level. The analysis of LLJ height variability (Section 4.2.2) performed in the current study indicating that GCMs are able to simulate this historical height fairly accurately. There is therefore valid precedent to consider the ability of these GCMs to assess projected changes of LLJ height over the South-Central Plains region.

The first two rows of Figure 18 consist of projections of LLJ height between the far future and historical time frames, and the bottom two rows represent near future minus historical projections. Otherwise, the maps are constructed in the same manner as in Figure 17. Much like in Figure 17, there is a lack of spatial consistency in these maps, regardless of time of day, season, or model enlisted. None of the maps possess a constant sign across all grid points. In fact, many grid points possess no change in height between time frames at all (black grid points), which is likely a consequence of changes in LLJ height being obtained from projections of discrete median height levels (see Section 3.3.1). There is an arguable tendency for the LLJ's median height to become lower in the coming decades, dropping by 1 to 2 levels in certain runs. This reduction is common between the far future and historical model runs, with maps of projected changes in spring, summer, and autumn for nighttime jet formation (first two rows of Figure 18) all showing this tendency, weak though it may be.

Across all of these maps, a tendency for reductions in LLJ height to the west and south can also be deduced, especially when considering height level differences from the far future and historical time frame maps (first two rows of Figure 18). However, none of these projections exceeded reductions of 1 to 2 height levels, regardless of the GCM, season, or time of day considered, with little to no tendency in these factors to note. These results do have some spatial consistency with the results of Figure 17, since the projected increases of LLJ speed also occurred mostly to the south and west of the South-Central Plains region. This result is consistent

with expectations from the literature. Shapiro and Fedorovich (2010) found in their analysis of vertical wind profiles produced by LLJs that increased jet speed and reduced jet height maxima occur concurrently. That being said, there is still an overall lack of consistency in the sign and magnitude of LLJ height changes, despite all of these projections of LLJ height possessing statistical significance ($p < 0.05$).

It should also be reiterated that despite the changes in the number of heights for two different GCMs being hypothetically the same, this does not mean that the change of the LLJ's median height in meters is the same. Differences in vertical height resolution between models (e.g., IPSL-CM5A-MR has 12 levels between the ground and 3000 meters, and ACCESS 1.0 has 16 levels) mean that a higher-resolution GCM that projects a median height decrease of one level constitutes a smaller reduction than that of a lower-resolution GCM. However, as discussed in Section 4.2.2, the categorical nature of these height levels makes representation of these heights in meters suspect.

4.3.3. Spatial Pattern of LLJ Frequency Projections

Much like when central tendency (Section 4.1) and variability (Section 4.2) of the three LLJ characteristics were considered, the most consistent and verifiable spatial patterns belong to projections of LLJ frequency. The results from examining this final LLJ characteristic are presented in Figure 19, again using the same diurnal, seasonal, and inter-model separation as before. Unlike Figures 17 and 18, there is a high consistency in the magnitude and direction of projected changes that can be seen when considering grid points on each map. Furthermore, even if there is a difference in sign at neighboring grid points, there is a clear progression of sign and magnitude from north to south or east to west, as in the second and third rows of Figure 16.

In many of these maps (except for the top row), increases in annual LLJ frequency between time frames are much larger to the north of the South-Central Plains region, with the higher resolution GCMs in particular (such as ACCESS 1.0 and HadGEM2-ES) projecting increases to the north that are 4 times greater than those to the south. In fact, some model outputs, such as springtime LLJ occurrences projected by HadGEM2-ES (third row, left), also show a slight reduction of LLJ frequency to the south of the region of study, but nevertheless more positive changes in LLJ frequency to the north. These results are all indicative of a poleward shift of LLJ formation in the coming decades, with as many as 100 more LLJs (+4.2%) forming in the near future and 300 more (+10.3%) in the far future time frames over the entire 25-year period, when compared to the output from the same GCM's historical time frame. Such a poleward shift of common LLJ formation sites has been found in several previous studies, such as Barandiran et al. (2013) and Harding and Snyder (2014).

Figure 19 also illustrates the greater increases of LLJ frequency projected by higher-resolution GCMs. For instance, projections of frequency by ACCESS 1.0 and HadGEM2-ES (second row of Figure 19) indicate frequency increases of as many as 300 extra LLJs, but IPSL-CM5A-MR's projections (which are also of summer nighttime LLJs) only amount to increases of up to 30 extra LLJs over the entire 25-years. This inconsistency could be a consequence of IPSL-CM5A-MR having a smaller number of height levels up to 3000 m AGL (per the definition used by Doubler et al. (2015) and Yu et al. (2017) in defining LLJ occurrences) than the former two GCMs. A final interesting result regarding inter-model differences is the negative projections of LLJ frequency by the GFDL GCMs enlisted for the current study (top row of Figure 19). There exists less of an obvious spatial pattern in the maps produced by these GCMs and

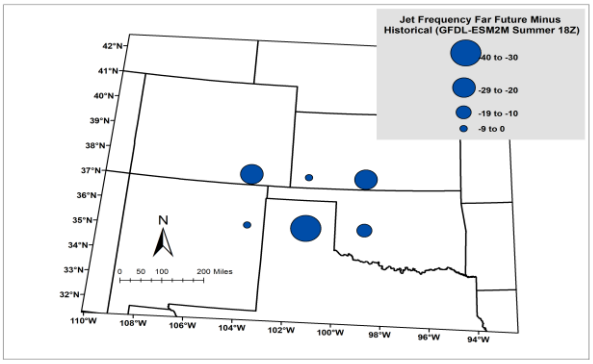

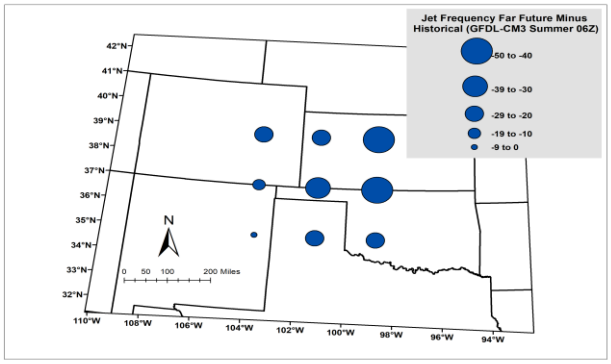

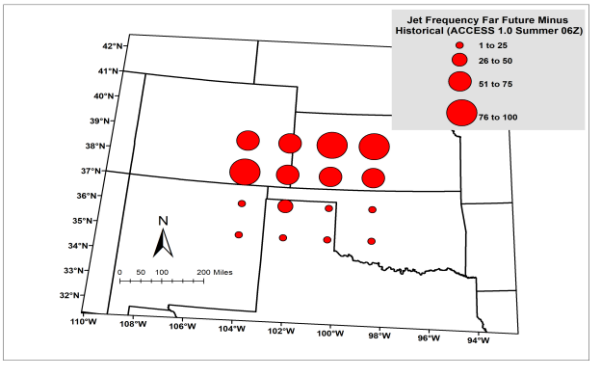

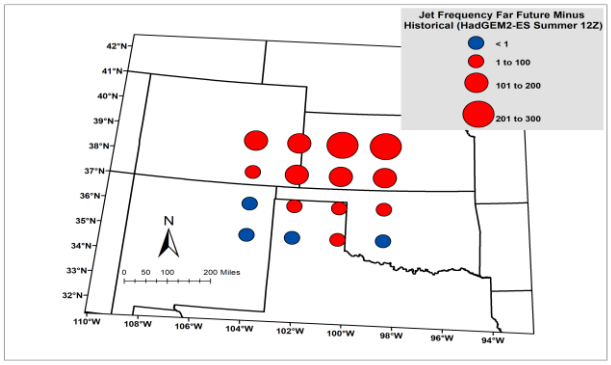

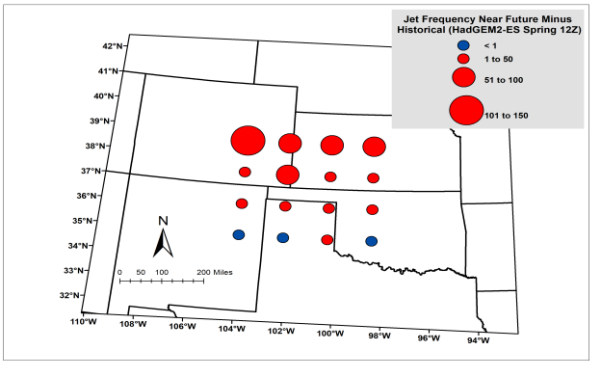

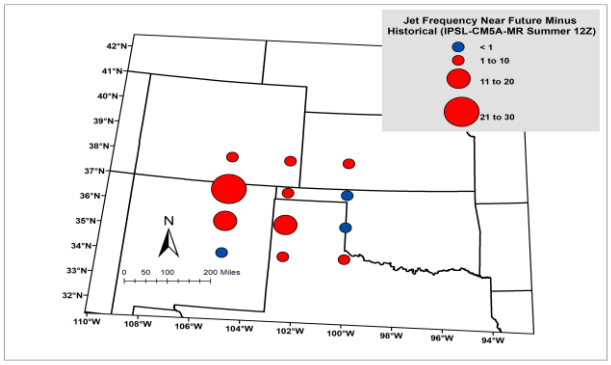

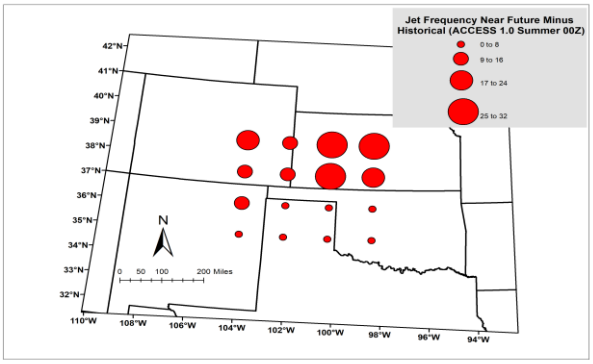

Figure 19: Same as Figure 17 but for counts of annual LLJ frequency.

the magnitude of these projected reductions in LLJ frequency are also smaller, maximizing at around 40 fewer LLJs between historical and future time frames.

This spatial reduction of LLJ frequency indicated by the GFDL models was also apparent in projections of LLJ's frequency's central tendency (Section 4.1) and variability (Section 4.2). These results again add to the general picture that the GFDL models do not agree with the projections of the other enlisted GCMs, but also do not project changes in frequency large enough to detract from the positive inter-model trend. The consequences of inter-model variability for the current study's results shall be discussed further in Chapter 6.

Chapter 5: Results – Wind Energy Metrics

5.1. Changes in Central Tendency of Wind Energy Metrics

Section 4.1 presented the projected changes in LLJ characteristics as percentage changes in central tendency between historical and future time frames (Tables 3 and 4). The same approach is taken for those of the wind energy metrics by enlisting the historical and future Oklahoma Mesonet estimates, as shown in Tables 6 and 7. These tables contain the percentage changes in each of these wind energy metrics between the near future and historical and the far future and historical time frames respectively. As with Tables 3 and 4, these percentage changes were broken down by enlisted GCM, season, and time of day, with statistically significant ($p < 0.05$) changes indicated by red-colored cells.

Consistent with the results from Section 4.1, the number of statistically significant results produced when comparing the far future and historical time frame (Table 7) greatly outnumbers those from the near future versus historical time frame (Table 6). Since the difference in time between the data frames that comprise Table 7 is greater, it is understandable that more statistically significant results would exist, providing that the long-term temporal change in these wind energy metrics is consistent. In fact, the patterns of these statistically significant changes are quite similar to those of Tables 3 and 4. For instance, Tables 6 and 7 demonstrate that statistically significant changes occur most frequently in summer and autumn, and less so in spring and winter, which is somewhat consistent with the pattern of projected changes shown in Tables 3 and 4.

Another consistent result is the tendency for higher resolution GCMs projecting a larger number of statistically significant changes, with HadGEM2-ES and IPSL-CM5A-MR in particular

presenting such a result in Table 7. These statistically significant changes can also be quite large, with HadGEM2-ES projecting far future reductions of WPD of up to -28% at certain times of day, constituting a large loss of wind energy resources. There is often, however, significant disagreement in the sign of statistically significant changes for the same wind energy metric projected by different GCMs. For instance, whereas GFDL-CM3 projects near future reductions of summer 12Z ramp up events of -15.7%, ACCESS 1.0 projects an increase in this particular quantity of 7.4%. Much like when LLJ characteristics were examined in Section 4.1, there appear to be considerable differences when comparing the magnitude and sign of statistically significant projections of wind energy metrics by different GCMs. The effects of grid resolution and differences in GCM constructions in terms of their effects on the results of the current study shall be discussed further in Chapter 6.

Despite the patterns in Tables 6 and 7 being like those of Tables 3 and 4 in terms of GCM and seasonal differences, the former set of tables possesses little diurnal consistency. Whereas projected changes of LLJ characteristics possessed a noticeably larger number of statistically significant changes at night, changes in wind energy metrics do not seem to favor a particular time of day, especially not in Table 7.

Concerning the sign and magnitude of the statistically significant changes presented in these tables, there are several results of interest. Models that project increases in wind speed and WPD are more likely to project decreases in the frequency of winds below V_{in} and increases in those above V_{out}. For instance, the ACCESS 1.0 GCM projects far future summertime wind speed increases of up to 19%, whilst at the same time projecting reductions of below V_{in} frequency of up to -44%. By contrast, the respective percentages projected by GFDL-CM3 are -18% and 58%. Such a relationship between different wind energy metrics might be expected to occur, since a

	ACCESS 1.0				GFDL-CM3				GFDL-ESM2G			
	Winter	Spring	Summer	Autumn	Winter	Spring	Summer	Autumn	Winter	Spring	Summer	Autumn
Below 3m/s - 00Z	-1.3	-2.1	-39.4	-17.1	9.7	1.3	15.3	-4.5	-0.4	-2.6	-1.1	-1.2
Below 3m/s - 06Z	6	1.1	-35.1	-13.3	9.5	-0.7	15.3	-3.8	2.6	-1.4	4.5	6
Below 3m/s - 12Z	6.9	3.8	-22	-9.7	2.5	8.9	34.5	-0.5	5.9	-1.6	-4.6	0.4
Below 3m/s - 18Z	4.9	-6.3	-28	-7.6	3.8	0.2	39.5	-8.2	0.4	-8.7	9.5	0.2
Above 25m/s - 00Z	8.7	-9.6	730.4	68.3	-39.3	-10.1	-40.8	34.2	6.7	44.1	2.5	0
Above 25m/s - 06Z	-6.8	4	438.1	90.2	-42.9	-0.2	-43.9	-11	-1.5	6.1	8.8	-40.9
Above 25m/s - 12Z	-6	38.4	520	84.8	-20.8	-28.7	-85.7	45.7	-6.7	14.5	0	-11.4
Above 25m/s - 18Z	-25.1	15.3	293.5	5	-13.7	0.6	-93.5	50.2	7.1	51.4	-29.7	-19.8
Ramp Up Events 00Z	3.7	-0.2	0.6	3.3	-5.4	0.9	-2.3	0.6	1	-0.3	-0.3	-0.2
Ramp Up Events 06Z	-0.3	0	15.9	2.9	-6.1	-0.8	-4.3	-2.2	0.3	3.9	2.2	-3.6
Ramp Up Events 12Z	-1	-1.1	7.4	-0.3	-3.2	-1.6	-15.7	1	0.2	2.2	-1.2	-3.4
Ramp Up Events 18Z	-1.9	0.1	5.4	-1.2	-0.6	0.1	-14.5	1.5	1.8	3.4	-2.4	-0.1
Ramp Down Events 00Z	0.6	0.3	0.4	0.8	-3.5	0.3	-2.3	0.5	-2	1	-2.7	0.6
Ramp Down Events 06Z	-6.1	4.5	14.9	2.2	-7.3	0.2	-5.3	-2.3	-8.5	2.7	-0.9	-5.1
Ramp Down Events 12Z	-5.1	-2.9	10.5	-6.1	-6.6	-0.5	-17.5	-9.5	-8.1	0.9	-2.8	0
Ramp Down Events 18Z	-3.3	1	5.1	-3.2	-2.6	-0.9	-21	-4.9	-6.4	4.2	-5	-0.5
Median WPD 00Z	2	0	70.5	12.9	-13.2	-3.4	-16.3	6.9	-4.1	6.3	0	0.5
Median WPD 06Z	-0.5	-5.2	77.5	6.6	-10.3	3.7	-22.7	-1	-7.5	-1.8	-4.3	-6.8
Median WPD 12Z	0	-3.4	31.3	3.4	-13	-6.5	-41.6	0.2	-8.9	0	5.8	-7.6
Median WPD 18Z	-4.9	8.9	54.4	10.4	-5.7	4.9	-37.6	5.9	-0.5	10.7	-4.8	-3.1
Median Speed 00Z	0	0	21.2	4.3	-4.8	0	-3.8	2.2	0	1.8	0	0
Median Speed 06Z	0	0	19.5	2.6	-2.6	0	-4.9	0	0	0	0	-2.6
Median Speed 12Z	0	0	11.1	0	-2.7	-2.3	-11.1	0	0	2.3	0	-2.7
Median Speed 18Z	-2	1.6	13.7	1.9	-2	1.6	-11.8	1.9	0	3.3	-2	-1.9

Table 6: Percentage changes of the six wind energy metrics selected for the current study between the historical and near future time frames.

- Changes in the wind energy metrics projected by the GCMs are separated by season and time of day. Red cells indicate changes in annual rank of a given wind energy metric that were statistically significant according to a Mann-Whitney U-test ($p < 0.05$).

	GFDL-ESM2M				HadGEM2-ES				IPSL-CM5A-MR			
	Winter	Spring	Summer	Autumn	Winter	Spring	Summer	Autumn	Winter	Spring	Summer	Autumn
Below 3m/s - 00Z	2.2	3.5	26.9	0.6	-9	-9.1	-17.2	-8.5	9.4	-0.1	-6.7	17.6
Below 3m/s - 06Z	0.7	1.3	14.9	0.1	2.5	-8.2	-21.2	-11.3	5.1	-3.6	9.4	8.5
Below 3m/s - 12Z	8.9	-1.1	14.1	-1.3	2.7	2.3	-25.8	-8.7	6.6	-2.1	13.7	15.3
Below 3m/s - 18Z	3.1	2.4	24.3	3.7	0.3	-4	-13.3	-4.1	9.5	3.1	-5	25
Above 25m/s - 00Z	-20.5	-11.2	-62.3	-16.5	50	58.9	87.3	-8.6	-31.5	35.8	17.9	-73.4
Above 25m/s - 06Z	-18	4.6	-36.7	-29.1	-50.9	74.1	89.7	-19.7	-29.1	15.7	-44	-75.2
Above 25m/s - 12Z	-47.3	-18.5	-33.3	31.1	-24.9	13.2	83.3	0	-34.3	-0.1	-66.7	-65.5
Above 25m/s - 18Z	-20.3	-8.3	-78.7	-30.9	-21.8	26.1	117.5	1.1	-32.3	-24.6	61.8	-78.5
Ramp Up Events 00Z	-2.2	-0.2	-5.6	-2.4	5.9	2.1	-1.8	0.8	-6.3	-1.7	-0.7	-9.9
Ramp Up Events 06Z	-2.1	-1	-4.9	-1.8	-2.4	2.8	4.7	-0.7	-3.4	-2	-10.2	-11
Ramp Up Events 12Z	-3.2	0	-5.6	1	0	-2.7	0	-0.5	-2.1	-1.5	-10.8	-7.8
Ramp Up Events 18Z	-1.3	-0.3	-6.8	-2.8	-1.7	-0.7	1.5	0.8	-3.7	-0.7	1.6	-10.8
Ramp Down Events 00Z	2.2	0.3	-1.3	2.5	-7.7	-5.2	-5	-13.2	-13.8	1	1.2	-13
Ramp Down Events 06Z	0.3	3.6	-3.5	3.2	-13.1	-1.3	-8	-15.4	-13.2	-4.5	-13	-19
Ramp Down Events 12Z	-1.3	1.9	-4.8	7.5	-15.1	-5.4	-8.8	-23.3	-10.9	-5.6	-11.3	-13.4
Ramp Down Events 18Z	-1.7	1.9	-4.1	0.3	-10.4	-5.2	-7.8	-12.8	-10.1	-4.6	4.1	-12.8
Median WPD 00Z	-4.5	0	-21.2	-4.1	21.1	6.1	28	6.3	-14.5	1.7	5.7	-18.5
Median WPD 06Z	-7	1.9	-14.1	-11.8	0	10.6	24.2	14	-10.2	13.8	-7.6	-15.8
Median WPD 12Z	-9.9	4.4	-23.5	-0.6	0.3	5.8	31.1	8.1	-6.4	0	-15.2	-21.2
Median WPD 18Z	-10.5	-3.7	-24.6	-10.5	-4.8	5.6	21.4	6.5	-6.5	-1.4	11.9	-27.2
Median Speed 00Z	-2.4	0	-7.7	-2.2	4.8	3.6	7.7	2.2	-2.6	2.1	2.2	-7.5
Median Speed 06Z	-2.6	0	-4.9	-2.6	0	4.5	7.3	2.6	-2.6	0	-5.6	-5.6
Median Speed 12Z	-2.7	0	-5.6	0	0	2.3	2.8	0	-2.4	0	-6.7	-9.1
Median Speed 18Z	-2	0	-7.8	-3.7	-2	1.6	5.9	1.9	-2	-1.6	3.7	-9.3

Continuation of Table 6.

higher median wind speed for a given year likely indicates a shift in distribution of most frequent wind speeds towards higher values. This difference in the signs of projected wind energy metrics by different models has been seen in previous studies, such as that of Johnson and Erhardt (2016), who also observed that downscaled GFDL GCMs had more of a tendency to project reductions of wind speed over the United States than other GCMs.

It should also be pointed out that the projections for frequency of winds above V_{out} can often be associated with large percentage changes, often in the hundreds of percent, which is particularly common for the ACCESS 1.0 GCM. These large changes can be attributed to the historical frequency of cut-out events over the Oklahoma Panhandle being small, with hub-height winds at most Mesonet stations rarely being greater than 25 m s^{-1}. In fact, ACCESS 1.0 often stands out amongst this collection of GCMs, since much more of its statistically significant projections are increases in wind energy metrics than the other five GCMs. Kulkarni and Huang (2014) also found that ACCESS 1.0 has a tendency to project increases in wind speed over the South-Central Plains region, unlike many other CMIP5 GCMs. Table 7 suggests such a result frequently, in which even the other higher-resolution GCMs, HadGEM2-ES and IPSL-CM5A-MR, project decreases in every metric except for the frequency of winds below V_{in}. This result again draws attention to the effects of inter-model variability on the results of the current study, which has also been seen in previous studies that examined biases of these GCMs, such as Harding et al. (2013) and Danco and Martin (2017).

It should be noted as well that this tendency to favor statistically significant reductions in wind speed and WPD over the Oklahoma Panhandle appears to contradict the results of previous work that studied this part of the United States, such as Pryor and Barthelmie (2011), Stadler et al. (2015), and Johnson and Erhardt (2016). This discrepancy with previous work could be a

	ACCESS 1.0				GFDL-CM3				GFDL-ESM2G			
	Winter	Spring	Summer	Autumn	Winter	Spring	Summer	Autumn	Winter	Spring	Summer	Autumn
Below 3m/s - 00Z	0.4	-12.6	-43.8	-16.6	10	3.4	15.8	0.4	7.9	-12.6	12.6	-3.9
Below 3m/s - 06Z	10.6	-1.1	-39.7	-19	13.4	-0.4	15.7	-1	14.9	-0.3	9.8	-0.7
Below 3m/s - 12Z	7.5	-2.6	-22.4	-13.6	12.2	1.4	36.5	6.7	12.7	1	11.5	1.1
Below 3m/s - 18Z	8.1	-8.4	-32.6	-5.5	8.2	5.2	58.9	5.9	12.9	-6.4	20	-0.2
Above 25m/s - 00Z	3.2	99.4	1066.4	68	-44.5	-24.1	-39.1	-10.5	-31.1	101.2	-39.2	24.8
Above 25m/s - 06Z	-48.5	84.4	430	74.5	-42.9	-8.2	-41.2	-13.4	-53.8	39.7	-21.7	-21.3
Above 25m/s - 12Z	-31.5	53.5	560	-12.1	-45	-29.4	-85.7	-71.4	-54.6	14.7	0	18.2
Above 25m/s - 18Z	-29.3	48.1	607.4	-15	-36.6	-31.6	-98.1	-33	-54.6	70.6	-68.3	-5
Ramp Up Events 00Z	1.7	1.5	1.5	2.3	-5.9	0.3	-1.5	0.2	-2.4	0.9	-2.6	1.6
Ramp Up Events 06Z	-6.6	5.4	13.5	0	-6.6	-0.3	-3.6	-2.5	-8	2.9	-0.5	-4.5
Ramp Up Events 12Z	-4.5	-1.8	8.3	-6.4	-7.4	1	-14.4	-5.9	-7.8	2.2	-2.5	-0.5
Ramp Up Events 18Z	-2.1	0.1	5	-4.2	-1.7	-1.3	-21.4	-4.5	-3.5	3.6	-5.5	1
Ramp Down Events 00Z	0.6	0.3	0.4	0.8	-3.5	0.3	-2.3	0.5	-2	1	-2.7	0.6
Ramp Down Events 06Z	-6.1	4.5	14.9	2.2	-7.3	0.2	-5.3	-2.3	-8.5	2.7	-0.9	-5.1
Ramp Down Events 12Z	-5.1	-2.9	10.5	-6.1	-6.6	-0.5	-17.5	-9.5	-8.1	0.9	-2.8	0
Ramp Down Events 18Z	-3.3	1	5.1	-3.2	-2.6	-0.9	-21	-4.9	-6.4	4.2	-5	-0.5
Median WPD 00Z	0	15.9	90.9	19.6	-16.8	-7.1	-16.3	0	-13.2	17.2	-11	5.2
Median WPD 06Z	-11.8	4	94.3	28.2	-10.3	6.5	-22.3	-1	-21.2	0.5	-13.8	-4.7
Median WPD 12Z	-8	5.1	33.6	15.8	-14.5	0	-41.2	-15	-19.5	-1.9	-14.8	-2.8
Median WPD 18Z	-4.9	15	59.9	0.8	-11.3	-7	-47.2	-12.9	-16.3	14.1	-16.2	0.4
Median Speed 00Z	0	5.5	25	4.3	-4.8	-1.8	-3.8	0	-2.4	5.5	-3.8	2.2
Median Speed 06Z	-5.3	4.5	19.5	2.6	-2.6	0	-4.9	0	-5.3	2.3	-2.4	-2.6
Median Speed 12Z	-2.7	0	8.3	-2.7	-2.7	-2.3	-11.1	-5.4	-5.4	0	-2.8	0
Median Speed 18Z	-2	3.3	17.6	-1.9	-4	-1.6	-17.6	-5.6	-6	4.9	-5.9	0

Table 7: Same as Table 6, but instead for changes in wind energy metrics selected for the current study between the historical and far future time frames.

- Changes in the wind energy metrics projected by the six GCMs are separated by season and time of day. Red cells indicate changes in rank of a given wind energy metric that were statistically significant according to a Mann-Whitney U-test ($p < 0.05$).

	GFDL-ESM2M				HadGEM2-ES				IPSL-CM5A-MR			
	Winter	Spring	Summer	Autumn	Winter	Spring	Summer	Autumn	Winter	Spring	Summer	Autumn
Below 3m/s - 00Z	0.1	-2.6	3.8	-10.5	13	24.2	-12.7	25.4	24.5	5.1	-18.8	20.3
Below 3m/s - 06Z	0.3	-2.5	1.4	-5.6	19.8	9.4	-18.2	8.9	20.2	6.4	1.5	11.5
Below 3m/s - 12Z	4.6	-6.1	7.2	-12.4	19	19.2	-23.7	18.2	21.8	10.3	3.3	22.4
Below 3m/s - 18Z	7.6	-5	17.4	-5.5	17.6	10.2	-9.8	10.3	30.3	11.6	-5	36.9
Above 25m/s - 00Z	6.7	37.6	-17.2	56.5	-59.9	-74.3	35.5	-87.9	-69.5	-9.7	76.4	-81.8
Above 25m/s - 06Z	-1.8	49.3	-16	37	-71.8	13.1	-17.8	-88.9	-74.1	-22.3	-40.5	-91.4
Above 25m/s - 12Z	-15.1	6.4	-16.7	166.7	-82.9	-52.6	-33.3	-100	-77.4	-33.7	-50	-77.4
Above 25m/s - 18Z	-26.8	15.4	-66.7	20.4	-78.9	-45.6	-56.7	-81.7	-83.2	-47	72.9	-91.4
Ramp Up Events 00Z	2.2	0	-1.9	3.2	-9	-5.4	-6	-14.5	-15.1	-0.5	3.3	-12.2
Ramp Up Events 06Z	-0.3	1.4	-2	1.8	-12.9	-0.3	-8.5	-16.7	-11.9	-5	-11.9	-19.9
Ramp Up Events 12Z	-2.9	2	-3.1	7.4	-13.5	-4.9	-6.8	-21.4	-7.8	-4	-10.2	-11.6
Ramp Up Events 18Z	-0.2	3	-4.3	0.6	-8	-4.7	-7	-11.1	-12.5	-3	3.6	-14.2
Ramp Down Events 00Z	2.2	0.3	-1.3	2.5	-7.7	-5.2	-5	-13.2	-13.8	1	1.2	-13
Ramp Down Events 06Z	0.3	3.6	-3.5	3.2	-13.1	-1.3	-8	-15.4	-13.2	-4.5	-13	-19
Ramp Down Events 12Z	-1.3	1.9	-4.8	7.5	-15.1	-5.4	-8.8	-23.3	-10.9	-5.6	-11.3	-13.4
Ramp Down Events 18Z	-1.7	1.9	-4.1	0.3	-10.4	-5.2	-7.8	-12.8	-10.1	-4.6	4.1	-12.8
Median WPD 00Z		6.7	-5.6	10.5	-17.6	-22.6	17.8	-28	-27.6	-4.2	28.2	-22.9
Median WPD 06Z	-2.8	9.8	-10	5.4	-20.7	-10.6	13	-3.5	-21.3	6.8	15.2	-10.2
Median WPD 12Z	-4	9.5	-14.3	8.5	-21.4	-13.1	17.3	-18.2	-20.3	-11	-6.5	-24.8
Median WPD 18Z	-9.3	2.3	-21.2	5.5	-21.2	-12.7	21.4	-19.5	-29.2	-13.1	12.3	-34.3
Median Speed 00Z	0	1.8	-1.9	4.3	-7.1	-7.3	1.9	-10.9	-7.9	0	6.7	-10
Median Speed 06Z	0	2.3	-2.4	2.6	-7.9	0	-2.4	-7.9	-7.9	-2.4	-5.6	-11.1
Median Speed 12Z	0	0	-2.8	2.7	-8.1	-4.7	-2.8	-13.5	-7.1	-3.8	-4.4	-11.4
Median Speed 18Z	-2	1.6	-5.9	1.9	-10	-6.6	0	-11.1	-11.8	-4.8	3.7	-13

Continuation of Table 7.

consequence of multiple factors, which shall be considered in the discussion of the current study in Chapter 6.

Much like when considering Tables 3 and 4, summarizing the multi-model projections of changes in wind energy metrics from Tables 6 and 7 is difficult, due to the large numbers of rows and columns that these tables contain. As such, Table 8 condenses Tables 6 and 7 and conveys the tendency for increases and decreases in each wind energy metric, whether the changes are statistically significant or otherwise. It is clear from this table that the proclivity for reductions in wind energy metrics is not limited to statistically significant changes. Whilst the trends when comparing the near future and historical time frames of the Mesonet data have less of an obvious overall trend, the far future minus historical time frames strongly favor reductions in wind speed, WPD, the frequency of ramp up/ramp down events, and the frequency of wind above V_{out}. The implication of these results is an overall reduction in hub-height level wind speeds and therefore in the Oklahoma Panhandle's wind energy resources in the coming decades. Furthermore, given the reduction of wind speeds projected by these GCMs, a negative relationship with the frequency of winds below V_{in} would be expected, therefore increasing the credibility of the projections presented in Tables 6, 7, and 8.

As stated above, this reduction in overall wind energy resources is not particularly consistent with the increases of wind speed and WPD that have been projected by multiple studies that considered the Oklahoma Panhandle in their spatial domains (Pryor and Barthelmie, 2011; Stadler et al., 2015; Johnson and Erhardt, 2016), since other studies have largely projected increases in the magnitude of these two wind energy metrics over this region. Based on Table 8, this lack of consistency between the current and previous studies is true for both statistically significant and non-significant changes in wind energy metrics.

	Near Future Positives vs Negatives			Far Future Positives vs Negatives		
	Positive	Negative	No Change	Positive	Negative	No Change
Below 3m/s - 00Z	9	15	0	15	9	0
Below 3m/s - 06Z	15	9	0	14	10	0
Below 3m/s - 12Z	14	10	0	18	6	0
Below 3m/s - 18Z	15	9	0	15	9	0
Above 25m/s - 00Z	13	11	0	11	13	0
Above 25m/s - 06Z	9	15	0	7	17	0
Above 25m/s - 12Z	8	14	2	6	17	1
Above 25m/s - 18Z	11	13	0	6	18	0
Ramp Up Events 00Z	9	15	0	11	12	1
Ramp Up Events 06Z	7	16	1	5	18	1
Ramp Up Events 12Z	5	16	3	5	19	0
Ramp Up Events 18Z	9	15	0	7	17	0
Ramp Down Events 00Z	13	11	0	13	11	0
Ramp Down Events 06Z	8	16	0	8	16	0
Ramp Down Events 12Z	4	19	1	5	18	1
Ramp Down Events 18Z	6	18	0	6	18	0
Median WPD 00Z	12	9	3	9	12	3
Median WPD 06Z	9	15	0	10	14	0
Median WPD 12Z	10	11	3	6	17	1
Median WPD 18Z	9	14	0	9	15	0
Median Speed 00Z	10	7	7	9	11	4
Median Speed 06Z	5	9	10	7	13	4
Median Speed 12Z	5	9	10	2	17	5
Median Speed 18Z	10	12	2	6	16	2

Table 8: A condensed form of Tables 6 and 7 that presents the number of cells in each row that possess increases, decreases, or no change for a given wind energy metric and time.
- The results from the near future minus historical time frames (Table 6) are shown on the left, with far future minus historical (Table 7) on the right. The blue cells indicate the most common sign for the changes of each wind energy metric and time combination, with the darker blue cells indicating signs that are deemed especially frequent in their occurrence (greater than 16 cells per row).

5.2. Changes in Variability of Wind Energy Metrics

Assessment of changes in the variability of the six wind energy metrics is also an important part of creating the desired holistic perspective on the potential future of Oklahoma's wind energy resources. Much like in Section 4.2, boxplots have been constructed that present the changes in annual median wind speed and wind power density, as well as annual counts of ramp up/down events and frequency of winds above V_{in}/below V_{out} (250 data points per boxplot – 25 from each Mesonet location). Those boxplots that possessed the most notable results are presented in this section, as was done in Section 4.2. Breaking down construction of these boxplots by GCM, season, and time of day again allows for a more complete analysis of changes in variability in these metrics. Due to the similarity of projected variability changes that some of these wind energy metrics possess, presentation of results is grouped together as such: wind energy and WPD, ramp up event frequency and ramp down event frequency, and frequency of winds above V_{out} and below V_{in}. It is also important to clarify that each individual boxplot presented is constructed using 25 annual wind energy metric values from all 10 Oklahoma Mesonet stations, totaling 250 data points in each boxplot.

5.2.1. Variability of Wind Speed and WPD

A result that is consistent across all of the presented boxplots, regardless of the wind energy metric(s) considered, is that the differences in variability that they possess are quite small. Diurnal, seasonal, across GCM, and across time frame differences all indicate such a result. Nevertheless, some notable results did arise from the analysis. Figure 20 (and Appendix B1) presents a collection of boxplots that illustrate the variability of median wind speed and WPD over the Oklahoma Panhandle. Many of these boxplots possess statistically significant ($p < 0.05$)

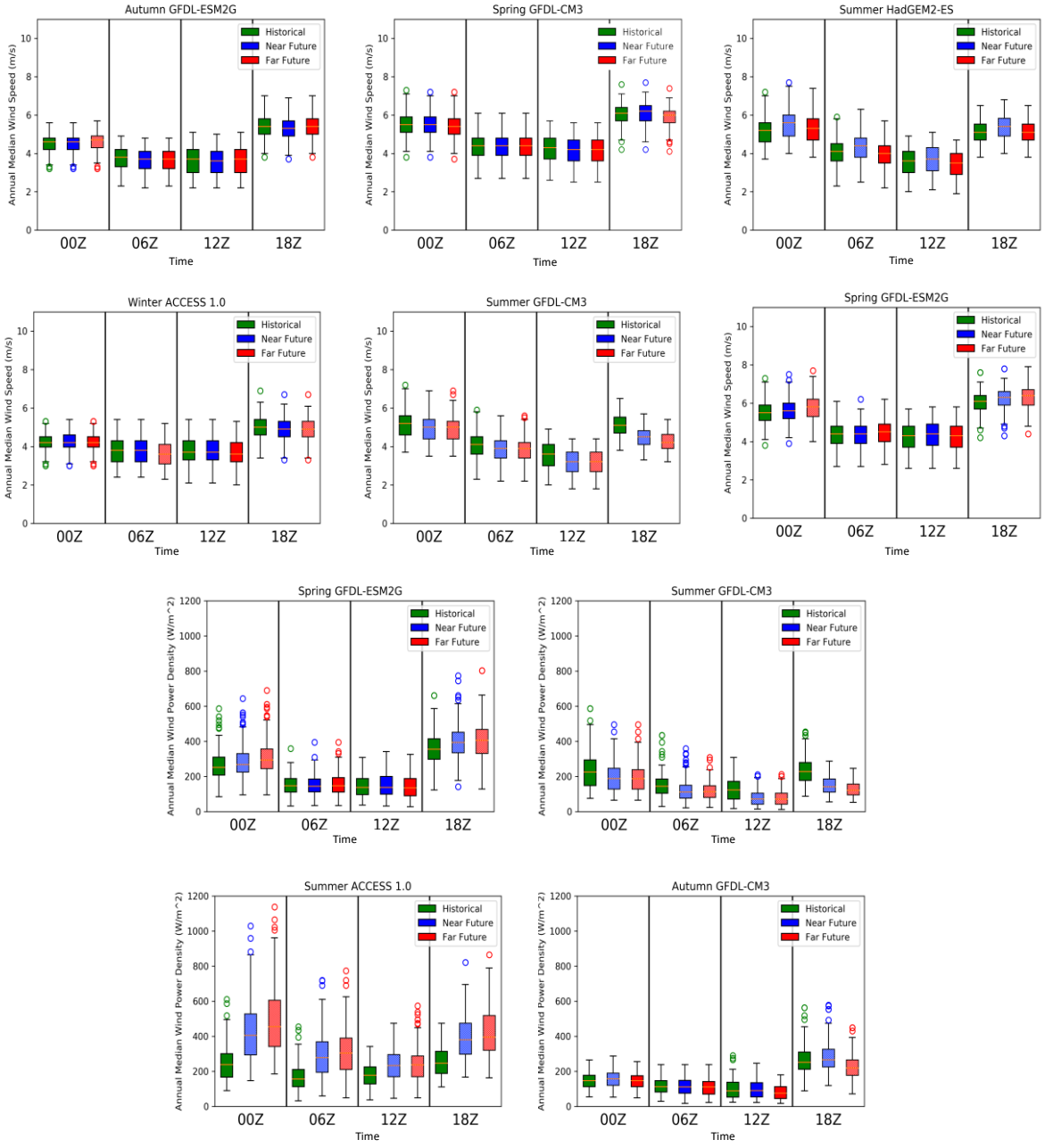

Figure 20: Boxplots showing median wind speed in (m s^{-1}, top two rows) and median WPD (W m^{-2}, bottom two rows) within the Oklahoma Panhandle for each individual time frame across each GCM's grid points. - The boxplots are grouped by season and the GCM that was used to produce them, with each set of three boxplots on a given pair of axes representing the historical (green), near future (blue), and far future (red) spread of median wind speeds and WPDs for a given time of day (00Z, 06Z, 12Z, 18Z). Statistically significant boxplots are indicated by lighter colors.

changes between historical and future time frames, especially those obtained for summer, since Tables 6 and 7 found such results to exist.

As stated above, median wind speed and WPD have been grouped together in Figure 20, since the trends in variability that they possessed were so similar, owing to WPD mainly being a function of the cube of the wind speed (see Equation 2 in Section 3.2). These similarities are especially true for diurnal variability – across all seasons but especially so in spring and summer, median wind speed was found to be 1-2 m s^{-1} greater at night than during the day. Several literature examples confirm the authenticity of this result. Both Dai and Deser (1999) and Zhang and Zheng (2004) found from observational studies of diurnal wind speed variability that wind speeds across the United States (including the Oklahoma Panhandle) tends to peak in strength in the early afternoon (to which 18Z is the closest daytime point used in the current study). These studies attributed this maximum daytime speed to enhanced surface level convergence associated with the convective boundary layer. It would therefore seem that the diurnal variability of projected future estimates of wind speed and WPD across the Oklahoma Panhandle is consistent with observed wind climatology.

Diurnal variability is not projected to notably change when comparing boxplots constructed from different time frames of data and/or different GCMs. This result agrees with those from Goddard et al. (2015) and Figure 11 that future changes in the United States' wind speed variability might be limited. Despite this agreement with previous work, an argument can be made for seasonal variability being larger in spring and summer than autumn and winter. Such a result is apparent when comparing the boxplots created using spring (second row, right) and autumn (first row, left) data projected by GFDL-ESM2G, with the former showing slightly higher variability in 00Z and 06Z annual median winds. In fact, some projections, such as those of WPD by spring GFDL-

ESM2G (third row, left) and summer ACCESS 1.0 (fourth row, left), seem to indicate that variability of these wind energy metrics is not only greater in spring and summer, but could also increase with time, given the greater spread in future median WPD that these boxplots present. These large WPD projections could in part be a consequence of not bias-correcting the GCM outputs used in the current study (as mentioned in Section 3.1), since any historical wind speed biases would be cubed in calculations of WPD, so importance attached to this result should be limited.

However, the general pattern presented by the boxplots is one of small changes in the spread of median WPD and wind speed, with changes in central tendency being larger overall. This pattern can be seen when considering wind speed and WPD outputs from summer GFDL-CM3 (second row, center) and just WPD outputs from spring GFDL-ESM2G. The fact that many of these boxplots possess statistically significant ($p < 0.05$) evolutions in these wind energy metrics without notable changes in the spread in the boxplot data indicates more notable changes in central tendency than their variability, which again agrees with expectations of previous literature (Goddard et al., 2015).

A final result of interest that these boxplots present concerns their comparison across time frames. It has already been seen that GCMs project slight reductions in wind speed and WPD, regardless of season or time of day (see Table 8). However, Figure 20 indicates that the increases projected by these GCMs (uncommon though they may be) can be much larger than projected decreases. These decreases typically do not exceed -0.5 m s^{-1} (-100 W m^{-2}), such is the case for wind speed (WPD) projections for summer GFDL-CM3. On the other hand, results for ACCESS 1.0 in summer project increases in WPD of over 200 W m^{-2}, which is a much larger although less common projection. Section 5.1 also stated that projections of wind energy metrics by ACCESS

1.0 did not often agree with those of the other GCMs, despite this model's projections being consistent with those from previous work, such as Kulkarni and Huang (2014) and Stadler et al. (2015). The overall picture from these results is one of little overall future change in central tendency of wind speed and WPD (except during spring and summer), and even smaller changes in their variability.

5.2.2. Variability of Ramp Up and Ramp Down Event Frequency

The next two wind energy metrics considered are the frequency of ramp up and ramp down events - descriptors of changes of wind power capacity in short spaces of time. A change in the climatological frequency of ramp events is potentially important, since a greater ramp up frequency, for instance, signifies rapid increases of wind speed over the Oklahoma Panhandle occurring more frequently. As discussed in Section 3.2.3, a larger number of ramp events results in more intermittent wind energy supply, and consequently greater difficulty in managing it for electricity demand. Figure 21 (and Appendix B2) shows a collection of boxplots that illustrate the variability in these two wind energy metrics, with the top two rows being boxplots for ramp up event frequency and the bottom two for ramp down event frequency. These two metrics were presented in the same figure because the variability patterns that transpired from them were quite similar.

This analysis of ramp up and ramp down event climatology across the Oklahoma Panhandle does have some consistency with observational studies. Sevlian and Rajagopal (2013) conducted statistical analysis on two years of wind power outputs from the Pacific Northwest and found that the seasonal patterns of ramp up and ramp down event frequency are indeed almost identical, with both metrics possessing higher frequency in spring and summer. Figure 21 shows

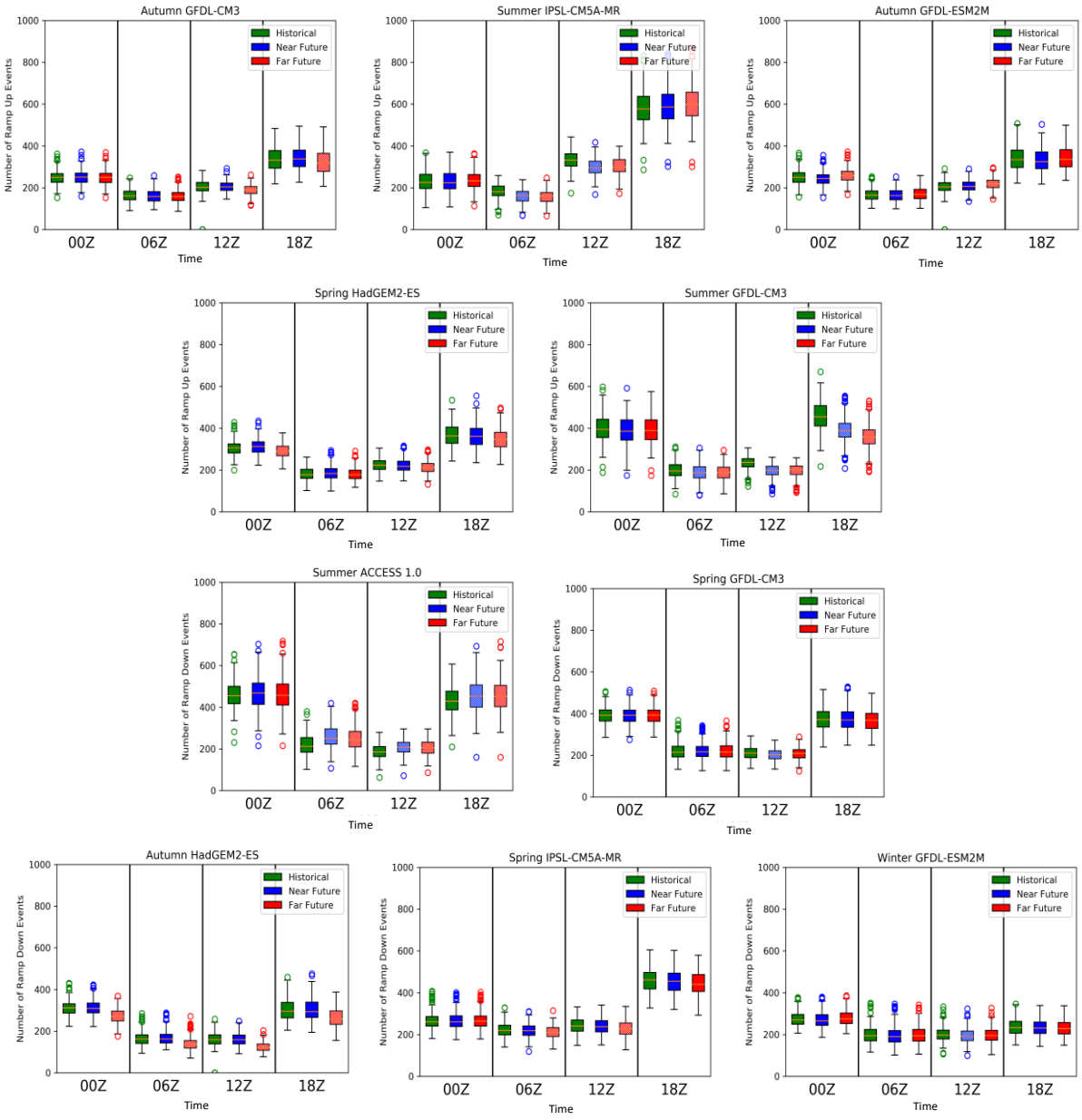

Figure 21: Same as Figure 20 but for frequency of ramp up events (top two rows) and ramp down events (bottom two rows).

consistency with this expectation, with median ramp up frequency from GFDL-CM3 at 00Z being approximately 400 ramp events per year in summer (second row, right), but only 250 ramp events per year in autumn (first row, left), with little to no difference in this value when comparing boxplots from different time frames.

Furthermore, the diurnal variability presented in this figure also agrees with previous work. A study conducted by Kamath (2010) considered historical patterns of ramp events using observed wind power outputs, and found that ramp events, particularly ramp up events, occur more frequently during the late morning and early afternoon than any other time of day. This greater daytime ramp event frequency does appear in Figure 21, which is captured especially well by IPSL-CM5A-MR, given the much greater recreated and projected daytime frequency that it presents for ramp up events in summer (top row, middle) and ramp down events in spring (bottom row, middle).

When comparing changes in ramp event frequency between historical and future time frames, the spread of ramp event counts does not seem to change as much as their median value. The predominant result from these projections is one of decreases in the number of ramp up and ramp down events across the Oklahoma Panhandle by the end of the century, with reductions of up to 50 fewer ramps in a given year in some cases, such as that projected by HadGEM2-ES in autumn (bottom row, left) and IPSL-CM5A-MR in summer. As in Section 5.2.1, ACCESS 1.0 again projects increases in ramp event frequency (third row, left), though less noticeably so than for the projections of wind speed and WPD presented in Figure 20. The overall picture remains one of future reductions in the number of ramp up and ramp down events across the region, with fewer ramp events resulting in slower and smaller changes of local wind speeds over short time periods. This reduction in the median count of future ramp events could be a result of a greater

LLJ frequency resulting in winds that are less variable in terms of their speed and direction, thus producing these smaller and slower wind power capacity changes. A more stable supply of wind energy from the Oklahoma Panhandle would therefore be produced, one that is less challenging for grid managers to control and distribute. Potential explanations for reduced ramp event frequency shall be explored specifically in Section 5.4, with the implications of fewer ramp events on the future of Oklahoma's wind energy resources considered in Chapter 6.

It is also important to highlight that the results presented in Figure 21 could have been different, had another definition of ramp event occurrence been used. The figure shows that the number of ramp events that occur over the Oklahoma Panhandle in a given season and time of day can range anywhere from only 100 events in a given year during autumn and winter at night, to close to 900 events in a given year during daytime spring and summer. These frequencies were obtained using the definition of ramp events enlisted by Bradford et al. (2010) and Kamath (2011), as discussed in Section 3.2.3. However, it was stated by Ela and Kemper (2009) in their analysis of ramp event occurrences in Colorado that the selected definition for a ramp event's occurrence can affect these numbers considerably, and by extension affect the extent of future changes in their variability. Chapter 6 considers the effects of selecting different ramp event definitions further.

5.2.3. Variability of Below Cut-In and Above Cut-Out Frequency

The final pair of wind energy metrics to consider in terms of their variability is frequency of winds below V_{in} and above V_{out}. Whilst their variability and projected changes are not necessarily similar, the language used to discuss them is similar, hence they have been grouped together. Figure 22 (and Appendix B3) displays the sets of boxplots for these two metrics, the top two rows being boxplots for V_{in} and the bottom two for $V_{out,}$ with the values in each boxplot

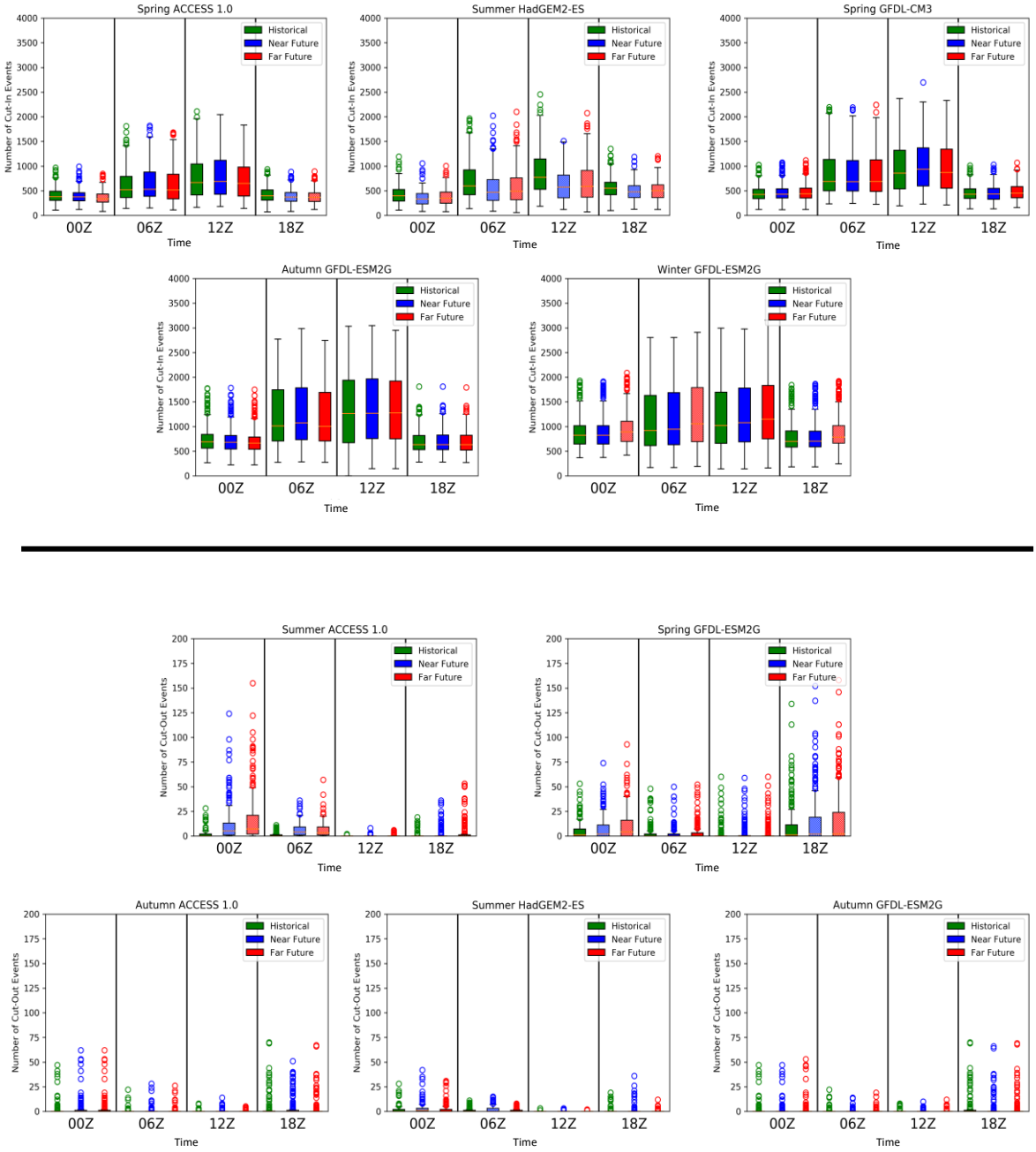

Figure 22: Same as Figure 20 but for frequency winds below V_{in} (top two rows) and above V_{out} (bottom two rows).

comprised of annual counts of wind speed occurrences that are below V_{in}/above V_{out}, broken down by GCM, time frame, season, and time of day. Drawing comparisons between previous literature and this figure is challenging, owing to the lack of studies that have considered the frequency of winds below and above these thresholds. As such, the current study represents a new attempt at not only quantifying the frequency of cut-in and cut-out events, but also examining these frequencies climatologically in the context of the availability of wind energy resources.

From studying the top two rows of Figure 22, it can be deduced that hub-height wind speeds are projected to be typically below the cut-in threshold much more often at night than during the day, but the spread of these occurrences is much larger. This diurnal variability and the spread of outcomes are particularly large in autumn and winter, with the median frequency of winds below V_{in} being up to 500 counts in a given year higher at night than during the day, and the spread of this frequency being up to 1000 counts in a given year higher. Outputs from GFDL-ESM2G for autumn and winter (second row of Figure 20) argue for this result. Figure 22's results seem to mirror those from Figure 20, with the latter showing that wind speed/WPD tended to be lower at night and during autumn and winter, hence the diurnal and seasonal cycle of V_{in} in Figure 22 appears to be credible.

Making deductions from the variability in frequency of V_{out} is difficult, since Figure 22 illustrates a low frequency in its value, regardless of the time of day, season, GCM, or time frame considered. The inability to make deductions is indicative of how infrequently hub-height winds exceed the cut-out threshold in this region. However, there are a few interesting results, such as outliers in counts of cut-out frequency being greater during the day than at night. These outliers occur frequently in autumn, with ACCESS 1.0 (bottom row, left) and GFDL-ESM2G

(bottom row, right) demonstrating annual frequency counts of up to 75 cut-out events at sunrise (00Z) and during the day (18Z), but then being around three times lower at all other times of day.

The GCMs all seem to agree on the existence of daytime maxima of V_{out} frequency, as well as it being more pronounced in autumn. Greater daytime cut-out frequencies could be linked to near-surface wind speeds over this region of the United States typically maximizing during the afternoon (Dai and Deser, 1999), therefore perhaps increasing the chance of outliers in cut-out frequency at this time of day. A greater cut-out frequency is reflective of the consequences of greater wind speed during the day, as in Figure 20. Greater median wind speed could accompany a distribution in which winds are more likely to exceed the cut-out threshold. The diurnal and seasonal patterns of frequency of winds below V_{in} and above V_{out} therefore seem to make sense in the context of previous studies of these patterns, such as Dai and Deser (1999) and Zhang and Zheng (2004).

Much like the results shown in Figure 20, changes in variability across time frames are generally small for both V_{in} and V_{out}. Some results, such as HadGEM2-ES in summer (top row, middle), and ACCESS 1.0 in summer (third row, left), suggest larger projected changes in frequency of winds below V_{in} and winds above V_{out}, both in terms of median value and their spread, many of which are statistically significant ($p < 0.05$). However, these outputs appear to be in the minority, with most differences between historical and future time frames being limited to ±20 cut-out events in a given year (bottom row in particular), and ±150 cut-in events in a given year. It appears from these boxplots that, despite there being strong diurnal and seasonal patterns in these two wind energy metrics, their variability in future decades could be quite similar to what has taken place in the historical time frame.

5.3. Spatial Patterns of Wind Energy Metrics

Having considered projected changes in the central tendency and variability of wind energy metrics, a final point of interest is the spatial patterns of these changes. The interest in examining these patterns is whether increases and decreases in these metrics are greater on one side of the Oklahoma Panhandle or another, and whether there is any consistency in these changes when considered diurnally, seasonally, or by GCM enlisted. As before, there are many maps that could potentially be made, so map presentation has been limited to those that possess results of particular note, with all maps possessing a statistically significant difference ($p < 0.05$) between the historical and selected future time frame for a particular wind energy metric.

Figure 23 shows the results from a collection of maps of projected changes in each of the six wind energy metrics across the Oklahoma Panhandle, with the location of each Mesonet station colored and sized according to the sign and magnitude of the projected change associated with it respectively. From examining the first two rows of maps, the largest changes of wind speed and WPD tend to occur towards the center of the Panhandle, with some GCMs occasionally projecting larger increases to the east, such as WPD for IPSL-CM5A-MR in summer at 06Z. The third, fourth, and fifth rows present maps of projected changes in ramp up/down event frequency, and frequency of winds below cut-in threshold respectively. These three metrics consistently experience greater changes on the east and west ends of the Panhandle, regardless of whether they are increases or decreases. The final row of the figure presents projected changes in the frequency of winds above the cut-out threshold, which all show greater changes in their number of occurrences on the west end of the Panhandle, again regardless of the sign of these projected changes.

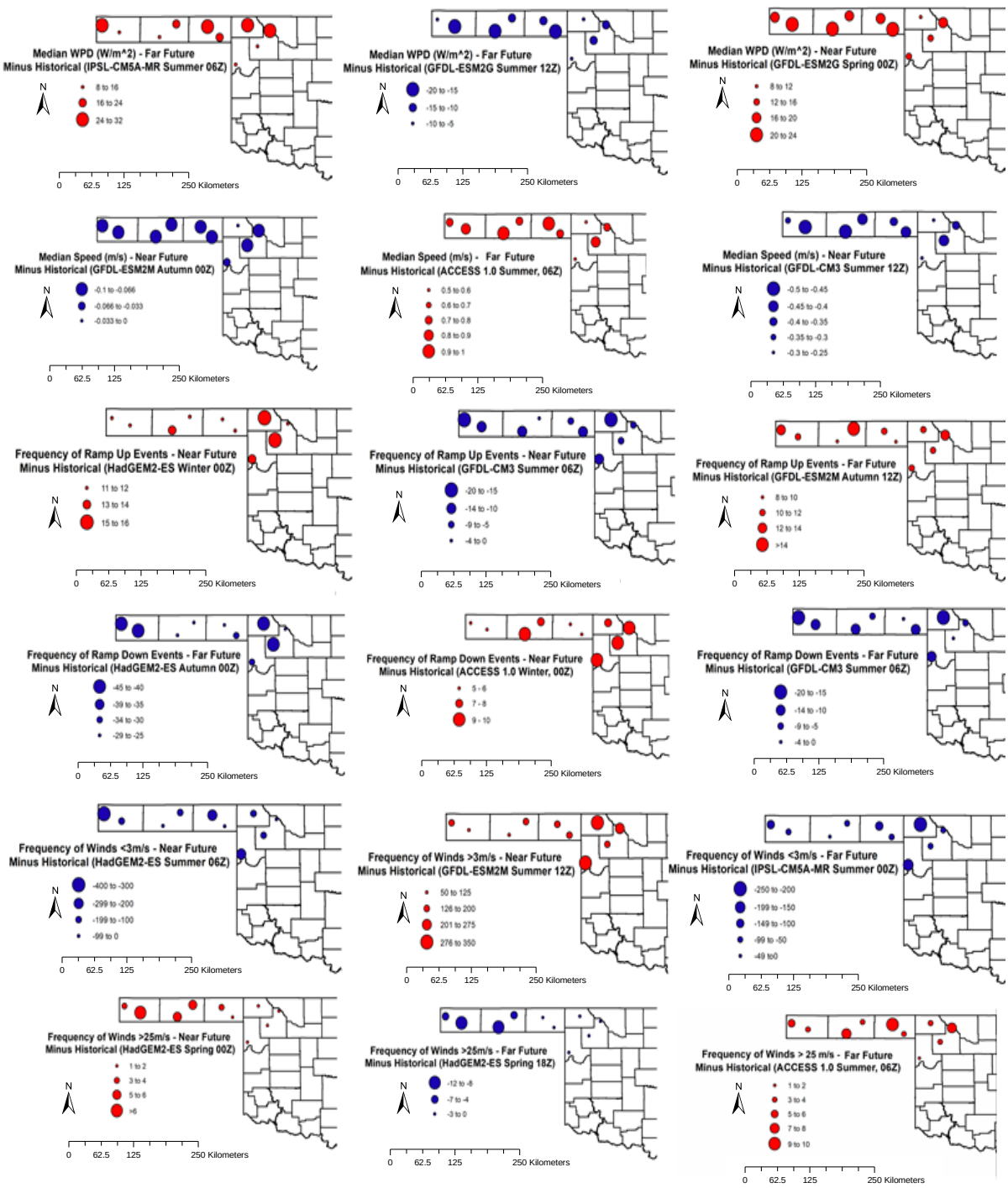

Figure 23: Changes in the six wind energy metrics across the Oklahoma Panhandle. - Projections were taken between the historical and near future (top row)/far future (remaining rows) time frames. Locations of each Oklahoma Mesonet station are colored based on increases (red) or decreases (blue) of each metrics with each point's size being proportional to the magnitude of the projected change. The projected changes presented in these maps are all statistically significant ($p < 0.05$).

In the case of all six of the wind energy metrics, there seems to be little of a diurnal, seasonal, or inter-timeframe pattern to the trends presented in this figure. This lack of trend can perhaps be attributed to the application of GCM outputs across the South-Central Plains region onto the smaller area that is the Oklahoma Panhandle, as discussed in Section 3.3.2. Figure 23 is a good example of how this limitation manifests – the application of a single factor change of median near-surface wind speed to all ten Mesonet locations may remove some of its spatial trends, which seems to have been the case. Despite the consequent loss of temporal detail in Figure 23, the results presented in Sections 5.1 and 5.2 were not affected by this, because central tendency and variability of wind energy metrics were evaluated across all 10 Mesonet locations, rather than individually.

5.4. Assessing the Linkage between LLJ Characteristics and Wind Energy Metrics

Thus far, the results chapters of the current study have presented potentially significant findings regarding both LLJ characteristics and wind energy metrics. Firstly, an overall projected increase in LLJ frequency with less of a definitive change in its speed or height (Section 4.1), with the biggest changes in LLJ frequency happening in summer, autumn, and at night (Section 4.2), as well as to the north of the South-Central Plains region (Section 4.3). Projected increases of frequency and increases to the north were more commonly projected by the higher-resolution GCMs, such as ACCESS 1.0 and HadGEM2-ES. Concerning wind energy metrics, the most notable results were slight reductions in wind speed and WPD, and larger decreases in the frequency of ramp up/down events and winds below V_{in}. As with the LLJ characteristics, the largest changes in these metrics were noted to occur in summer and autumn (Section 5.1), but with little pattern in projected changes diurnally (Section 5.2). It was also noted that the decision to downscale GCM outputs onto a small-scale, high resolution dataset over the Oklahoma

Panahndle has the weakness of reducing details in spatial variability (Section 5.3). The majority of GCMs were consistent in the signs of their projections of these wind energy metrics, with ACCESS 1.0 frequently standing out for its incongruent outputs, despite being consistent with its application in previous work.

Section 2.3 provided evidence for a link between the state of the LLJ and wind energy generation that has been seen in various observational studies (Cosack et al., 2007; Emeis, 2014b; Lampert et al., 2016). Having considered the projected changes in multiple LLJ characteristics and wind energy metrics across the South-Central Plains region, it is now possible to evaluate the linkage between these two features and how important it is for Oklahoma's wind climatology. This link was evaluated by conducting simple linear regression analysis on separate LLJ characteristics and wind energy metrics, with statistical significance ($p < 0.05$) determined using Spearman's Rho analysis (Yue et al., 2002). Linear regression was used to fit the LLJ and wind energy data against each other, since the most common type of relationship that they possessed was one with a linear shape when plotted. A similar approach was taken by Wimhurst et al. (2017) in their analysis of projected changes in near-surface wind speeds over the United Kingdom and their relationship with projected changes in the speed and latitude of the North Atlantic Jet. Owing to the large number of different combinations of time of day, season, GCM enlisted, time frame considered, and Oklahoma Mesonet location, thousands of simple linear regression analyses were created as part of the current study. As such, the analyses presented here are limited to those that possessed a statistically significant link for a given LLJ characteristic and wind energy metric, as well as those that summarize the most consistent and notable results of the conducted research. It is also important to point out that many of the figures presented in this section possess different axes scales, owing to the range of values that LLJ characteristics and wind

energy metrics can potentially possess. As such, it is necessary to take care when interpreting these figures, since the strength of the relationships that they each possess can be quite different, even if several of them look similar at first glance.

5.4.1. Linkage between LLJ Speed and Various Wind Energy Metrics

The approach taken to present the results from these regression analyses is to examine the relationship between the wind energy metrics and each of the three LLJ characteristics separately, starting with LLJ speed. An attempt was made at conducting a factor analysis that combined LLJ speed, height and frequency into a single characteristic and regressing the standardized outputs against the wind energy metrics, but the results of this analysis have not been included due to the lack of results that were conceptually sound or consistent with previous literature. Figure 24 presents the results from a selection of regression analyses of LLJ speed against various wind energy metrics, with each row representing results from a different metric. In these regression analyses, each plot point represents the value of median LLJ speed and a wind energy metric for a single season and time of day, such that the number of plot points is equal to the number of years of data enlisted in a single time frame (25 years = 25 plot points). Confidence intervals around each regression line are shown in a lighter blue, and the Rho-value is also given.

The relationship that LLJ speed seems to have with wind energy metrics is not particularly consistent. For example, the HadGEM2-ES GCM indicates that summers that experience greater hub-height wind speeds are associated with greater LLJ speeds in the far future time frame, regardless of time of day or Mesonet station considered, but are also associated with lower LLJ speeds in the near future time frame (rows a and b of Figure 24). It does not appear to make conceptual sense that the sign of the relationship

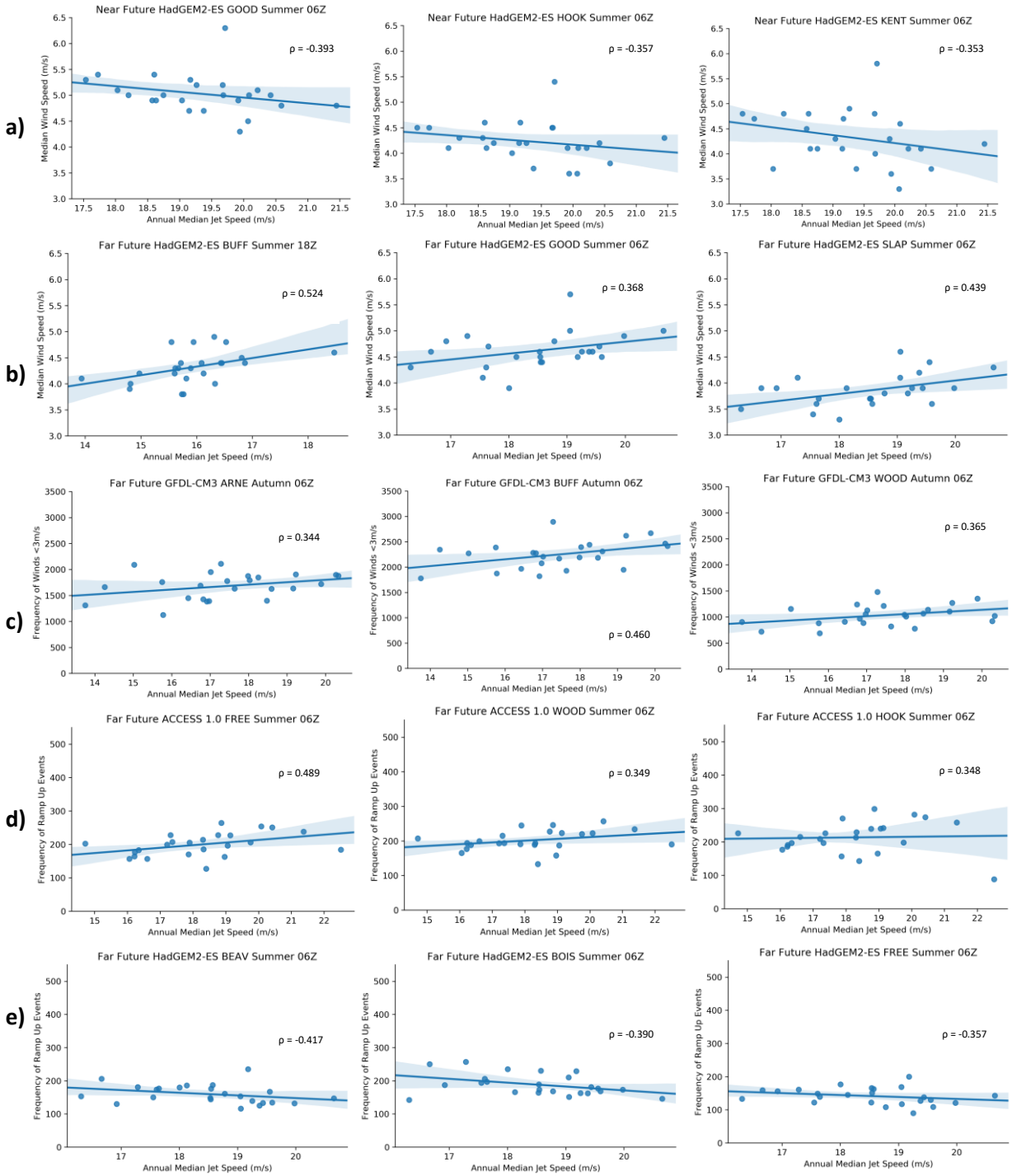

Figure 24: Linear regressions for LLJ speed against wind energy metrics.
- Each regression line and confidence interval (light blue shading) describes a statistically significant relationship ($p < 0.05$) based on a Spearman's Rho test. Each line (lettered) represents regression analyses using a different wind energy metric. Plot points represent the value of median LLJ speed in each year broken down by season, time of day, and corresponding wind energy metric. Regression analyses are also broken down by GCM, Mesonet station, and time frame considered.

between hub-height winds and LLJ speed would be negative as it is projected to be in the near future time frame, given the relationship indicated by previous literature (such as Lampert et al. (2016)), let alone that the sign in subsequent future time frames would reverse. This lack of a sensible and consistent relationship exists when considering other wind energy metrics as well. For instance, the GFDL-CM3 GCM suggests that a greater speed for far future nighttime (06Z) autumnal LLJs is associated with an increased frequency of winds below V_{in} (row c of Figure 24). This result seems counterintuitive, since one might expect that greater LLJ speed would be associated with greater hub-height winds and therefore a reduction in the frequency of cut-in events. The LLJ speed's relationship with these metrics is not particularly consistent when comparing the outputs of different GCMs either. Whereas ACCESS 1.0 projects greater numbers of ramp up events when far future summer nighttime (06Z) LLJs are faster (row d of Figure 24), the relationship projected by HadGEM2-ES is of opposite sign (row e of Figure 24).

Despite the large number of statistically significant links that LLJ speed and wind energy metrics possess, their lack of consistency on various temporal scales and when comparing outputs of different GCMs means that the relationships displayed in Figure 24 are often inconsistent with prior expectations. LLJ speed therefore perhaps lacks a strong influence on these metrics compared to other LLJ characteristics, or perhaps other climatological features that are connected to the LLJ, which shall be addressed in Chapter 6.

5.4.2. Linkage between LLJ Height and Various Wind Energy Metrics

Conducting regression analyses of LLJ height against the six wind energy metrics could be viewed as inappropriate, owing to its height having been evaluated in the current study using GCM height levels with a relatively coarse resolution (see Section 3.3.1). The consequent effect is several plot points in a given regression analysis possessing the same LLJ

height over a range of values for a particular wind energy metric (expressing LLJ height in meters would not rectify this), thus making it difficult to make any valid or conclusive remarks, regardless of whether the relationship that LLJ height and the metric possess is statistically significant. Linear regression should also not be performed with categorical and discrete data, such as LLJ height levels, which is another reason why such data presentation is inappropriate. For the sake of completeness of the current study, however, Figure 23 shows example regression analyses of LLJ height and a range of wind energy metrics to illustrate this point. Whilst it is possible that the lack of detail in height level changes between time frames could be making much of the relationship between LLJ height and wind energy metrics less clear, there is little to be concluded from the relationships presented in this work. Much like LLJ speed, LLJ height seems to have little of a consistent or notable influence on wind energy metrics.

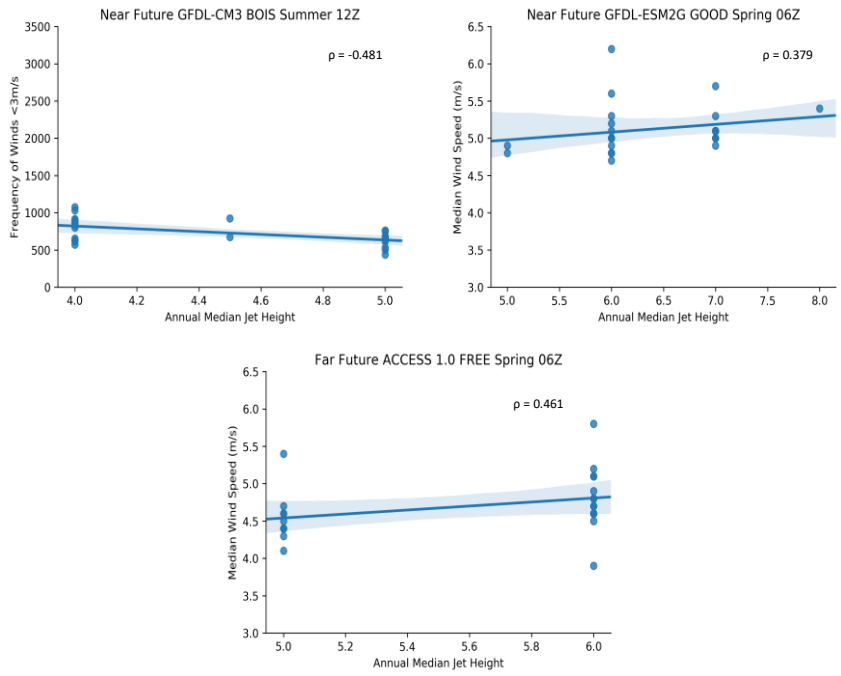

Figure 25: Same as Figure 24 but for relationships between LLJ height and various wind energy metrics.

5.4.3. Linkage between LLJ Frequency and Various Wind Energy Metrics

Unlike LLJ speed and height, LLJ frequency has relationships with wind energy metrics that are extremely consistent and conceptually sound. Figure 26 shows a collection of regression analyses of LLJ frequency against the six metrics. Overall, a much larger number of statistically significant links existed between LLJ frequency and wind energy metrics than existed for LLJ speed and height, with the majority of them occurring at night (06Z), near sunrise (12Z), and spring and summer – times of typically greater LLJ frequency (Doubler et al., 2015). More importantly, many of these statistically significant relationships fit an intuitive understanding and the previous results from the literature. Several GCMs indicate that a greater LLJ frequency is associated with greater hub-height speed and WPD. GFDL-ESM2G projects such a result for near future time frames for nighttime summertime LLJs (row a of Figure 26), as do ACCESS 1.0 and IPSL-CM5A-MR (row b of Figure 26). Since the LLJ is associated with more powerful winds across the South-Central Plains region (Shapiro and Fedorovich, 2010), it should be expected that the median hub-height level winds and WPD over the Oklahoma Panhandle would be higher in the presence of a greater number of LLJs.

The relationship that LLJ frequency has with the occurrence of ramp events is also highly consistent. The most common relationship presented is that greater LLJ frequency occurs with a simultaneous reduction in the number of ramp up (row c of Figure 26) and ramp down (row c of Figure 26) events, implying that the variability of hub-height winds is lower when the LLJ is more frequently present. This linkage appears when considering the outputs of multiple GCMs, such as projections by HadGEM2-ES (row c) for future autumnal LLJs that occur near sunrise as well as by GFDL-CM3 (row d) for future spring LLJs at multiple times of day. Whilst it has been found by Weaver and Nigam (2008) that the LLJ does possess a degree of

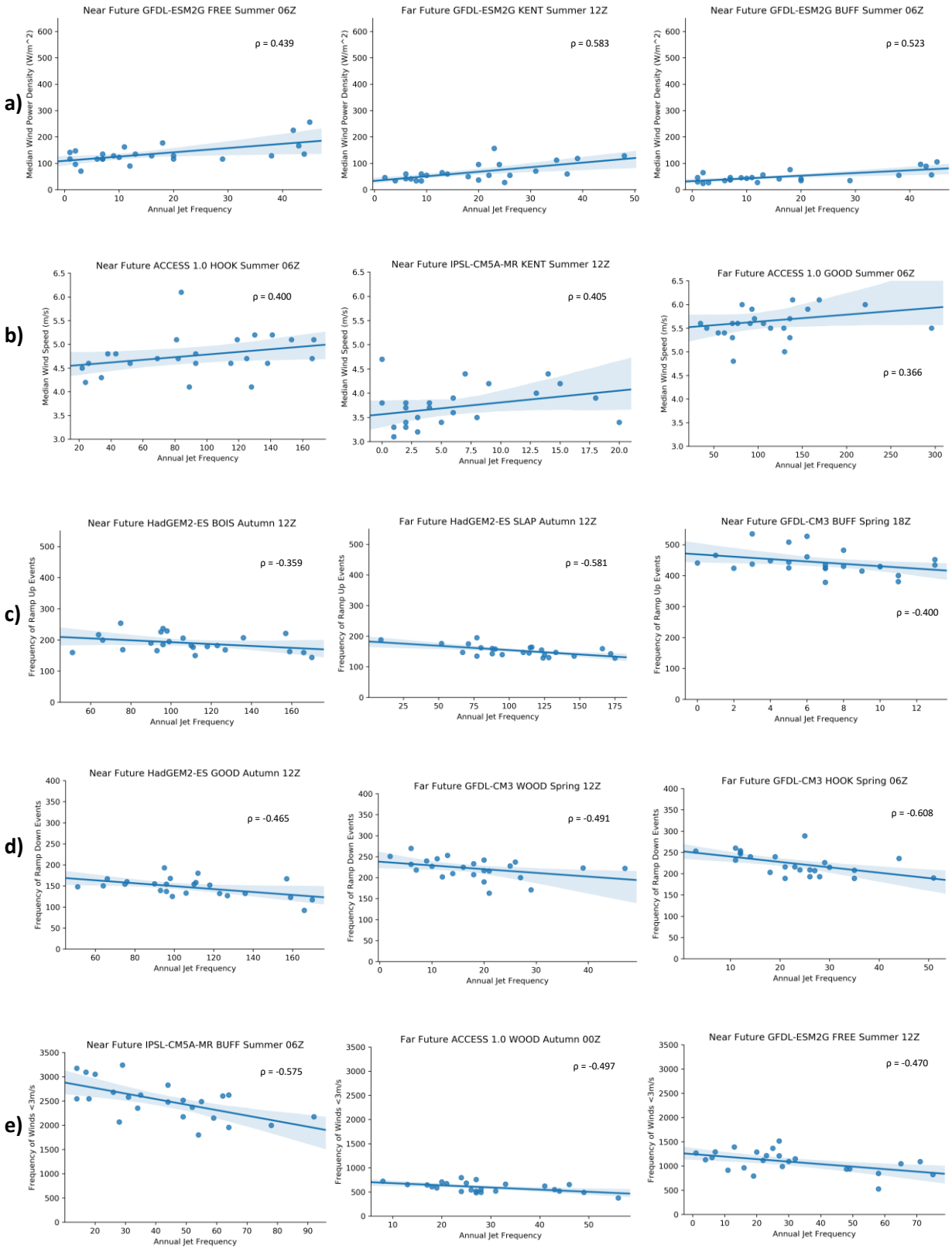

Figure 26: Same as Figure 24 but for relationships between LLJ frequency and various wind energy metrics.

diurnal variability in its speed and that this variability tends to increase with latitude, therefore contributing to the occurrence of ramp events, a consistent southerly direction is still most common (Shapiro and Fedorovich, 2010). Recall also from Kamath (2010) that the frequency of ramp events is typically lower at night – the time at which LLJs form more frequently in their diurnal cycle. It could therefore be argued that the LLJ's presence contributes to winds that are less variable than those that occur during the day, therefore resulting in a reduction in the number of ramp events in a given time period when the LLJ occurs more frequently.

Finally, there are a large number of regression analyses that show a consistent and understandable relationship between LLJ frequency and frequency of winds below V_{in} (due to the lack of occurrences of winds above V_{out}, regression analyses against this metric were inconclusive). It can be seen from row e of Figure 26 that the typical relationship is such that greater LLJ frequency commonly occurs along with fewer cut-in events. All GCMs produce this result, but most consistently for spring and summer, and during times of the day when the LLJ occurs more commonly (e.g. 06Z and 12Z). Recall from rows a and b of Figure 24 that a greater LLJ frequency is associated with greater wind speed at hub-height. With this wind energy metric being larger, a lower frequency of cut-in events is a consistent result.

It is quite clear from these results that LLJ frequency is the only characteristic of the three examined that has a consistent relationship with wind energy metrics over the Oklahoma Panhandle that also makes conceptual sense. LLJ frequency is most likely not, however, the sole factor that explains the projected changes in wind energy metrics that were presented in Sections 5.1, 5.2, and 5.3. Firstly, correlation between two variables does mean that a change in one causes a change in the other. Secondly, it is possible that other climatological factors and climate variability cycles may be just as, if not more, important than the LLJ. This second reason is

especially important, since the projected changes in wind energy metrics shown throughout this chapter were predominantly negative (positive for the frequency of winds below V_{in}), meaning that LLJ frequency could only have important effects on the climatological frequency of ramp up and ramp down events. The relative significance of the linkage between LLJ characteristics and projected changes in wind energy metrics shall be discussed further in Chapter 6.

Chapter 6: Summary, Limitations, and Future Work

The objective of the current study was to determine whether or not projected evolutions in the state of Oklahoma's wind energy resources have a relationship with the future state of the LLJ that frequently forms over the United States' Central Plains. The motivation for analyzing the LLJ's influences on these resources came from several research examples that discovered a link between the two in analysis of observations (Emeis, 2014a; Lampert et al., 2016), as well as research that projected increases in both hub-height wind speed/WPD (Greene et al., 2010; Stadler et al. 2015) and the LLJ's speed and frequency (Cook et al., 2008; Tang et al., 2017) over the South-Central Plains region. Given the consistent changes observed in previous work and the relationship that the two features have been found to possess, it was therefore reasonable to examine links between various wind energy metrics and LLJ characteristics on climatological timescales out to the end of the 21st Century. Using this information, it therefore allows for suggestions to be made concerning why Oklahoma's wind energy resources could evolve in a manner that could be incongruent with the rest of the contiguous United States.

6.1. Answering the Questions Posed in Chapter 1

6.1.1. Question 1 – Projections of LLJ Characteristics

In answering this topic, the current study proposed three questions in Section 1.2, the first of which read as follows: "In what way does using more recent climate model outputs of wind speed and consideration of a wider range of low-level jet characteristics change the current understanding of projected low-level jet climatology over the South-Central Plains region?". There are two reasons why an update to the results of previous studies that had considered projected changes in LLJ climatology is needed. Firstly, few studies of historical versus future

LLJ climatology have been conducted previously, and many of them were done using climate model outputs from the Third Generation of the Coupled Model Intercomparison Project (CMIP3; Cook et al., 2008; Barandiran et al., 2013; Tang et al., 2017). Studies that have enlisted Fifth Generation (CMIP5) climate model outputs that focused on the United States either did not consider outputs from multiple GCMs (Harding and Snyder, 2014), or focused their analysis on historical timeframes (Harding et al., 2013; Danco and Martin, 2017). Secondly, projected changes in LLJ speed and frequency have been commonly studied, but LLJ height is not a factor that has been considered much in previous work on this subject, hence there existed a possibility to broaden the set of LLJ characteristics that such studies consider.

By enlisting the methods of previous LLJ climatology studies (Doubler et al., 2015; Yu et al., 2017) that include information about LLJ height (as well its speed and frequency at a given point in time), the outputs of six GCMs (Table 1) were used to project changes in these three characteristics across the South-Central Plains region (Figure 8). These projections suggest increases in LLJ frequency across the region of study (Tables 3 and 4), with these increases being at their largest by the end of the 21st Century, during summer and autumn, and also at times of day when LLJ formation is typically favored – near sunset and at night (Shapiro and Fedorovich, 2010). By contrast, projected changes in median LLJ speed and height were not as consistent, with the former indicating some tendency towards increases in its value at night (Table 5).

The biggest changes in all three of these characteristics came from the higher-resolution GCMs enlisted in the current study – ACCESS 1.0, HadGEM2-ES, and IPSL-CM5A-MR. The lower-resolution GCMs had a greater tendency to project decreases in LLJ speed and frequency, but these decreases were less common and smaller in magnitude than the increases projected by the

higher-resolution GCMs. It is important to also recognize that these lower-resolution GCMs are all variants of the GFDL model, meaning that common differences in model physics compared to other GCMs could also explain this discrepancy in projected LLJ speed and frequency. Recall that all of these models may be biased such that they underestimate historical LLJ speed and frequency (Doubler et al., 2015; Danco and Martin, 2017), so such discrepancy is to be expected. The inter-model result is one of the same sign, if not slightly higher in magnitude than the projections of LLJ frequency that were found in studies such as Tang et al. (2017), though the slight overall increase in LLJ speed constitutes a departure from that study's projection of no overall change.

Analysis of the spatial patterns of these projections showed that these increases in LLJ frequency tend to be larger toward the poleward edge of the South-Central Plains region (Figure 19), especially in spring and summer, with much less consistent spatial patterns for LLJ speed and height (Figures 17 and 18). A poleward shifting of the most frequent LLJ occurrences has been seen in several previous studies (Barandiran et al., 2013; Harding and Snyder, 2014), but what is interesting about the current study is that not all GCMs were consistent in this regard.

As with the results for projected percentage changes in Tables 3 and 4, poleward shifts of greater LLJ frequency were consistently projected by the higher-resolution GCMs enlisted in the current study, with those possessing a lower resolution (namely GFDL-CM3, GFDL-ESM2G, and GFDL-ESM2M) being more likely to project inconclusive or negative changes in LLJ frequency. Higher resolution GCMs are more likely to capture occurrences of LLJs due to the greater density of grid points and larger number of height levels that they possess, perhaps resulting in larger changes in LLJ characteristics. It may also be the case that some of these GCMs do not represent the effects of climate variability cycles that influence the LLJ, such as ENSO (Danco

and Martin, 2017), the AMO and PDO (Weaver and Nigam, 2008), and the Bermuda High (Holt and Wung, 2012) as accurately as others. The differences in outputs seen in the current study nevertheless exemplify the importance of analyzing outputs from multiple GCMs.

This study also examined the variability of these projections in LLJ characteristics on various temporal scales, by showing results that decomposed the characteristics diurnally, seasonally, by GCM, and by time frames considered (historical versus near future or historical versus far future). In the case of all three characteristics, it resulted that diurnal and seasonal variability within one time frame tended to exceed the projected change in each one's magnitude across time frames, with the central tendency of the changes that do occur between time frames exceeding the spread of potential values. There was also some evidence to suggest that, particularly in projections of LLJ frequency, the spread of projected LLJ characteristics could become wider in future decades, implying greater extremes in their occurrence. This finding is consistent with conclusions from Cosack et al. (2007) that the presence of the LLJ is typically associated with greater magnitude and spread in observed wind speeds.

These results also illustrated a weakness in the method of determining LLJ height (Figure 15) using the outputs of GCMs. The number of height levels that these GCMs possessed between ground level and 3000 meters above (as per the definition enlisted for the current study) ranged from 12 to 16 levels, depending on the GCM considered. Even in proximity to the ground, these height levels can still be as much as 50 meters apart, meaning that detection of changes in height level between time frames was only possible when they were large enough to occur at a different level. A reduction in details of detected height levels consequently occurred, as shown by the occasional lack of a classic box-and-whisker structure in the boxplots shown in Figure 15, but the GCMs nevertheless succeeded in obtaining LLJ heights that were realistic and comparable to

the results of previous observational studies, such as Emeis (2014a). There was some evidence to suggest that the spread of LLJ heights was much greater in autumn and winter across all time frames. However, there was much disagreement between GCMs in terms of the extent of this spread, with some of the lower-resolution GCMs (such as GFDL-CM3) indicating a much greater spread in values. It is apparent from these results that the approach used to determine and project changes in LLJ height used in the current study do function at a basic level, but the imprecision of the GCMs' height levels creates a need to examine this characteristic with higher-resolution data in future.

6.1.2. Question 2 – Projections of Wind Energy Metrics

The second question posed by the current study concerned the six wind energy metrics described in Section 3.2, and read as follows: "Does using more recent climate model projections to calculate changes in a range of wind energy metrics yield notable results concerning Oklahoma's future wind energy resources?". Much like previous studies that have considered projected changes in LLJ characteristics, the CMIP5 generation of climate models has not been enlisted in many studies (other than Kulkarni and Huang (2014)) that have examined the United States' wind energy resources since their outputs became available, whether in studies that have projected trends nationally (Johnson and Erhardt, 2016) or over the state of Oklahoma (Stadler et al., 2015). As such, there was an interest to consider projections with a more recent set of climate model outputs. Furthermore, almost all previous studies of changes in the United States' wind energy resources have used wind speed and/or WPD as their wind energy metric, examples including Sailor et al. (2008), Pryor and Barthelmie (2011), and Greene et al. (2012). Observational studies of the frequency of ramp up and ramp down events have been conducted before, such as Kamath (2010) and Ela and Kemper (2009), but none of these studies considered

climatological time scales or anything beyond observed wind power output. Moreover, frequency of winds below cut-in and above cut-out thresholds is not a commonly studied topic. Ramp event frequency and the frequency of cut-in/cut-out events are unlike wind speed/WPD, in the sense that they evaluate the ability to extract wind energy, rather than quantifying the wind energy resource itself. Evaluating this wider range of wind energy metrics therefore allowed for the current study to consider changes in Oklahoma's wind energy resources more holistically, in ways that previous studies have not considered that are also relevant to grid managers and wind turbine manufacturers.

Projection of future pseudo-observations from 10 Oklahoma Mesonet locations (Table 2) were obtained by statistically downscaling each GCM's outputs onto these locations using the climatological delta method (Déqué, 2007; Maraun et al., 2010; Walsh et al., 2018). The intention of this downscaling was to create high-resolution estimates of future wind speed over a part of the United States that has seen much recent interest in developing wind power capacity (Section 3.3.2). Projection of wind energy metrics from these historical and future Mesonet values led to several interesting results. Percentage changes of the six wind energy metrics showed somewhat of a lack of consistency with previous work. Whereas studies such as Stadler et al. (2015) had projected mid-to-late century increases in wind speed and WPD across the Oklahoma Panhandle (Figure 3), the GCMs enlisted in the current study tended more to project decreases in these metrics, as shown by Tables 6, 7, and 8. The only GCM outputs that showed agreement with the results of previous work were those of ACCESS 1.0, with this model even projecting the decreases in the Panhandle's summer hub-height wind speed also found in Stadler et al. (2015).

It is difficult to reason, however, why the overall slight decrease in these two metrics projected by the other five GCMs would not agree with prior expectations. This inconsistency perhaps resulted from the climate model changes that happened as part of CMIP's fifth generation update (Taylor et al., 2012), or perhaps the decision to statistically downscale several GCM grid points onto a smaller area (the Oklahoma Panhandle). Another possibility is the known biases in resolving wind speed that these GCMs possess, such as a tendency to underestimate the strength of the 850 hPa winds sometimes used to characterize the LLJ (Danco and Martin, 2017). Another point to make is that CMIP5-based studies of wind speed projection do not use the same emissions scenarios (RCP, Riahi et al., 2011) as some of these earlier studies (SRES, Nakićenović et al. (2000)), which could also impact inconsistency between literature examples. It is worth mentioning, however, that Johnson and Erhardt (2016) found in their study of climate model projections of wind speed that the GFDL GCM that they enlisted projected decreases in future wind speed over the South-Central Plains region, much like the GFDL GCMs enlisted in the current study. Kulkarni and Huang (2014) also verifies the projections of wind energy metrics produced by ACCESS 1.0, since their study found increases in wind speed over the South-Central Plains region to also occur in their analysis of its outputs.

With an overall reduction in projected wind speed and WPD by most GCM outputs, it therefore made sense that increases in the frequency of cut-in events and small reductions of that of cut-out events would also be projected, as also shown by Tables 6, 7, and 8. With cut-out events originally being a low-frequency occurrence across the Oklahoma Panhandle, as shown in boxplots of Figure 22, a large percentage change in their frequency of occurrence has little significance for changes in extractable wind energy. The same cannot be said, however, for changes in cut-in event frequency. Figure 22 showed that the median number of cut-in events for

a given season and time of day can be anywhere from 500 to 1000 events per year, meaning that an increase in the number of these events could result in notable reductions in wind power production across the Oklahoma Panhandle.

The changes in the frequency of ramp up and ramp down events were shown to have similar patterns. Much like wind speed and WPD, decreases in their frequency of occurrence were projected (Table 8), with only the decreases projected by models such as GFDL-CM3 and HadGEM2-ES being large enough to match the scale of the diurnal and seasonal variability that ramp event frequency seemed to possess (Figure 21). These ramp event frequencies, across all temporal scales and GCMs enlisted, seemed to match the observed expectations of previous literature, which were greater in frequency in spring and summer (Sevlian and Rajagopal, 2013) as well as during the day (Kamath, 2010). The ability of observational data forced by GCMs to capture these variability trends gives credibility to the consideration of ramp event frequency on climatological timescales. It should be pointed out, however, that the frequency of ramp up and ramp down events shown in the current study could be affected by selecting a different definition of ramps. It was stated by Ela and Kemper (2009) that enlisting shorter time periods to judge the occurrence of ramp events is more appropriate, given the ability of ramp events to occur in a matter of minutes. That being said, studies such as Ferreira et al. (2010) have used periods as long as four hours at a time to allow for ramp event occurrence.

The spatial patterns of these projections of wind energy metrics were also considered (Figure 23), since previous studies such as Stadler et al. (2015) have shown there to be notable differences in projected wind speed on different sides of the Oklahoma Panhandle. What this study's results showed was that the projected change by a particular GCM, hour, and season combination is typically constant across the entire Panhandle, with the largest changes in ramp

event frequency and cut-in/cut-out frequency typically projected at its eastern and western extremities. However, there was little else to be interpreted from these projected spatial patterns. Recall from Section 3.3.2 that the creation of these future pseudo-observations was achieved by applying the delta method to a coarse grid of GCM outputs, and subsequently applying the factor changes to the much finer Oklahoma Mesonet locations. The consequent resolution of the metrics' spatial trends was quite coarse, and therefore less able to accurately capture the trends in wind speed across the Oklahoma Panhandle as studies that enlisted higher-resolution GCM outputs, such as Stadler et al. (2015). Despite the limitation of this approach, the spatial domain of the Oklahoma Panhandle is so small that, even when applying the GCMs' median projected wind speed changes to create projections of high-resolution wind speed changes, an average overview of the projected change across the Oklahoma Panhandle can still be obtained, as seen in Figure 23.

6.1.3. Question 3 – Linking LLJ Characteristics and Wind Energy Metrics

Having examined projected changes in a wide range of LLJ characteristics and wind energy metrics, the final step was to consider any linkage that could exist between them, as posed by the third question asked by the current study: "How can changes in the low-level jet climatology projected in the current study be linked to changes in Oklahoma's wind energy resources in ways that make sense conceptually, owing to suggested influences of the low-level jet on near-surface winds?" Using the same GCM outputs and Oklahoma Mesonet data as those enlisted in answering questions one and two, simple linear regression was used to determine whether any combinations of LLJ characteristics and wind energy metrics had notable relationships with each other, in a similar fashion to work by Wimhurst et al. (2017). Whilst LLJ speed and height did not seem to have much of a consistent or sensible relationship with any wind energy metrics

(Figures 24 and 25), LLJ frequency possessed relationships with several wind energy metrics that were statistically significant and also are consistent with pre-conceptions and much existing research on this topic. As was shown in Figure 26, within any time frame or at any location considered, increased LLJ frequency was consistently associated with greater hub-height wind speed/WPD, lower ramp up/ramp down event frequency, and a decreased number of cut-in events. Each of the six GCMs were consistent concerning the relationships that they asserted to exist between LLJ frequency and wind energy metrics, with all of them broadly agreeing with the overall message asserted by Figure 26. These consistent relationships were also found to occur more often at times of day (nighttime) and during seasons (spring and summer) when LLJ formation is typically more common (Doubler et al., 2015).

These regression analyses provided needed context to the relationship that LLJ characteristics and wind energy metrics have been implied to possess in previous work. As has been seen before, the LLJ is associated with stronger observed winds at hub-height (Cosack et al., 2007; Emeis, 2014a; Lampert et al., 2016), and these regression analyses show that this relationship also exists climatologically. However, the current study has shown that most GCMs project overall decreases in near-surface wind speed/WPD over the Oklahoma Panhandle in the decades to come (Table 8), with only ACCESS 1.0 projecting increases in these two metrics (Tables 6 and 7). Whilst this overall result is not consistent with previous work, such as Stadler et al. (2015) and Johnson and Erhardt (2016), reduced wind energy resources over the Panhandle is consistent with the poleward shift of the LLJ's greatest frequency that was found in Figure 19 and the results of studies such as Barandiran et al. (2013) and Harding and Snyder (2014). It is therefore possible that the positive relationship between LLJ frequency and hub-height wind speed/WPD manifested in the current study's results, which demonstrates the LLJ's influences

on wind speed also existing on climatological scales. By the same logic, a reduction of the number of cut-in events over the Oklahoma Panhandle in tandem with this poleward LLJ frequency increase is an understandable result. Dai and Deser (1999) and Zhang and Zheng (2004) both showed that diurnal variability of near-surface wind speeds typically results in the greatest wind speeds over this part of the United States in the afternoon, owing to the influences of the daytime convective boundary layer. It is also important to realize that many other climatological variables bear a degree of responsibility for projected changes in wind climatology, such as changes in the strength and intensity of extratropical cyclones (Woollings and Blackburn, 2012), and influences of climate variability cycles such as the NAO (Weaver and Nigam, 2008) and ENSO (Danco and Martin, 2017). With the multitude of processes that can influence hub-height level winds, the climatological influence of the LLJ on these particular wind energy metrics appears quite limited.

The relationship between LLJ frequency and occurrence of ramp up/down events is also of interest. As shown by Figure 26, increases in LLJ frequency were consistently associated with a smaller number of ramp events, particularly at night. This relationship is intuitive and followed previous studies, which have shown that ramp events have been observed to occur less frequently at night (Kamath, 2010), and that the LLJ's existence is characterized by consistent southerly winds (Shapiro and Fedorovich, 2010). As such, it is therefore conceivable that an increase in nighttime LLJ frequency could contribute to a reduction in the variability of the wind, and therefore a reduction in the number of ramp events. A reduction in ramp events would result in smaller and slower changes in the hourly power capacity of wind turbines, thus reducing future concerns for grid managers that control supply of wind-sourced electricity. It is worth pointing out, however, that grid management techniques and their evolution go beyond the scope

of this work, so comments about impacts of ramp event frequency can be made based only on what is known currently about grid management in Oklahoma.

This negative relationship also transpired in the projections shown throughout the current study, with projected increases of LLJ frequency (see Tables 3, 4, and 5) occurring alongside projected reductions in the frequency of ramp up and ramp down events over the Oklahoma Panhandle (see Tables 6 and 7). As above, the observed relationship between LLJ frequency and ramp event frequency could be a coincidence. Owing to the conceptual basis of this relationship and the fact that projections of these quantities could evolve in the same manner as the sign of said relationship, there is an argument to be made that a greater LLJ frequency could have an important influence on the climatology of future ramp events over the South-Central Plains region.

6.2. Limitations of the Current Study and Potential Future Work

The current study has come to the conclusion that, despite some departures from previous studies that examined projected changes in wind energy metrics, there is evidence to suggest that the LLJ could have noteworthy influences on the future of Oklahoma's wind energy resources. This is particularly true when considering the relationship and projected changes of LLJ frequency and the occurrence of ramp up and ramp down events. There were, however, some limitations in the current study that may have impacted the results. Some of these limitations have been discussed above, including, for example, the decision to downscale coarse GCM outputs onto a much smaller region, and the consequent loss of detailed spatial patterns of wind energy metrics across the Oklahoma Panhandle. This study possessed some other limitations that may have impacted the results of this work.

Firstly, only GCM outputs for the future time frames forced by the RCP 8.5 emissions scenario were enlisted. This RCP represents the "business as usual" scenario, in which little to no effort would be made to mitigate carbon dioxide emissions and subsequent climate change impacts (Riahi et al., 2011). Of course, there are several other scenarios in which mitigation efforts would be hypothetically made, and it would have been interesting for the current study's purposes to have seen how other scenarios could have affected projections of LLJ characteristics and wind energy metrics. That being said, there is still much worth in focusing on RCP 8.5 in the current study, since the consequences of a business as usual emissions scenario are of interest to many different groups, and the use of GCMs forced by this scenario produced interesting results, as discussed in Section 6.1. It is also important to realize that only six GCMs were used in the current study, three of which were GFDL models. This could have limited the range of potential projections in LLJ characteristics and wind energy metrics, and also skewed the perception of bias in the current study's results.

Another limitation of this work was the use of the Mann-Whitney U-test for judging statistical significance of changes in LLJ characteristics and wind energy metrics between time frames. The motivation for using this particular test was twofold – the tendency for wind speed data to have a skewed frequency distribution, therefore rendering changes in the median as a more valid quantity for projection (as in Greene et al. (2012)), and the use of Mann-Whitney U-tests in studies relating to wind energy in the past (Baidya Roy and Traiteur, 2010). Since this type of test judges statistical significance based on changes in the rank order of a particular LLJ characteristic or wind energy metric between two time frames (historical and near/far future), what occasionally happened was that a significant difference in rank order occurred without any change in the median value of the quantity being tested, e,g, the red cells in Tables 3, 4, 6, and 7

that contain a 0% change. Whilst such a result was uncommon, it nevertheless represents a weakness of using this particular test for analyzing statistically significant changes in the current study. A means to get around this issue could be to flag statistically significant changes that were associated with a 0% change in a particular LLJ characteristic/wind energy metric, so that overstatement of the results associated with them is avoided. It is also important to point out that other tests of statistical significance, such as the student's t-test (as used by Tang et al. (2017)), were not used due to the mean being considered a less appropriate measure of wind speed's central tendency. Despite the limitations of enlisting Mann-Whitney U-tests as the means of determining statistical significance, its suitability for testing ranked data such as that used in the current study made it a better choice than other test types.

A third important limitation to address is the temporal offset between the GCM outputs and the Oklahoma Mesonet data. As mentioned in Section 3.1, due to the Oklahoma Mesonet not being formed until January 1st 1994, and most GCM outputs of historical wind speeds stopping on December 31st 2005, there existed a 13-year offset in the historical GCM outputs (1981-2005) and the Oklahoma Mesonet observations (1994-2018). The current study did take measures to ensure that this offset would not greatly affect the results, such as by verifying the lack of significant change in historical wind speed trends over the Oklahoma Panhandle and South-Central Plains region (Figures 12 and 13), and also corroborating this lack of change by drawing comparisons with previous work (Pryor et al., 2009; Torralba et al., 2017). As such, there is still validity in combining these two sets of data, despite the 13-year difference in the model run period. Whilst this assumption is acceptable on climatological timescales, the temporal offset does become important when considering historical wind energy metrics and LLJ characteristics of individual years of data. Note that in Figures 24, 25, and 26, none of the presented

relationships were taken over the historical time frame, since at least 13 data points (out of 25) in each regression analysis would have been comprised of data from different years, which would have been meaningless. It was therefore considered better to not perform linear regression on data from the historical timeframe, and focus instead on regression of outputs from the future time frames.

The limitations that the current study possesses do not detract from the sense of what this study has presented. Much care was taken to minimize the effects of these limitations, and meaningful results relating to the linkage between LLJ characteristics and wind energy metrics were found despite them. One overarching means of removing many of these limitations in future would be to enlist GCM outputs that had been previously downscaled to the resolution of the Oklahoma Mesonet data. Many previous studies that sought finer details of projected changes in LLJ characteristics (Tang et al., 2017) and wind energy metrics (Stadler et al., 2015) did so using downscaled projections of GCM outputs. Access to finer resolution outputs (both temporally and spatially) would have reduced the issues concerning relatively low horizontal resolution (such as the GFDL GCMs) that some of the enlisted models had. For instance, it was discussed in Section 4.2.3 that lower-resolution GCMs are biased to underestimate LLJ frequency when compared to results from observational/reanalysis studies (Doubler et al., 2015). Use of GCM outputs with greater spatial and temporal resolution would have also eliminated the need to enlist observations from the Oklahoma Mesonet. The creation of pseudo-observations using median projected changes in near-surface wind speed has already been mentioned as a potential limitation of the current study in Section 6.1, since the ability to use interpolated GCM outputs to force projections (such as in Eames et al. (2012)) was not possible. Future studies of LLJ characteristics and wind energy metrics should therefore enlist higher-resolution GCM outputs

than those used in the current study, preferably from models as part of the Sixth Generation of the Coupled Model Intercomparison Project (CMIP6; Eyring et al., 2016) or beyond, once more of them become available.

A second subject to consider in future work would be greater analysis of LLJ height climatology. This study showed that GCMs were able to recreate and project changes in LLJ height that were sensible, but they often lacked precision due to the discrete nature of the height levels that GCMs typically possess. Due to the influence that LLJ height has been shown to have on observations of wind turbine hub-height (Emeis, 2014a; Lampert et al, 2016) and the results of the current study, further analysis of the climatology of LLJ height is certainly warranted. Doubler et al. (2015) previously considered this climatology over the historical timeframe, but the current study showed that this same analysis can be conducted in the context of climate change. With a more detailed understanding of the LLJ's height climatology, assertions of its linkage with wind energy metrics would be more appropriate than those presented in the current study. One could thus examine whether long-term changes in its height produce detectable wind shear changes in the vicinity of wind turbine blades, as has been seen in observational studies (Emeis, 2014b). Other aspects of LLJ climatology could also be considered, such as spatial and temporal changes in its width. Weaver and Nigam (2008) used empirical orthogonal function analysis to find that changes in the LLJ's spatial and temporal extent constitute notable portions of its variance. It is therefore of interest to determine whether climatological patterns in its width and exact position across the South-Central Plains region exist. Such a result would provide useful context to the spatial patterns of LLJ characteristics shown in the current study (Section 4.3).

A third avenue of future work would be the effects of enlisting different definitions of ramp events in future studies of its climatology. As with LLJ height and frequency of cut-in/cut-out

events, the climatology of ramp events has not been frequently studied in previous work. The current study only considered one definition of ramp events in deducing their climatological frequency – at least a 20% change in wind power capacity in an hour or less (Bradford et al., 2010; Kamath, 2011). It would be of interest to find out whether ramp event climatological patterns, and their strong relationship with LLJ frequency, could be affected by changing the enlisted ramp event definition. Another important consideration is what grid operators prioritize in terms of ramp events. It is possible that grid operators care less about the selected ramp event definition than those researching these events, thus warranting future study into ramp events in the context of grid demands and management.

Finally, refinement of the empirical formula used to extrapolate near-surface winds to hub-height is another area of future research that would be pertinent to the current study. As discussed in Section 3.2.1, upscaling of winds in the presence of an LLJ was done using an empirical linear formula derived from the findings of several research examples, such as Baas et al. (2009), Lampert et al. (2016), and Pichugina et al. (2016). It is reasonable to assume, however, that the winds of stable boundary layers that exist in the presence of LLJs (Stull, 1988) are seldom describable by a linear equation with a constant coefficient of 0.05 s^{-1}, as laid out in Equation 3. Despite being more appropriate than a logarithmic upscaling of near-surface wind speed, this equation still may result in some error in estimating hub-height speed in an LLJ's presence, owing to its empirical nature. Such an underestimation could have also led to some inaccuracies in the occurrence of ramp events and cut-in/cut-out events. For example, the presence of an LLJ in one point in time but its absence in the next (meaning a change in the formula used to extrapolate wind speed) could have produced artificial ramp down events/cut-in events at hub-height, even if the change in near-surface wind speed between the two points in time was in fact

quite small. In order to improve future research of hub-height wind climatology, equations that more accurately describe vertical wind profiles in the vicinity of an LLJ should be derived.

Although this study did encounter multiple limitations and identified several possible subjects to consider in future work, many results were found that supplement and consolidate current understanding regarding the low-level jet and its relationship with Oklahoma's wind energy resources. This study showed that increases in LLJ frequency are a feature that is still projected by multi-model ensembles of more recent GCM outputs, with these increases being larger to the north of the South-Central Plains region. The analysis of various wind energy metrics presented some disagreement with the results from previous work, namely slight decreases in wind speed and wind power density over the Oklahoma Panhandle. This study also examined various features relating to wind climatology and wind energy production that had not previously been considered, such as LLJ height, and the frequency of ramp up/down and cut-in/cut-out events. Analysis of such a broad range of features revealed a consistent and conceptually sound relationship between increases in future LLJ frequency and simultaneous reductions in the frequency of ramp events. Such a result accredits the importance of future LLJ climatology for the production of wind energy resources over the South-Central Plains region. This has important implications for the future of grid management for wind energy. These implications include greater consistency in extractable wind energy resources over this region, such that management of supply without worrying about sudden power increases and drops in accordance with ramp events would happen less frequently. An implication that follows from this is the suitability of the Oklahoma Panhandle as a site for long-term wind energy extraction, based on the consistency and ease of management of extractable resources that this region could possess in future.

The projected increases in LLJ frequency presented in the current study have implications that go beyond impacts on the wind energy industry. With southerly winds across the South Central Plains region becoming more consistent, poleward transport of objects advected by these winds could be enhanced, such as transportation of pollen from ecosystems south of this area. Moisture transport from the Gulf of Mexico could also be enhanced by an increased LLJ frequency, potentially having implications for air mass and moisture combinations that favor tornadogenesis over Oklahoma and the surrounding states. The implications of changing future states of the LLJ could therefore have other noteworthy consequences, which would be worth considering in future work.

References.

Abdullah, M. A., A. H. M. Yatim, C. W. Tan, and R. Saidur, 2012: A review of maximum power point tracking algorithms for wind energy systems. *Renewable and Sustainable Energy Reviews*, **16**, 5, 3220-3227, doi:10.1016/j.rser.2012.02.016.

Altunkaynak, A., T. Erdik, I. Dabanli, and Z. Şen, 2012: Theoretical derivation of wind power probability distribution function and applications. *Applied Energy*, **92**, 809-814, doi:10.1016/j.apenergy.2011.08.038

American Electric Power, 2018: Wind Catcher Energy Connection Project – Fact Sheet. Accessed 20 March 2018. Available online at http://www.windcatcherenergy.com/docs/4405_PSO_FactSheet_v19%20-%20REV6-Digital%20(3).pdf#view=Fit

American Wind Energy Association, 2018: Wind Energy in Oklahoma – Fact Sheet. Accessed 31 January 2019. Available online at http://awea.files.cms-plus.com/FileDownloads/pdfs/Oklahoma.pdf.

Baas, P., F. C. Bosveld, K. Klein Baltnik, and A. A. M. Holtslag, 2009: A Climatology of Nocturnal Low-Level Jets at Cabauw. *Journal of Applied Meteorology and Climatology*, **48**, 8, 1627-1642, 10.1175/2009JAMC1965.1.

Baidya Roy, S., and J. J. Traiteur, 2010: Impacts of wind farms on surface air temperatures. *PNAS*, **107**, 42, 17899-17904, doi:10.1073/pnas.1000493107.

Barandiran, D., S. Wang, and K. Hilburn, 2013: Observed trends in the Great Plains low-level jet and associated precipitation changes in relation to recent droughts. *Geophysical Research Letters*, 40, 23, 6247-6251, doi:10.1002/2013GL058296.

Bengtsson, L., K. I. Hodges, and E. Roeckner, 2006: Storm Tracks and Climate Change. *Journal of Climate*, **19**, 15, 3518-3543, doi:10.1175/JCLI3815.1.

Bingman, B., and E. Sears, 2015: SB 808 – Wind energy facilities; requiring evidence of financial security prior to construction of new facilities. Accessed 2 April 2019. Available online at http://oklegislature.gov/Billinfo.aspx?Bill=SB808&Session=1500.

Blackadar, A. K., 1957: Boundary Layer Wind Maxima and Their Significance for the Growth of Nocturnal Inversions. *Bulletin of the American Meteorological Society*, **38**, 5, 283-290.

Boccard, N., 2009: Capacity factor of wind power realized values vs. estimates. *Energy Policy*, **37**, 7, 2679-2688, doi:10.1016/j.enpol.2009.02.046.

Bradford, K. T., R. L. Carpenter, Jr., and B. L. Shaw, 2010: Forecasting Southern Plains Wind Ramp Events using the WRF Model at 3-km. *9th Student Conference*, Atlanta, GA, American Meteorological Society, 10pp, http://downdraft.caps.ou.edu/reu/reu09/papers/Bradford.pdf.

Breslow, P. B., and D. J. Sailor, 2002: Vulnerability of wind power resources to climate change in the continental United States. *Renewable Energy*, **27**, 4, 85-598, doi:10.1016/S0960-1481(01)00110-0.

Brock, F. V., K. C. Crawford, R. L. Elliott, G. W. Cuperus, S. J. Stadler, H. L. Johnson, and M. D. Eilts, 1995: The Oklahoma Mesonet: A Technical Overview. *Journal of Atmospheric and Oceanic Technology*, **12**, 1, 5-19, doi:10.1175/1520-0426(1995)012<0005:TOMATO>2.0.CO;2.

Carvalho, D., A. Rocha, M. Gómez-Gesteira, and C . Silva Santos, 2017: Potential impacts of climate change on European wind energy resource under the CMIP5 future climate projections. *Renewable Energy*, 101, 29-40, doi: 10.1016/j.renene.2016.08.036.

Clarke, G.M., and D. Cooke, 1998: *A Basic Course in Statistics*, Arnold Publishing, 672pp.

Collier, M., and P. Uhe, 2012: CMIP5 datasets from the ACCESS1.0 and ACCESS1.3 coupled climate models. CAWCR Technical Report No. 59, 32pp, http://cawcr.gov.au/technical-reports/CTR_059.pdf.

Cook, K.H., E. K. Vizy, Z. S. Launer, and C. M. Patricola, 2008: Springtime Intensification of the Great Plains Low-Level Jet and Midwest Precipitation in GCM Simulations of the Twenty-First Century. *Journal of Climate*, **21**, 23, 6321-6340, doi:10.1175/2008JCLI2355.1.

Cosack, N., S. Emeis, and M. Kühn, 2007: On the Influence of Low-Level Jets on Energy Production and Loading of Wind Turbines. **In:** *Wind Energy: Proceedings of the Euromech Colloquium*, 325-328, doi:10.1007/978-3-540-33866-6_61.

Cox, R. A., M. Drews, C. Rode, and S. Balslev Nielsen, 2015: Simple future weather files for estimating heating and cooling demand. *Building and Environment*, **83**, 104-114, doi:10.1016/j.buildenv.2014.04.006.

Dai, A., and C. Deser, 1999: Diurnal and semidiurnal variations in global surface wind and divergence fields. *Journal of Geophysical Research*, **104**, D24, 31109-31125, doi:10.1029/1999JD900927.

Danco, J. F., and E. R. Martin, 2017: Understanding the influence of ENSO on the Great Plains low-level jet in CMIP5 models. *Climate Dynamics*, 22pp, doi:10.1007/s00382-017-3970-9.

Department of Energy, 2018: Wind Vision – A New Era for Wind Power in the United States. Accessed November 21 2018. Available online at https://www.energy.gov/sites/prod/files/WindVision_Report_final.pdf

Déqué, M., 2007: Frequency of precipitation and temperature extremes over France in an anthropogenic scenario: Model results and statistical correction according to observed values. *Global and Planetary Change*, **57**, 1-2, 16-26, doi:10.1016/j.gloplacha.2006.11.030.

Djurić, D., and D. S. Ladwig, 1983: Southerly Low-Level Jet in the Winter Cyclones of the Southwestern Great Plains. *Monthly Weather Review*, **111**, 11, 2275-2281, doi:10.1175/1520-0493(1983)111<2275:SLLJIT>2.0.CO;2.

Doane, D. P., and L. E. Seward, 2017: Measuring Skewness: A Forgotten Statistic? *Journal of Statistics Education*, **19**, 2, 18pp, doi:10.1080/10691898.2011.11889611.

Donner, L. J., and Coauthors, 2011: The Dynamical Core, Physical Parameterizations, and Basic Simulation Characteristics of the Atmospheric Component AM3 of the GFDL Global Coupled Model CM3. *Journal of Climate*, **24**, 13, 3484-3519, doi:10.1175/2011JCLI3955.1.

Doubler, D. L., J. A. Winkler, X. Bian, C. K. Walters, and S. Zhong, 2015: An NARR-Derived Climatology of Southerly and Northerly Low-Level Jets over North America and Coastal Environs. *Journal of Applied Meteorology and Climatology*, **54**, 7, 1596-1619, doi:10.1175/JAMC-D-14-0311.1.

Dufresne, J. -L., and Coauthors, 2013: Climate change projections using the IPSL-CM5 Earth System Model: from CMIP3 to CMIP5. *Climate Dynamics*, **40**, 9-10, 2123-2165 doi:10.1007/s00382-012-1636-1.

Eames, M., T. Kershaw, and D. Coley. 2012: A comparison of future weather created from morphed observed weather and created by a weather generator. *Building and Environment*, **56**, 252-264, doi:10.1016/j.buildenv.2012.03.006.

Ela, E., J. Kemper, 2009: Wind Plant Ramping Behaviour. National Renewable Energy Laboratory, 44pp, available online at https://www.nrel.gov/docs/fy10osti/46938.pdf.

Emeis, S., 2014a: Review – Current issues in wind energy meteorology. *Meteorological Applications*, **21**, 4, 803-819, doi:10.1002/met.14772.

Emeis, S., 2014b: Wind speed and shear associated with low-level jets over Northern Germany. *Meteorologische Zeitschrift*, **23**, 3, 295-304, doi:10.1127/0941-2948/2014/0551.

Energy Information Administration, 2018: Levelized Cost and Levelized Avoided Cost of New Generation Resources in the Annual Energy Outlook 2018. Accessed 21 November 2018. Available online at https://www.eia.gov/outlooks/aeo/pdf/electricity_generation.pdf.

Engineering Toolbox, 2003: Air – Altitude, Density and Specific Volume. Accessed April 30 2018. Available online at https://www.engineeringtoolbox.com/air-altitude-density-volume-d_195.html.

Eyring, V., S. Bony, G.A. Meehl, C.A. Senior, B. Stevens, R.J. Stouffer, and K.E. Taylor, 2016: Overview of the Coupled Model Intercomparison Project Phase 6 (CMIP6) – experimental design and organisation. *Geoscientific Model Development*, **9**, 1937-1958, doi: 10.5194/gmd-9-1937-2016.

Ferreira, C., J. Gama, L. Matias, A. Botterud, and J. Wang, 2010: A Survey on Wind Power Ramp Forecasting. ANL/DIS-10-13, 40pp, https://digital.library.unt.edu/ark:/67531/metadc832671/m2/1/high_res_d/1008309.pdf

Fiebrich, C. A., C. R. Morgan, A. G. McCombs, P. K. Hall Jr., and R. A. McPherson, 2010: Quality Assurance Procedures for Mesoscale Meteorological Data. *Journal of Atmospheric and Oceanic Technology*, **27**, 10, 1565-1582, doi:10.1175/2010JTECHA1433.1.

Gallego, C., A. Cuerva, A. Costa, 2014: Detecting and characterising ramp events in wind power time series. *Journal of Physics: Conference Series*, **555**, 7pp, doi:10.1088/1742-6596/555/1/012040.

Goddard, S. D., M. G. Genton, A. S. Hering, and S. R. Sain, 2015: Evaluating the impacts of climate change on diurnal wind power cycles using multiple regional climate models. *Environmetrics*, **26**, 3, 192-201, doi:10.1002/env.2329.

Greaves, B., J. Collins, J. Parkes, and A. Tindal, 2009: Temporal Forecast Uncertainty for Ramp Events. *Wind Engineering*, **33**, 4, 309-320, doi:10.1260/030952409789685681.

Greene, J. S., McNabb, K., Zwilling, R., Morrissey, M., and S. Stadler, 2009: Analysis of Vertical Wind Shear in the Southern Great Plains and Potential Impacts on Estimation of Wind Energy Production. *International Journal of Global Energy Issues*, **32**, 3, 191-211, doi:10.1504/IJGEI.2009.030651.

Greene, J. S., M. Morrissey, and S. E. Johnson, 2010: Wind Climatology, Climate Change, and Wind Energy. *Geography Compass*, **4**, 11, 1592-1605, doi:10.1111/j.1749-8198.2010.00396.x.

Greene, J. S., M .Chatelain, M. Morrissey, and S. Stadler, 2012: Projected Future Wind Speed and Wind Power Density Trends over the Western US High Plains. *Atmospheric and Climate Sciences*, **2**, 32-40, doi:10.4236/acs.2012.21005.

Groeneveld, R. A., and G. Meeden, 1984: Measuring Skewness and Kurtosis. *Journal of the Royal Statistical Society*, **33**, 4, 391-399, doi:10.2307/2987742.

Gutierrez, W., A. Ruiz-Columbie, M. Tutkun, and L. Castillo, 2017: Impacts of the Low-Level Jet's Negative Wind Shear on the Wind Turbine. *Wind Energy Science*, **2**, 2, 533-545, doi:10.5194/wes-2-533-2017.

Harding, K. J., P. K. Snyder, and S. Liess, 2013: Use of dynamical downscaling to improve the simulation of Central U.S. warm season precipitation in CMIP5 models. *Journal of Geophysical Research*, **118**, 22, 12522-12536, doi:10.1002/2013JD019994.

Harding, K. J., and P. K. Snyder, 2014: Examining Future Changes in the character of Central U.S. warm-season precipitation using dynamical downscaling. *Journal of Geophysical Research - Atmospheres*, 119, 13, 13,116-13,136, doi:10.1002/2014JD022575.

Holt, E., and J. Wung, 2012: Trends in Wind Speed at Wind Turbine Height of 80 m over the Contiguous United States Using the North American Regional Reanalysis (NARR). *Journal of Applied Meteorology and Climatology*, **51**, 2188-2202, doi:10.1175/JAMC-D-11-0205.1.

Höök, M., and X. Tang, 2013: Depletion of fossil fuels and anthropogenic climate change – A review. *Energy Policy*, **52**, 797-809, doi:10.1016/j.enpol.2012.10.46.

Johnson, D. L., and R. J. Erhardt, 2016: Projected impacts of climate change on wind power density in the United States. *Renewable Energy*, **85**, 66-73, doi:10.1016/j.renene.2015.06.005.

Jones, C. D., and Coauthors, 2011: The HadGEM2-ES implementation of CMIP5 centennial simulations. *Geoscientific Model Development*, **4**, 543-570, doi:10.5194/gmd-4-543-2011.

Kallistratova, M. A., R. D. Kouznetsov, V. F. Kramar, and D. D. Kuznetsov, 2013: Profiles of Wind Speed Variances within Nocturnal Low-Level Jets Observed with a Sodar. *Journal of Atmospheric and Oceanic Technology*, **30**, 9, 1970-1977, doi:10.1175/JTECH-D-12-00265.1.

Kamath, C., 2010: Understanding Ramp Events Through Analysis of Historical Data. *IEEE PES T&D 2010*, 6pp, doi:10.1109/TDC.2010.5484508.

Kamath, C., 2011: Associating weather conditions with ramp events in wind power generation. *IEEE PES Power Systems Conference and Exposition 2011*, 8pp, doi:10.1109/PSCE.2011.5772527

Karnauskas, K. B., J. K. Lundquist, L. Zhang, 2018: Southward shift of the global wind energy resource under high carbon dioxide emissions. *Nature Geoscience*, **11**, 1, 38-43, doi:10.1038/s41561-017-0029-9.

Kulkarni, S., and H. Huang, 2014: Changes in Surface Wind Speed over North America from CMIP5 Model Projections and Implications for Wind Energy. *Advances in Meteorology*, **3**, 10pp, doi:10.1155/2014/292768.

Lampert, A., B. B. Jimenez, G. Gross, D. Wulff, and T. Kenull, 2016: One-year observations of the wind distribution and low-level jet occurrence at Braunschweig, North German Plain. *Wind Energy*, **19**, 10, 1807-1817, doi:10.1002/we.1951.

McCall, C., and T. Schulz, 2017: HB 2298 – Zero Emission Facility Tax Credit Amendments Act of 2017. Accessed 3 March 2019. Available online at http://webserver1.lsb.state.ok.us/cf_pdf/2017-18%20INT/hB/HB2298%20INT.PDF

McPherson, R. A., and Coauthors, 2007: Statewide Monitoring of the Mesoscale Environment: A Technical Update on the Oklahoma Mesonet. *Journal of Atmospheric and Oceanic Technology*, **24**, 3, 301-321, doi:10.1175/JTECH1976.1.

Mabel, M. C., and E. Fernandez, 2007: Analysis of wind power generation and prediction using ANN: A case study. *Renewable Energy*, **33**, 5, 986-992, doi:10.1016/j.renene.2007.06.013.

Maraun, D., and Coauthors, 2010: Precipitation downscaling under climate change: recent developments to bridge the gap between dynamical models and the user. *Reviews of Geophysics*, **48**, 3, 34pp, doi:10.1029/2009RG000314.

Meehl, G. A., C. Covey, T. Delworth, M. Latif, B. McAvaney, J. F. B. Mitchell, R. J. Stouffer, and K. E. Taylor, 2007: The WRCP CMIP3 Multimodel Dataset – A New Era In Climate Change Research. *Bulletin of the American Meteorological Society*, **88**, 9, 1383-1394, doi:10.1175/BAMS-88-9-1383.

Mesonet, 2018: Daily Data Retrieval. Accessed April 4 2018. Available online at https://www.mesonet.org/index.php/weather/daily_data_retrieval.

Nakićenović, N., and Coauthors, 2000: Summary for Policymakers – Emissions Scenarios: A Special Report of Working Group III of the Intergovernmental Panel on Climate Change. 27pp, http://pure.iiasa.ac.at/id/eprint/6101/2/sres-en.pdf.

NARCCAP, 2012: NARCCAP – Project Overview. Accessed 30 March 2018. Avaiable online at http://www.narccap.ucar.edu/doc/about/NARCCAP_Intro_manager_meet.pdf.

Oklahoma State Courts Network, 2015: Chapter 22 – Oklahoma Energy Security Act – Chapter 801.4 – Renewable Energy Standard - Establishment - Resources - Determination of Renewable Energy – Reports. Accessed 20 March 2018. Available online at http://www.oscn.net/applications/oscn/DeliverDocument.asp?CiteID=459329**.**

Pichugina, Y. L., and Coauthors, 2016: Properties of the offshore low level jet and rotor layer wind shear as measure by scanning Doppler Lidar. *Wind Energy*, **20**, 6, 987-1002, doi: 10.1002/we.2075.

Pourmokhtarian, A., C. T. Driscoll, J. L. Campbell, K. Hayhoe, and A. M. K. Stoner, 2016: The effects of climate downscaling technique and observational data set on modeled ecological responses. *Ecological Applications*, **26**, 5, 1321-1337, doi:10.1890/15-0745.

Pryor, S. C., J. T. Schoof, and R. J. Barthelmie, 2005: Empirical downscaling of wind speed probability distributions. *Journal of Geophysical Research*, **110**, D19, 12pp, doi:10.1029/2005JD005899.

Pryor, S. C., and Coauthors, 2009: Wind speed trends over the contiguous United States. *Journal of Geophysical Research*, **114**, D14, 18pp, doi:10.1029/2008JD011416.

Pryor, S.C, and R.J. Barthelmie, 2010: Climate change impacts on wind energy: A review. *Renewable and Sustainable Energy Reviews*, **14**, 1, 430-437, doi:10.1016/j.rser.2009.07.028.

Pryor, S. C., and R. J. Barthelmie, 2011: Assessing climate change impacts on the near-term stability of the wind energy resource over the United States. *PNAS*, **108**, 20, 8167-8171, doi:10.1073/pnas.1019388108.

Riahi, K., and Coauthors, 2011: RCP8.5 – A scenario of comparatively high greenhouse gas emissions. *Climate Change*, **109**, 33-57, doi: 10.1007/s10584-011-0149-y.

Riaz, M., 2013: On Enhanced Interquartile Range Charting for Process Dispersion. *Quality and Reliability Engineering International*, **31**, 3, 389-398, doi:10.1002/qre.1598.

Sailor, D. J., M. Smith, and M. Hart, 2008: Climate change implications for wind power resources in the Northwest United States. *Renewable Energy*, **33**, 2393-2406, doi:10.1016/j.renene.2008.01.007.

Segal, M., Z. Pan, R. W. Arritt, and E. S. Takle, 2001: On the potential change in wind power over the US due to increases of atmospheric greenhouse gases. *Renewable Energy*, **24**, 235-243, doi:10.1016/S0960-1481(00)00194-4.

Sevlian, R., and R. Rajagopal, 2013: Detection and Statistics of Wind Power Ramps. *IEEE Transactions on Power Systems*, **28**, 4, 3610-3620, doi:10.1109/TPWRS.2013.2266378

Shapiro, A., and E. Fedorovich, 2010: Analytical description of a nocturnal low-level jet. *Quarterly Journal of the Royal Meteorological Society*, **136**, 650, 1255-1262, doi:10.1002/qj.628.

Song, J., K. Liao, R. L. Coulter, and B. M. Lesht, 2005: Climatology of the Low-Level Jet at the Southern Great Plains Atmospheric Boundary Layer Experiments Site. *Journal of Applied Meteorology*, **44**, 10, 1593-1606, doi:10.1175/JAM2294.1.

Stadler, S., J. M. Dryden, Jr, and J. S. Greene, 2015: Climate Change Impacts on Oklahoma Wind Resources: Potential Energy Output Changes. *Resources*, **4**, 203-226, doi:10.3390/resources4020203.

Storm, B., J. Dudhia, S. Basu, A. Swift, and I. Giammanco, 2009: Evaluation of the Weather Research and Forecasting Model on Forecasting Low-level Jets: Implications for Wind Energy. *Wind Energy*, **12**, 1, 81-90, doi:10.1002/we.288.

Stull, R. B., 1988: *An Introduction to Boundary Layer Meteorology*. Springer Science and Business Media, 670pp.

Tang, Y., S. Zhong, J. A. Winkler, and C. K. Walters, 2016: Evaluation of the southerly low-level jet climatology of the central United States as simulated by NARCCAP regional climate models. *International Journal of Climatology*, **36**, 13, 4338-4357, doi:10.1002/joc.4636.

Tang, Y., J. Winkler, S. Zhong, X. Bian, D. Doubler, L. Yu, and C. Walters, 2017: Future changes in the climatology of the Great Plains low-level jet derived from fine resolution multi-model simulations. *Nature Scientific Reports*, 7, 10pp, doi:10.1038/s41598-017-05135-0.

Taylor, K.E., R.J. Stouffer, and G.A. Meehl, 2012: An overview of CMIP5 and the experiment design. *Bulletin of the American Meteorological Society*, **93**, 4, 485-498, doi:10.1175/BAMS-D-11-00094.1

Tobin, I., and Coauthors, 2016: Climate change impacts on the power generation potential of a European mid-century wind farms scenario. *Environmental Research Letters*, **11**, 3, 9pp, doi: 10.1088/1748-9326/11/3/034013.

Torralba, V., F. J. Doblas-Reyes, and N. Gonzalez-Reviriego, 2017: Uncertainty in near-surface wind speed trends: a global reanalysis intercomparison. *Environmental Research Letters*, **12**, 11, 9pp, http://iopscience.iop.org/article/10.1088/1748-9326/aa8a58/pdf.

Uccellini, L. W., 1980: On the Role of the Upper Tropospheric Jet Streaks and Leeside Cyclogenesis in the Development of Low-Level Jets in the Great Plains. *Monthly Weather Review*, **108**, 10, 1689-1696, doi:10.1175/1520-0493(1980)108<1689:OTROUT>2.0.CO;2.

Walsh, J. E., and Coauthors, 2018: Downscaling of climate model output for Alaskan stakeholders. *Environmental Modelling & Software*, **110**, 38-51, doi:10.1016/j.envsoft.2018.03.021.

Weaver, S. J., and S. Nigam, 2008: Variability of the Great Plains Low-Level Jet: Large-Scale Circulation Context and Hydroclimate Impacts. *Journal of Climate*, **21**, 7, 1532-1551, doi:10.1175/2007JCLI1586.1.

Wexler, H., 1961: A Boundary Layer Interpretation of the Low-Level Jet. *Tellus*, **13**, 3, 368-378, doi:10.3402/tellusa.v13i3.9513.
Wimhurst, J. J., D. J. Brayshaw, and G. Zappa, 2017: Understanding the Role of the North Atlantic Jet in Projections of UK Wind Power Resource by 2100. Undergraduate thesis, Department of Meteorology, University of Reading, 40pp.
WINDExchange, 2018a: U.S. Installed and Potential Wind Power Capacity and Generation. Accessed 12 January 2019. Available online at https://windexchange.energy.gov/files /docs/installed_wind_capacity_by_state.xls
WINDExchange, 2018b: Oklahoma 80-Meter Wind Resource Map. Accessed 30 March 2018. Available online at https://windexchange.energy.gov/maps-data/101.
Wind Turbine Models, 2014: General Electric GE 2.5 – 120. Accessed 2 April 2018. Available online at https://www.en.wind-turbine-models.com/turbines/310-general-electric-ge-2.5-120.
Woollings, T., and M. Blackburn, 2012: The North Atlantic Jet Stream under Climate Change and Its Relation to the NAO and EA Patterns. *Journal of Climate*, **25**, 3, 886-902, doi:10.1175/JCLI-D-11-00087.1.
World Meteorological Organization, 2011: Commission for Climatology – Over Eighty Years of Service. Accessed 30 March 2018. Available online at http://www.wmo.int/pages/prog/wcp/ccl/documents/WMO1079_web.pdf.
WRCP, 2019: World Climate Research Programme – CMIP6 model output database. Accessed 12 January 2019. Available online at https://esgf-node.llnl.gov/search/cmip6/.
Yin, J. H., 2005: A consistent poleward shift of the storm tracks in simulations of 21st Century climate. *Geophysical Research Letters*, **32**, 18, 4pp, doi:10.1029/2005GL023684.
Yu, L., S. Zhong, J. A. Winkler, D. L. Doubler, X. Bian, and C. K. Walters, 2017: The inter-annual variability of southerly low-level jets in North America. *International Journal of Climatology*, **37**, 1, 343-357, doi:10.1002/joc.4708.
Yuan, J., 1999: Testing Linearity For Stationary Time Series Using the Sample Interquartile Range. *Journal of Time Series Analysis*, **21**, 6, 713-722, doi:10.1111/1467-9892.00206.
Yue S., P. Pilon, and C. Cavadias, 2002: Power of the Man-Kendall and Spearman's rho tests for detecting monotonic trends in hydrological series. *Journal of Hydrology*, **259**, 1, 254-271, doi:10.1016/S0022-1694(01)00594-7.
Zappa, G., L.C. Shaffrey, K.I. Hodges, P.G. Sansom, and D.B. Stephenson, 2013: A Multimodel Assessment of Future Projections of North Atlantic and European Extratropical Cyclones in the CMIP5 Climate Models. *Journal of Climate*, **26**, 16, 5846-5862, doi: 10.1175/JCLI-D-12-00573.1.
Zhang, D., and W. Zheng, 2004: Diurnal cycles of surface winds and temperatures as simulated by five boundary layer parameterizations. *Journal of Applied Meteorology*, **43**, 1, 157-169, doi:10.1175/1520-0450(2004)043<0157:DCOSWA>2.0.CO;2.
Zhang, J., M. Cui, B. Hodge, A. Florita, and J. Freedman, 2017: Ramp forecasting performance from improved short-term wind power forecasting over multiple spatial and temporal scales. *Energy*, **122**, 528-541, doi:10.1016/j.energy.2017.01.104.
Zhu, J., and X. Liang, 2013: Impacts of the Bermuda High on Regional Climate and Ozone over the United States. *Journal of Climate*, **26**, 3, 1018-1032, doi:10.1175/JCLI-D-12-00168.1.

Appendix.

A1: The remaining 14 boxplots showing variability of LLJ speed that were not shown as part of Figure 14.

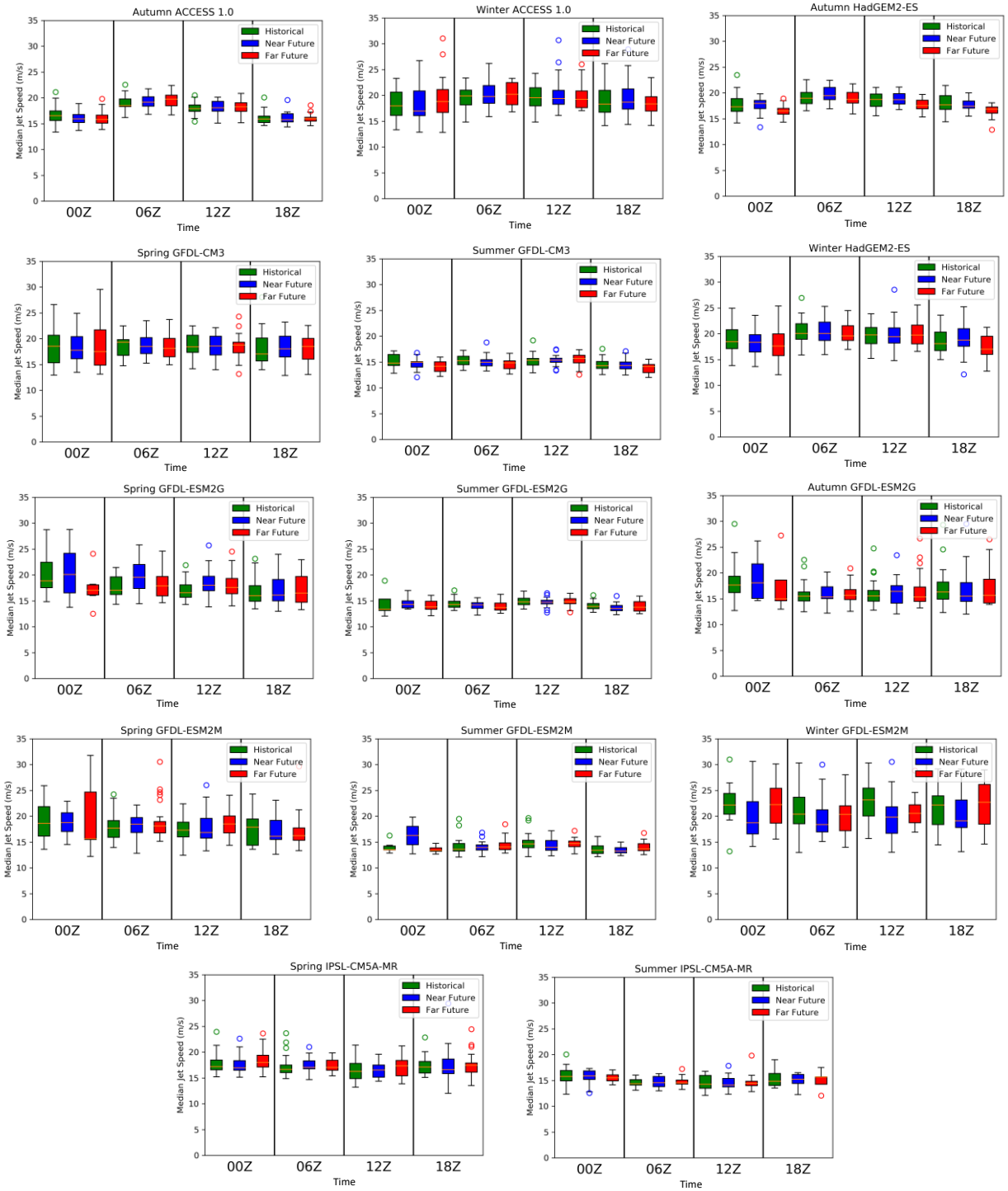

A2: The remaining 15 boxplots showing variability of LLJ height that were not shown as part of Figure 15.

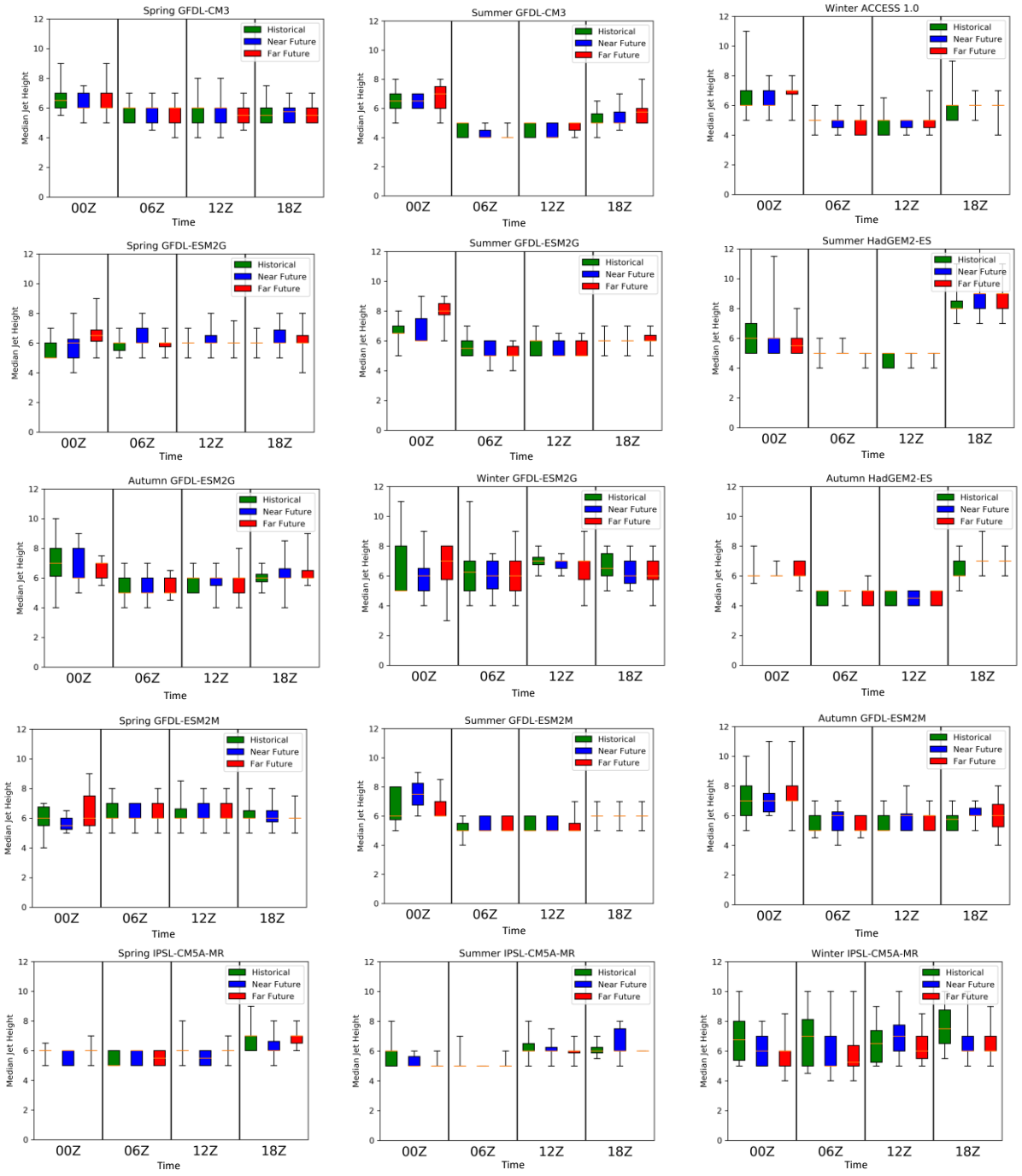

A3: The remaining 14 boxplots showing variability of LLJ frequency that were not shown as part of Figure 16.

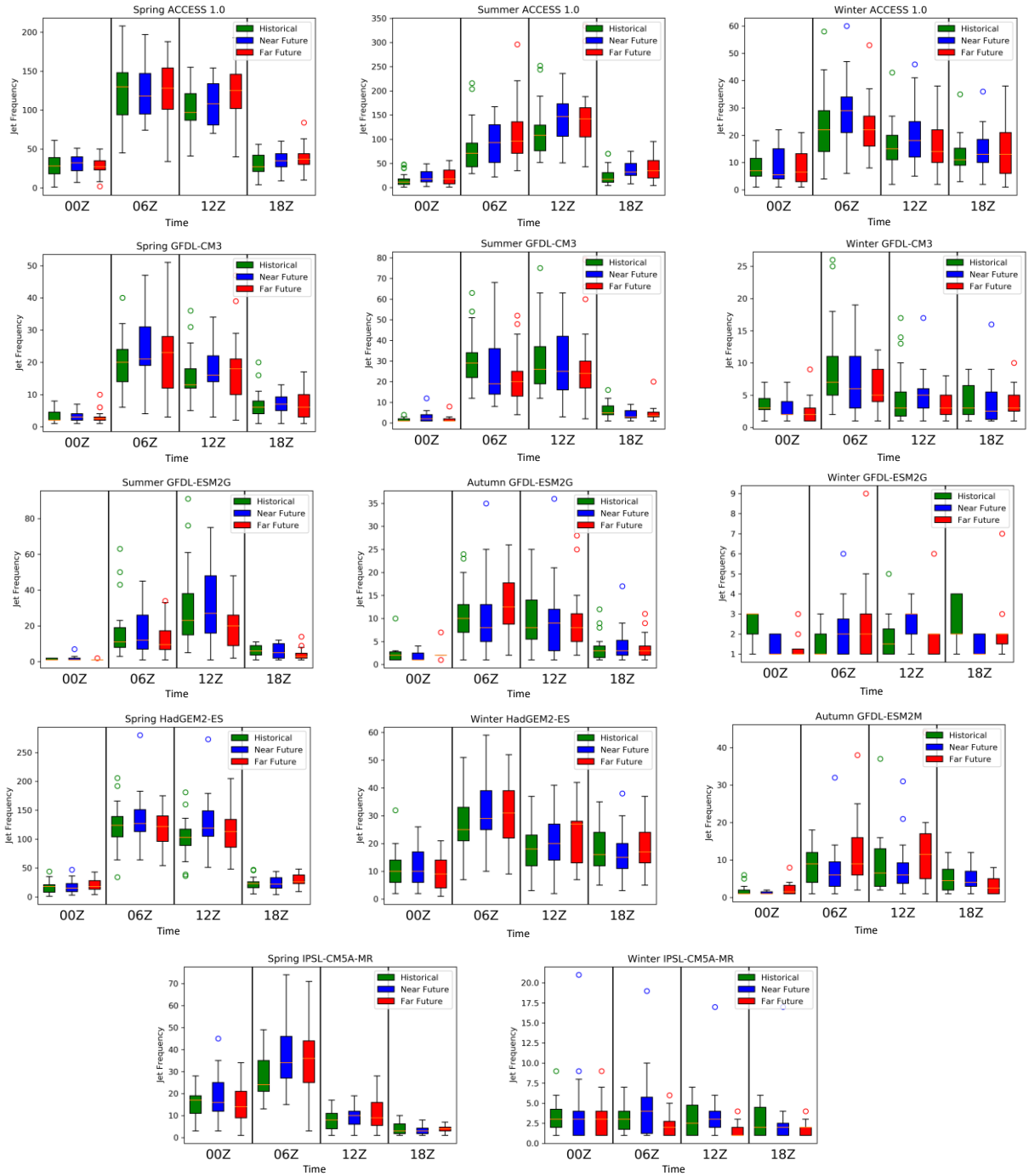

B1: The remaining 38 boxplots showing variability of median wind speed and WPD that were not shown as part of Figure 20.

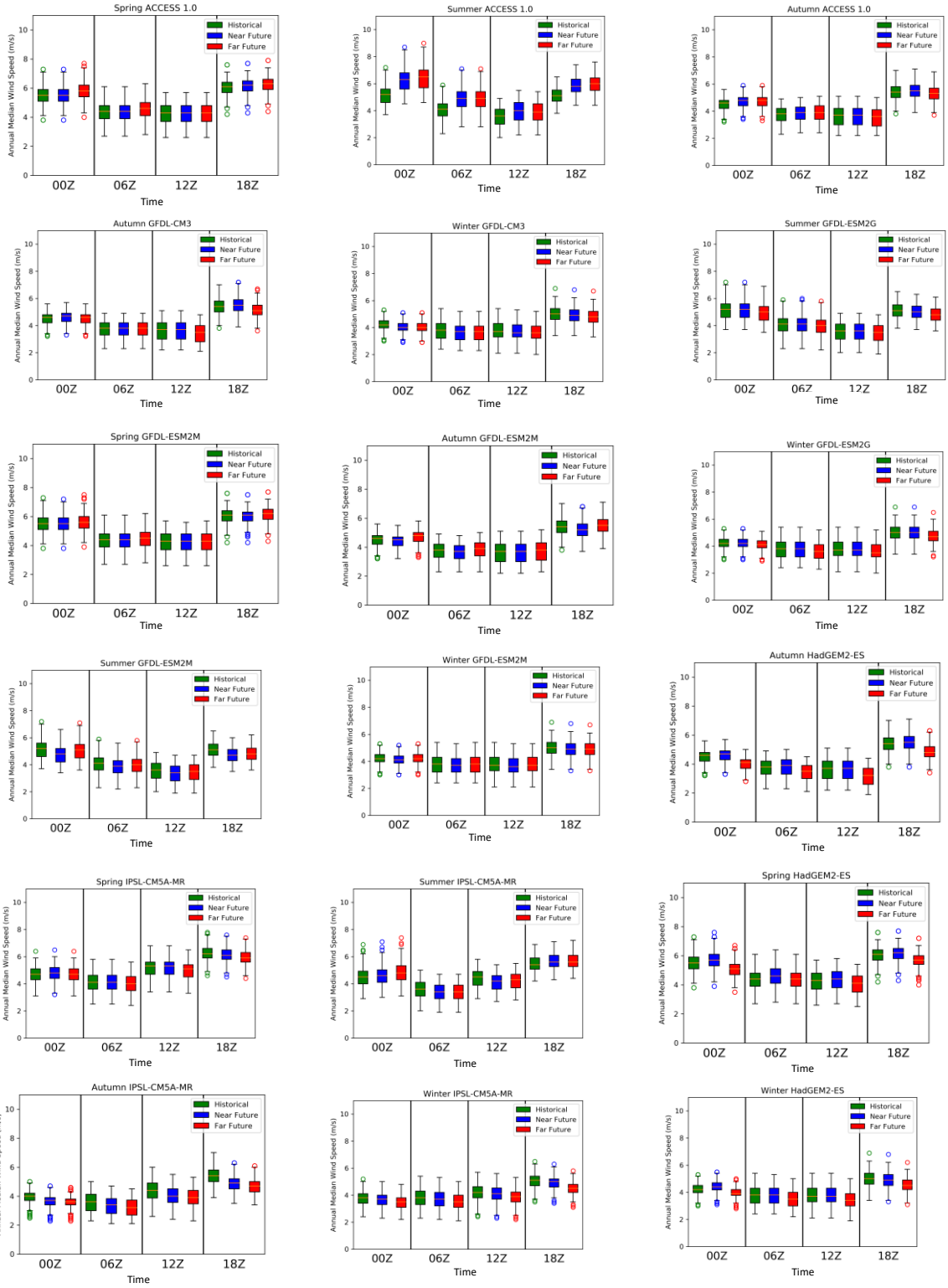

Continuation of B1.

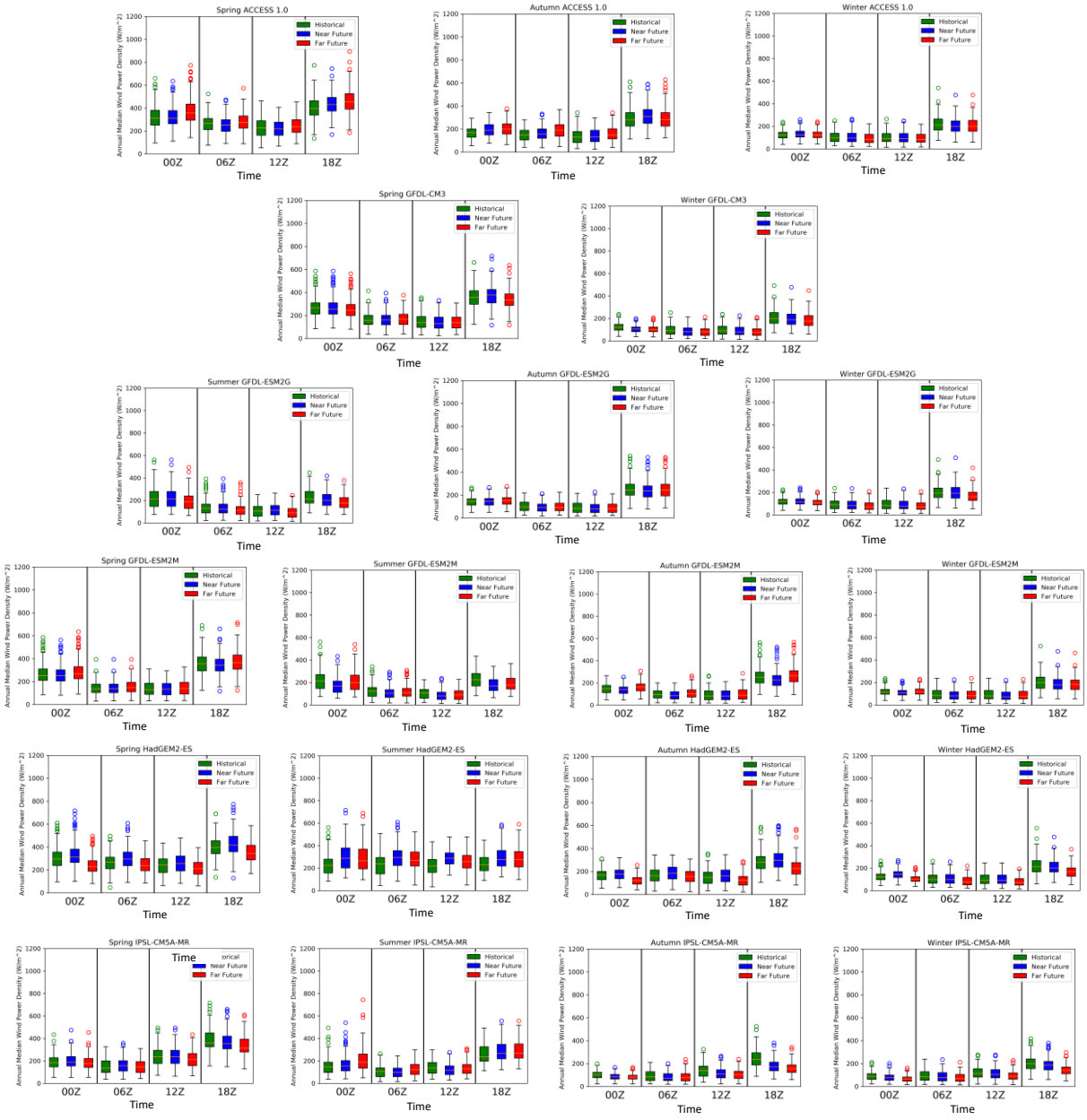

B2: The remaining 37 boxplots showing variability of ramp up and ramp down frequency that were not shown as part of Figure 21.

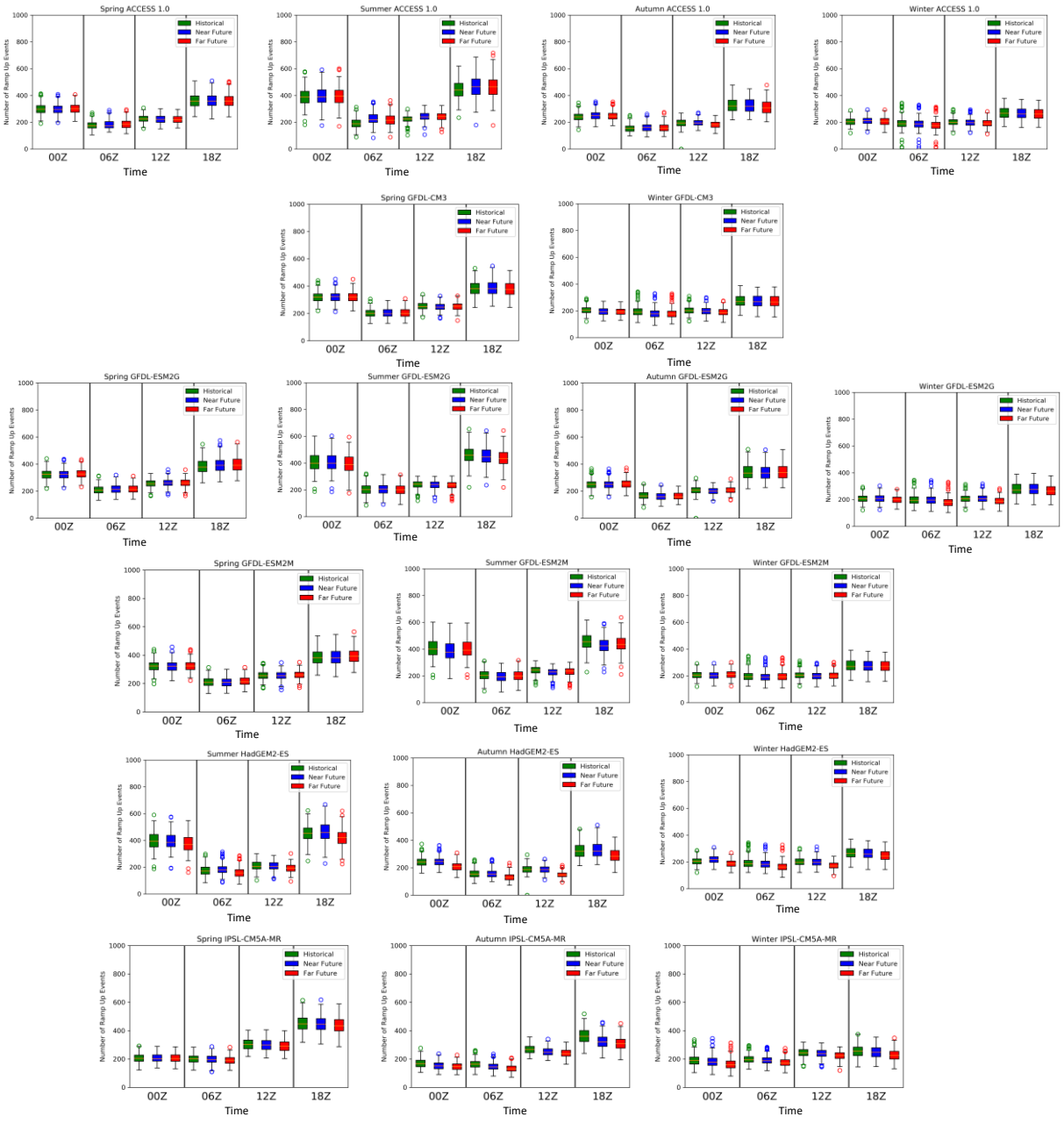

Continuation of B2.

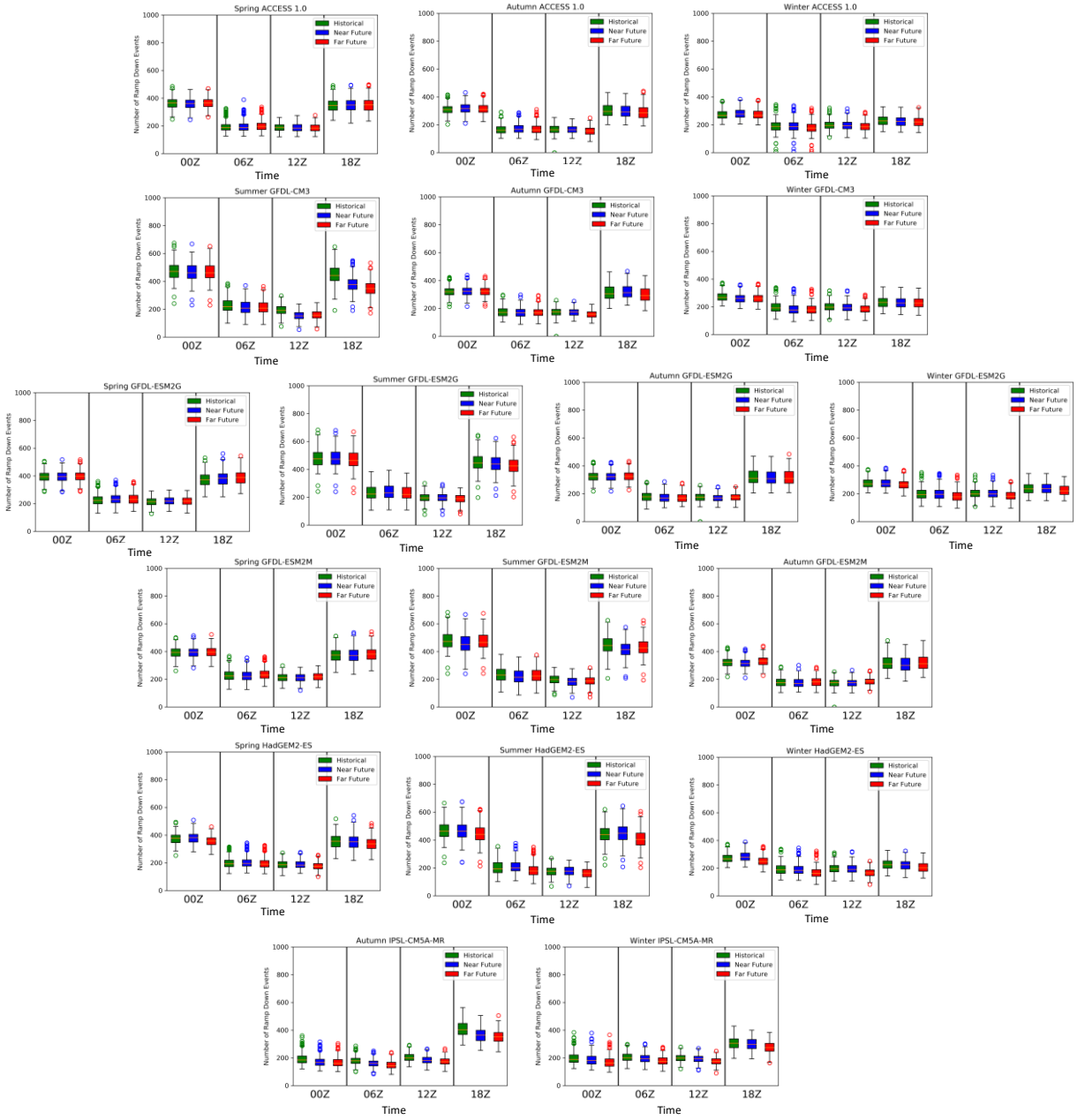

B3: The remaining 38 boxplots showing variability of cut-in and cut-out frequency that were not shown as part of Figure 22.

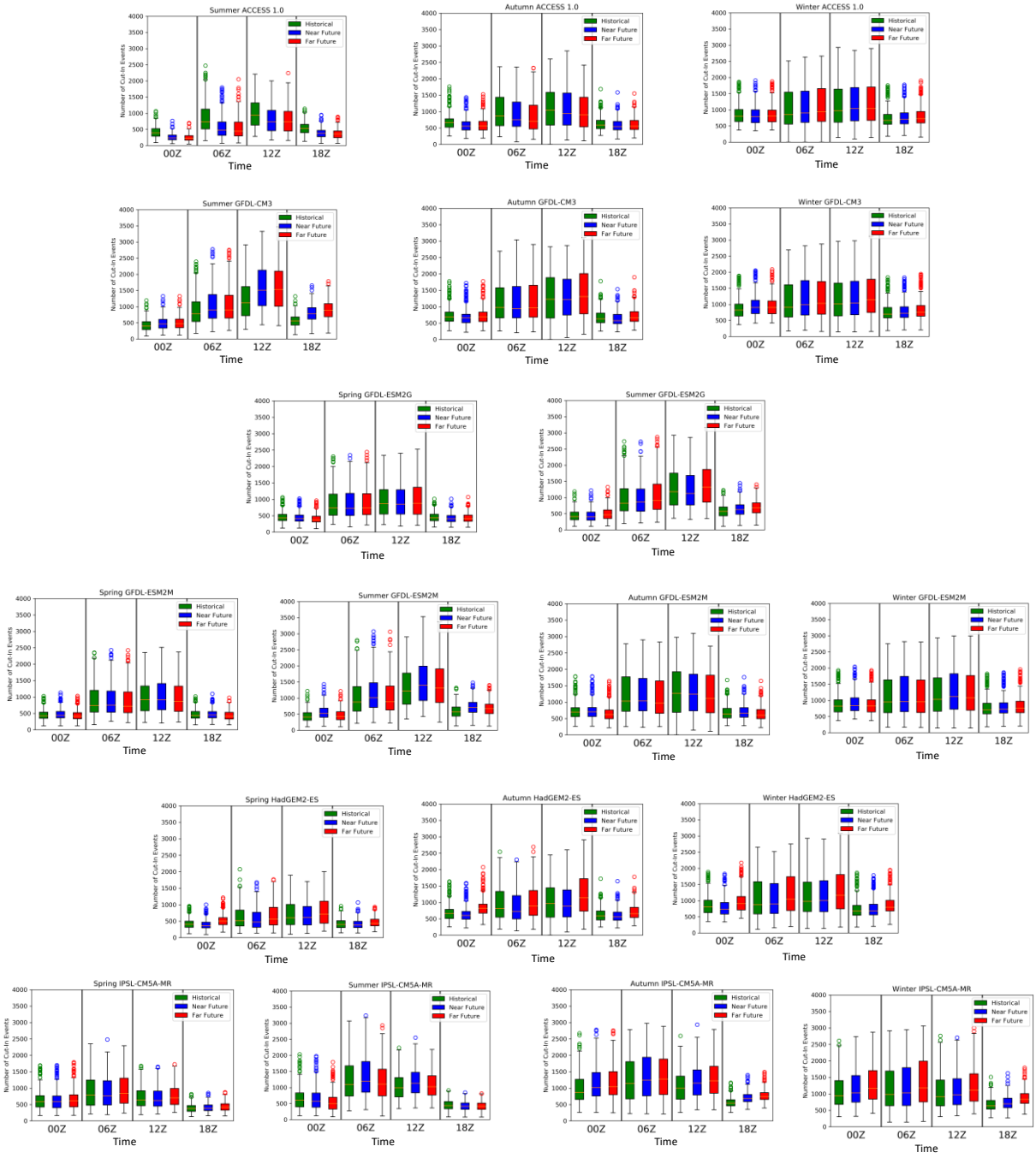

Continuation of B3.